



Universität Hamburg

Unchaining the biomarker potential of aerobic methanotrophic bacteria

Dissertation
zur Erlangung des Doktorgrades der Naturwissenschaften

Dr._rer._nat._

an der Fakultät für Mathematik, Informatik und Naturwissenschaften
Fachbereich Geowissenschaften
der Universität Hamburg

vorgelegt von

Alexmar del Carmen Córdova González

Hamburg, 2022

Department of Earth Sciences

Date of Oral Defense:

14.06.2022

Reviewers:

Prof. Dr. Jörn Peckmann

Dr. Daniel Birgel

Members of the examination commission:

Prof. Dr. Wolfgang Streit

PD Dr. Christian Knoblauch

Prof. Dr. Johanna Baehr

Chair of the Subject Doctoral Committee

Earth System Sciences:

Prof. Dr. Hermann Held

Dean of Faculty MIN:

Prof. Dr. Heinrich Graener

To my dad, my eternal love

Acknowledgments

To my supervisors Prof Dr. Jörn Peckmann and Dr. Daniel Birgel for their support and guidance through all these years of research and hard work, and for believing in my scientific criteria.

To the lab technician Sabine Beckmann for her assistance in the chromatographic analyses of the samples and lab work, and for all the technical knowledge she shared with me throughout the development of my doctorate.

To my colleagues in the research group Mathia Sabino, Lydia Baumann, Nicola Krake and Simon Rouwendaal for the company in the long hours in the lab and throughout this path of ups and downs. Special thanks to Mathia for being the best office mate I could ever have; you know I will always treasure our long talks. I also thank to other members of the Geology in the Earth System working group for the timeshare.

To the Prof Dr. Andreas Kappler of the University of Tübingen, for providing the infrastructure for the performance of the culturing experiments of my research. Also, to the lab technician Lars Grimm for his assistance in the cultivation of the strains and microbiological analyses, as well as to the other members of the Geomicrobiology Group.

The most special thanks go to my loving family. To my siblings Córdova González, Alejandro, Alejandra, Alexia and Isaac, for always being willing to listen to me, regardless of the time difference. Mami, thank you for your advice and your love. Papi, I would give anything to share this achievement with you, but I know that from wherever you are you are celebrating it with me. I love you to infinity “∞” and beyond. These thanks are extensive to my beloved nieces and siblings-in-law.

To my husband John Cárdenas for his love, patience, and support during these years together. Thank you for always showing me new and interesting perspectives, and for the adventure that is our life together. I love so much.

To my lifelong friends Gibran Romero, Khelymey Uzcátegui, Ana Karina Faraco, Henry Gómez, and Nadeztha Hernandez. “If a friendship lasts longer than seven years, psychologists say it will last a lifetime”, ours has no turning back. Also, to the new friends I met during my time in Germany, specially to Oscar Sánchez, Jonas Moe and Rob Steenkamp for all the laughter, drinks and delicious food.

To the German Academic Exchange Service–DAAD for the scholarship they granted me to finance my doctoral studies (program number “57299294 – Research Grants Doctorate 17/18”).

Abstract

Unchaining the biomarker potential of aerobic methanotrophic bacteria

The aim of this project was to increase the knowledge on the lipid biomarker inventory of aerobic methanotrophic bacteria, regarding their lipid biomarker patterns and their stable carbon isotopic fingerprint, facilitating the recognition and interpretation of this important group of bacteria in marine and other highly alkaline and saline environments. To fulfil this objective, the biomarker distribution and compound-specific carbon isotopic composition of the strains *Methylovimicrobium alcaliphilum* and *Methylovimicrobium kenyense* were studied. Both strains can tolerate high alkalinity and salinity conditions similar to those typifying marine methane seeps. Their unique cyclic terpenoid inventory comprises 4-methyl steroids, 3-methyl- and desmethyl bacteriohopanepolyols (aminotetrol and aminotriol), and tetrahymanol, all of which are ^{13}C -depleted. The average carbon isotope fractionation between methane and the respective lipid ($\Delta\delta^{13}\text{C}_{\text{terpenoid-methane}}$) is found to be -25‰ for *M. kenyense* and -16‰ for *M. alcaliphilum*. These data shed new light on the previously reported compound and carbon stable isotope patterns of cyclic terpenoids from methane-seep environments, particularly, ^{13}C -depleted tetrahymanol and its degradation product gammacerane, which are reinterpreted as biomarkers of aerobic methanotrophic bacteria based on their occurrence in methane-seep deposits in association with other biomarkers of aerobic methanotrophs.

In culture experiments at varying conditions, the hopanoid abundance of *M. alcaliphilum* was increased at lower salinity and higher nitrate concentration. The production of pentacyclic triterpenoids, but especially aminotriol, was favored at low salinity. Interestingly, 3-methyl-aminotetrol and tetrahymanol were favored at higher salinity. Bacteriohopanepolyols (BHPs) increased considerably at higher nitrate concentrations, particularly aminotriol and 3-methyl-aminotriol. The changes on the hopanoid production of *M. alcaliphilum* under varying conditions highlights the significance of environmental factors for bacterial lipid production.

Aerobic methanotrophs have been considered to cause carbonate dissolution in natural environments. To understand the role of aerobic methanotrophic bacteria on the biocorrosion of carbonates, a carbonate corrosion experiment was performed at a modern marine methane seep (REGAB Pockmark, Congo area). Carbonate cubes exposed to active seepage showed visible traces of microbioerosion, visualized by epoxy casts. The corrosion traces are accompanied by unique and strongly ^{13}C -depleted fatty acids, 4-methyl sterols and diplopterol on the corroded surface of the carbonates, most likely produced by aerobic methanotrophs. 16S rRNA analyses confirm the predominance of methanotrophs among bacteria and support aerobic methanotrophic bacteria as potential cause of biocorrosion. The outcome of the obtained data demonstrate that carbonate corrosion is potentially caused by aerobic methanotrophic bacteria, supporting the hypothesis that aerobic methanotrophy can be a trigger for carbonate biocorrosion at marine methane seeps.

Zusammenfassung

Die Überprüfung des Biomarkerpotenzials aerober methanotropher Bakterien

Das Ziel dieses Projekts war es, das Wissen über das Lipid-Biomarker-Inventar aerober methanotropher Bakterien hinsichtlich ihrer charakteristischen Lipid-Biomarker-Muster und ihres stabilen Kohlenstoffisotopen-Fingerabdrucks zu erweitern. Im Vordergrund stand dabei, diese wichtige Gruppe von Bakterien in marinen und anderen nicht-marinen, aber stark salzhaltigen, und alkalinen Umgebungen besser erkennen und interpretieren zu können. Um dieses Ziel zu erreichen, wurde die spezifische Biomarkerverteilung und die Kohlenstoffisotopenzusammensetzung einzelner organischer Verbindungen der beiden Stämme *Methylovimicrobium alcaliphilum* und *Methylovimicrobium kenyense* untersucht. Beide Stämme können Umweltbedingungen mit hohen Alkalinitäten und normal marinen Salzgehalten tolerieren, welche den Bedingungen ähneln, die für kalte Methanquellen (cold seeps) typisch sind. Ihr einzigartiges Inventar zyklischer Terpenoide umfasst 4-Methylsterioide, 3-Methyl- und Desmethyl-Bakteriohopanpolyole (Aminotetrol und Aminotriol) und Tetrahymanol, die alle ^{13}C -verarmte Isotopenverhältnisse zeigen. Die durchschnittliche Kohlenstoffisotopenfraktionierung zwischen Methan und dem entsprechenden Lipid ($\Delta\delta^{13}\text{C}_{\text{Terpenoid-Methan}}$) beträgt -25‰ für *M. kenyense* und -16‰ für *M. alcaliphilum*. Diese Ergebnisse werfen ein neues Licht auf die bisher berichteten Muster von Verbindungen und stabilen Kohlenstoffisotopen von zyklischen Terpenoiden aus cold seeps, insbesondere von ^{13}C -verarmtem Tetrahymanol und seinem Abbauprodukt Gammaceran. Tetrahymanol und Gammaceran müssen als Biomarker für aerobe methanotrophe Bakterien an cold seeps neu interpretiert werden, vor allem wenn andere, aus Kulturen bekannte Biomarker von aeroben methanotrophen Bakterien in Umweltproben vertreten sind.

In Kulturexperimenten unter variierenden Salzgehalten und Nitratkonzentrationen war die Hopanoid-Häufigkeit von *M. alcaliphilum* bei jeweils niedrigerem Salzgehalt und

höheren Nitratkonzentrationen erhöht. Die Produktion von pentazyklischen Triterpenoiden, insbesondere aber von Aminotriol, wurde bei niedrigem Salzgehalt begünstigt. Interessanterweise wurden 3-Methylaminotetrol und Tetrahymanol bei höherem Salzgehalt bevorzugt. Bacteriohopanepolyole (BHPs) nahmen bei höheren Nitratkonzentrationen deutlich zu, insbesondere die BHPs Aminotriol und 3-Methylaminotriol. Die Veränderungen der Hopanoid-Produktion von *M. alcaliphilum* unter unterschiedlichen Bedingungen verdeutlichen die Bedeutung sich verändernder Umweltfaktoren für die Lipidproduktion.

Es wird angenommen, dass aerobe methanotrophe Bakterien in deren natürlichen Umgebungen durch ihren Metabolismus zu einer Herabsetzung der Alkalinität beitragen können, und dadurch die Korrosion von Karbonaten herbeiführen. Um die Rolle aerober methanotropher Bakterien bei der Biokorrosion von Karbonaten zu untersuchen, wurde ein Karbonatkorrosionsexperiment an einem aktiven cold seep (REGAB Pockmark, vor der Küste der Republik Kongo) durchgeführt. Es wurden Karbonatwürfel ausgebracht, die für 4 Jahre aktivem Ausströmen von Methanausgesetzt waren. Die Würfel zeigten sichtbare Spuren von Mikrobioerosion, die durch Epoxidgüsse sichtbar gemacht wurden. Begleitet werden die Korrosionsspuren von einzigartigen und stark ^{13}C -verarmten Fettsäuren, 4-Methylsterolen und Diplopterol auf der korrodierten Oberfläche der Karbonate. Das einzigartige Biomarkerinventar deutet auf aerobe methanotrophe Bakterien als Produzenten hin. 16S-*r*RNA-Analysen bestätigen die Dominanz methanotropher Bakterien auf den korrodierten Karbonaten und unterstützen die Hypothese, dass aerobe methanotrophe Bakterien die mögliche Ursache von Biokorrosion an Karbonaten darstellen.

List of publications

Chapters II, III and IV of the present thesis are either published as articles in peer-reviewed journals or are in preparation for submission. Individual contributions of the doctoral candidate to publications can be found in Appendix D

Published as in peer-reviewed journals

Cordova-Gonzalez, A., Birgel, D., Kappler, A., & Peckmann, J., 2020. Carbon stable isotope patterns of cyclic terpenoids: A comparison of cultured alkaliphilic aerobic methanotrophic bacteria and methane-seep environments. *Organic Geochemistry*, 139, 103940. DOI: 10.1016/j.orggeochem.2019.103940. (Chapter II)

Cordova-Gonzalez, A., Birgel, D., Kappler, A., & Peckmann, J., 2021. Variation of salinity and nitrogen concentration affects the pentacyclic triterpenoid inventory of the haloalkaliphilic aerobic methanotrophic bacterium *Methylovulum alcaliphilum*. *Extremophiles* 25(3):285-299. DOI: 10.1007/s00792-021-01228-x. (Chapter III)

In preparation

Cordova-Gonzalez A., Birgel D., Wisshak M., Urich T., Brinkmann F., Marcon Y., Bohrmann G. & Peckmann J. A carbonate corrosion experiment at a marine methane seep: The role of aerobic methanotrophic bacteria. (Chapter IV).

Table of contents

	Page
1. Chapter I.....	1
Introduction	1
1.1 Background.....	1
1.1.1 Aerobic methanotrophic bacteria	1
1.1.2 Lipid biomarkers and aerobic methanotrophy.....	5
1.1.3 Aerobic methanotrophs in marine cold seep systems	10
1.2 Research questions and hypotheses	12
1.3 Objectives and structure	15
2. Chapter II.....	17
Carbon stable isotope patterns of cyclic terpenoids produced by aerobic methanotrophic bacteria.....	17
2.1 Abstract	17
2.2 Introduction	18
2.3 Material and methods	22
2.3.1 Cultures of aerobic methanotrophs	22
2.3.2 Lipid extraction.....	22
2.3.3 Biomarker analysis	23
2.3.4 Stable carbon isotopic composition of methane	24
2.4 Results and compilation of previous data.....	24
2.4.1 Results: Biomarker patterns of <i>Methylomicrobium kenyense</i> and <i>M. alcaliphilum</i>	24
2.4.2 New results and compilation of previous data: Biomarker patterns and compound-specific $\delta^{13}\text{C}$ values of aerobic methanotrophs in modern and ancient seep deposits.....	27
4-Methyl steroids.....	28
Hopanoids and 3-methyl hopanoids.....	29
Tetrahymanol and gammacerane.....	30
2.5 Discussion.....	34
2.5.1 Cyclic triterpenoids of Type I methanotrophs and their carbon stable isotope composition.....	34
2.5.2 Comparison of carbon isotope fractionation patterns	38
Cultures and methane-seep deposits.....	38
How to constrain the carbon isotope composition of methane at ancient seeps ...	40
2.6 Conclusions.....	43
3. Chapter III.....	45
Effect of varying conditions in the pentacyclic triterpenoid inventory of aerobic methanotrophic bacteria.....	45

3.1	Abstract	45
3.2	Introduction	46
3.3	Materials and methods.....	49
	3.3.1 Culture conditions	49
	3.3.2 Extraction and derivatization	49
	3.3.3 Gas chromatography and high-performance liquid chromatography	50
3.4	Results and discussion	52
	3.4.1 Novel N-containing BHPs.....	52
	3.4.2 Effect of salinity and nitrate concentration on growth rates	58
	3.4.3 Effect of salinity and nitrate concentration on the pentacyclic triterpenoid inventory	59
3.5	Conclusions.....	66
4.	Chapter IV	67
	Carbonate corrosion at marine methane seeps induced by aerobic methanotrophy.....	67
4.1	Abstract	67
4.2	Introduction	68
4.3	Geological setting	70
4.4	Methods.....	71
4.5	Results	74
	4.5.1 Carbonate corrosion features.....	74
	4.5.2 Composition of the microbial community	76
	4.5.3 Lipid biomarkers	77
	<i>CAB-B</i>	78
	<i>CAB-C</i>	80
	<i>CAB-D</i>	81
4.6	Discussion.....	82
	4.6.1 Are aerobic methanotrophic bacteria corroding carbonate at seeps?.....	82
	4.6.2 Carbonate microbioerosion and aerobic methanotrophy.....	88
4.7	Conclusions.....	90
5.	Chapter V	91
5.1	Outcomes.....	91
5.2	Perpectives	93
6.	References.....	95
	Appendix A	111
	Appendix B	113
	Appendix C	117
	Appendix D:.....	119
	Eidesstattliche Versicherung	121

List of figures

Figure 1.1 Classification of aerobic methanotrophic bacteria	3
Figure 1.2 Pathways of carbon metabolism in methanotrophs	3
Figure 1.3 Cell lipid membranes with insertion of (a) sterols (eukaryotes) and (b) hopanols (bacteria). (c) Selected common fatty acids in methanotrophic bacteria.....	7
Figure 1.4 Biosynthetic pathway for steroids from squalene in methanotrophic bacteria	8
Figure 1.5 (a) Biosynthetic pathway for hopanoids from squalene. (b) Selected common hopanoids (side chain structures) synthesized by methanotrophic bacteria. (c) Ring A with methylation at C-3.....	9
Figure 1.6 Schematic overview of the microbial metabolisms consuming methane at seeps.....	11
Figure 2.1 Relative contents (in relation to all extracted lipids) of a) lipid biomarkers, b) 4-methylated sterols and c) hopanoids in <i>M. alcaliphilum</i> and <i>M. kenyaense</i>	27
Figure 2.2 Offset of $\delta^{13}\text{C}$ values ($\Delta\delta^{13}\text{C}$) between methane and terpenoid biomarkers of aerobic methanotrophs in cultures and seep deposits	41
Figure 3.1 Comparison of quantification of BHPs of <i>M. alcaliphilum</i> as (a) hopanol products after periodic acid cleavage using GC–FID and (b) intact hopanols using LC–MS reflecting different salinities and nitrate concentration	53
Figure 3.2 Partial HPLC–MS chromatograms showing BHPs in the acetylated total lipid extract of <i>M. alcaliphilum</i> grown at 3% salinity and 100 mM KNO_3	53
Figure 3.3 HPLC–MS spectra of acetylated (a) aminodiol I, (b) 3-methyl-aminodiol II, isomers of (c-d) aminotriol IIIa,b and (e-f) 3-methyl-aminotriol IVa,b of <i>M. alcaliphilum</i>	54
Figure 3.4 (a) HTGC–MS partial chromatograms (m/z 492; m/z 191; m/z 205) of acetylated total lipid extract of <i>M. alcaliphilum</i> . (b) EI mass spectrum of acetylated isomer of aminotriol b IIIb. (c) EI mass spectra of acetylated 3-methyl-aminotriol b IVb. (d) EI mass spectra of acetylated 3-methyl-aminotriol a IVa	56
Figure 3.5 Partial GC–MS chromatograms (m/z 291; m/z 277; m/z 263) of hopanol products obtained after periodic acid cleavage.....	58
Figure 3.6 Distribution of pentacyclic triterpenoids in response to variations in salinity (1% and 3%): (a) total pentacyclic triterpenoids, (b) aminotetrol, (c) aminotriol isomers, (d) C_{30} hopanes, (e) C_{30} hopanols, (f) tetrahymanol.	62
Figure 3.7 Relative abundance in percent of main pentacyclic triterpenoids of <i>M. alcaliphilum</i> in response to variations in salinity (1% and 3%).	63
Figure 3.8 Distribution of pentacyclic triterpenoids in response to variations in nitrate concentration (10 mM and 100 mM): (a) total pentacyclic triterpenoids, (b) aminotetrol, (c) aminotriol isomers, (d) C_{30} hopanoids, (e) C_{30} hopanols, (f) tetrahymanol.	65
Figure 4.1 Location of the study area within the REGAB Pockmark	71

- Figure 4.2** Carbonate experiments with four limestone cubes each, deployed for 2.5 years within the REGAB Pockmark in the Lower Congo Basin at ca. 3170 m water depth. (a) Upon deployment of CAB-B in a mussel bed, gas escaped from the sediment. (b) CAB-C placed onto an active hydrate site with mussels and tubeworms; yellow arrow indicating a shrimp, white arrow pointing to a crab. (c) CAB-D located in a reference area with no apparent seepage activity.72
- Figure 4.3** Scanning electron imaging of experimental marble substrates CAB-C (a) and epoxy casts thereof (b-f), showing distinctive signs of microbioerosion: (a) intense surface pitting in the coarsely crystalline carbonate matrix (m); (b) epoxy cast with circumradial microboring structure; (c-d) dense clusters of the same type of microborings; (e-f) close-ups of individual tunnels radiating and ramifying from a central point of entry towards slightly widened terminations.....75
- Figure 4.4** Diversity and relative abundance (%) of dominant phylogenetic groups in the corroded surface of CAB-C. Each color represents the percentage of the total sample contributed by each taxon group at (a) phylum level, except for Proteobacteria and Bacteroidetes, which are shown by class; (b) order level (dominant phylotypes with relative abundance $\geq 3\%$), (c) family level (dominant phylotypes with relative abundance $\geq 3\%$).....77
- Figure 4.5** Partial gas chromatograms of alcohol (a) and fatty acid (b) fractions of CAB-C biofilm.79
- Figure 4.6** Relative abundance of lipids in the alcohol (a) and fatty acid (b) fractions of biofilms from CAB-B, CAB-C, and CAB-D cubes.....81

List of tables

Table 2.1 Contents and $\delta^{13}\text{C}$ values of lipid biomarkers from cultures of aerobic methanotrophs; n.d. = not detected; tr = traces.	26
Table 2.2 Average compound-specific $\delta^{13}\text{C}$ values (‰ V-PDB) of lipids from four species of aerobic methanotrophs bacteria, two mussel symbionts, one sediment sample from Haakon Mosby (H.M.), two subrecent carbonates (A.C. = Alaminos Canyon 645, Makr = Makran) and eight ancient seep carbonates; Pietr = Pietralunga (Miocene), Marm = Marmorito (Miocene), Buje (Eocene), Tepee Buttes (Late Cretaceous), C.C. = Cold Fork of Cottonwood Creek (Early Cretaceous), W.S. = Wilbur Springs (Early Cretaceous), Zizin (Early Cretaceous), PSK = Paskenta (Late Jurassic); tr = traces	32
Table 2.3 Offset of $\delta^{13}\text{C}$ values ($\Delta\delta^{13}\text{C}$) between methane and lipid biomarkers	37
Table 3.1 Growth rates for each condition tested	59
Table 3.2 Contents of pentacyclic triterpenoids in cultures of <i>M. alcaliphilum</i> grown at different salinities	60
Table 3.3 Contents of pentacyclic triterpenoids in cultures of <i>M. alcaliphilum</i> grown with varying amounts of nitrate	61
Table 4.1. Contents ($\mu\text{g/g}$) and $\delta^{13}\text{C}$ (‰ vs V-PDB) values of lipid biomarkers from biofilms attached to CAB-B, CAB-C, and CAB-D cubes	78

1. Chapter I

Introduction

Aerobic methanotrophic bacteria are a subset of methylotrophic bacteria, which utilize methane (CH_4) as only carbon and energy source (Hanson & Hanson, 1996). Aerobic methane oxidation, which is performed by aerobic methanotrophic bacteria, is an important process regulating the amount of methane released into the environment, (Chistoserdova, 2018). Methane is among the most severe greenhouse gases next to carbon dioxide (CO_2) and nitrous oxide (NO_x), making aerobic methanotrophs of great interest for paleoclimate and carbon cycling studies. Besides their relevance in methane consumption, there has been a considerable interest over the years in the use of aerobic methanotrophic bacteria for biotechnological purpose (Trotsenko & Murrell, 2008; Khider et al., 2021).

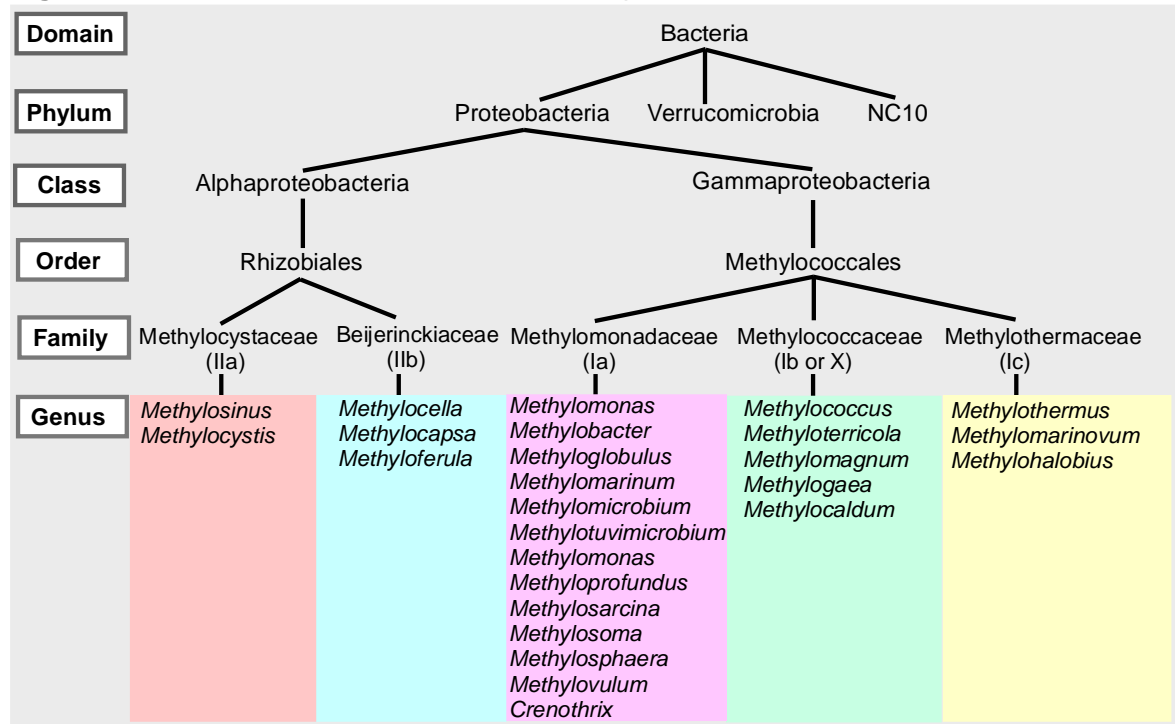
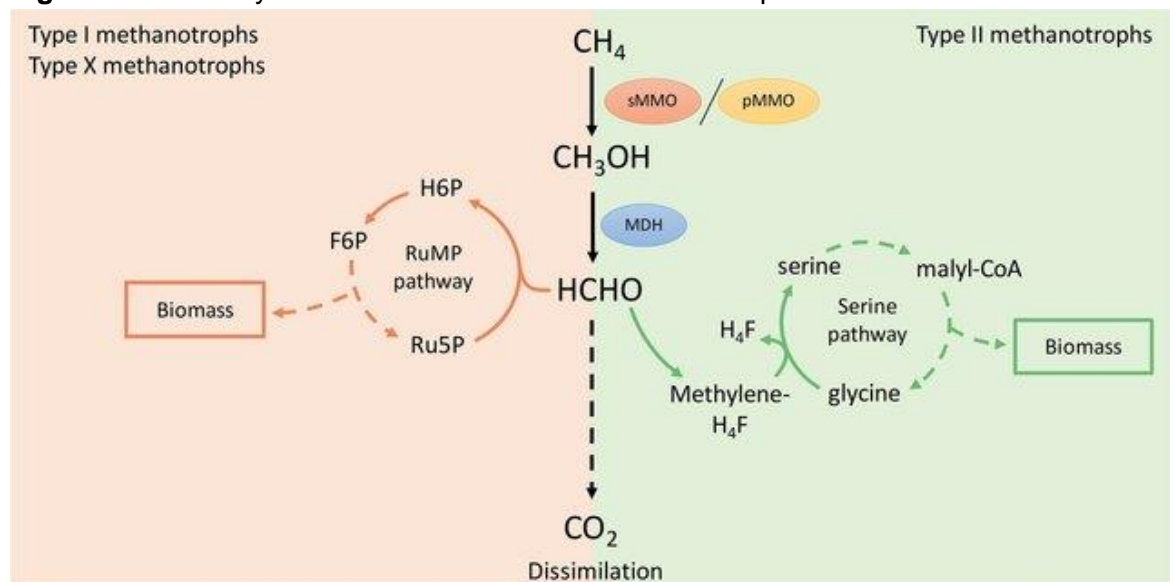
1.1 Background

1.1.1 Aerobic methanotrophic bacteria

Aerobic methanotrophic bacteria (methanotrophs) are a group of gram-negative bacteria that use methane as carbon and energy source (Hanson & Hanson, 1996), playing an important role in the oxidation of methane and attenuating the fluxes of this potent greenhouse gas to the atmosphere (Smith et al., 2010). Aerobic methanotrophic bacteria are widely distributed in the environment, occurring in terrestrial, aquatic, and marine ecosystems, preferably at oxic-anoxic interfaces, where sufficient oxygen is available as electron acceptor and methane as carbon and energy source (Nazaries et al., 2013; Knief, 2015). Generally, methanotrophic bacteria belong to the Phylum Proteobacteria, but representatives of the Phylum

Verrucomicrobia—a unique group of methanotrophs capable of growing at very low pH—and the candidate phylum NC10—which possess an intra-aerobic pathway of methane oxidation—(Fig. 1.1; Khmelenina et al., 2018) are known. The proteobacterial aerobic methanotrophs are classified into two major groups, based on physiological, biochemical, morphological, ultrastructural and chemotaxonomic characteristics (Figs. 1.1 and 1.2): (1) Gammaproteobacteria (Type I methanotrophs) and (2) Alphaproteobacteria (Type II methanotrophs) (Hanson & Hanson, 1996; Dedysh & Knief, 2018). Major distinctive features between various types of methanotrophs are (1) the arrangement of their intracytoplasmic membranes (ICM) as stacks of vesicular discs (Type I), or as layers parallel to the cell periphery (Type II); (2) the predominance of specific C₁₆ (Type I) or C₁₈ (Type II) phospholipid fatty acids (PLFAs); (3) the capability of nitrogen fixation (few Type II methanotrophs); and (4) the carbon fixation mechanism via the ribulose monophosphate pathway (RuMP, Type I) or serine cycle (Type II; Dedysh & Knief, 2018).

Aerobic methanotrophs fix carbon in the form of formaldehyde and they possess two pathways of methane assimilation, assimilatory and dissimilatory. In the dissimilatory pathway, aerobic methanotrophs completely oxidize methane to carbon dioxide, producing energy. In the assimilatory pathway, methane-derived carbon becomes cellular material or biomass (Khider et al., 2021). The initial step of both pathways is the conversion of methane to methanol, which is then oxidized to formaldehyde (Fig. 1.2), the compound through which methanotrophs obtain most of their cellular carbon (Bowman, 2006). A proportion of the formaldehyde is either oxidized to formate and then to carbon dioxide, or assimilated through the RuMP cycle (Type I methanotrophs), or via the serine cycle (Type II methanotrophs) (Fig. 1.2; Khider et al., 2021). The conversion of methane to methanol, central to the growth of methanotrophs, is catalyzed by the enzyme methane monooxygenase (MMO). There are two structurally and biochemically distinct forms of MMO, a copper-dependent particulate methane monooxygenase (pMMO) and a soluble methane monooxygenase (sMMO). All known methanotrophs, except for the genus *Methylocella*, are capable of expressing pMMO, when grown in the presence of copper, but the ability to form sMMO has been observed only in some Type II methanotrophs (Hanson & Hanson, 1996; Kalyuzhnaya et al., 2019).

Figure 1.1 Classification of aerobic methanotrophic bacteria**Figure 1.2** Pathways of carbon metabolism in methanotrophs

Source: Khider et al. (2021).

Type I methanotrophs belong to the order Methylococcales, which includes the three family members Methylomonadaceae, Methylococcaceae, and Methylothermaceae (Fig. 1.1; Orata et al., 2018), corresponding to Type Ia, Ib or X, and Ic, respectively (Knief, 2015). Type II methanotrophs belong to the order Rhizobiales and are grouped in two families called Methylocystaceae and Beijerinckiaceae (Orata et al., 2018; Kalyuzhnaya et al., 2019), corresponding to Type IIa and IIb, respectively (Knief,

2015). Representatives of Type II methanotrophic bacteria (Fig. 1.1) have been mostly isolated in peats, soils, and lakes, whereas Type I methanotrophic bacteria (Fig. 1.1) are more versatile, also dwelling in the marine realm (Knief, 2015). Most methanotrophic bacteria are mesophilic and neutrophilic, but some strains are adapted to more extreme habitats, for example, verrucomicrobial strains, as well as some Type I *Methylocaldum* and *Methyloccoccus* strains, outstand for being thermophilic; some Type II *Methylocystis* strains and the Type I *Methylomonas paludis* adapt to low pH, while there are some Type I methanotrophs, particularly within the genus *Methylomicrobium*, that are adapted to high pH (Knief, 2015). Some alkaliphilic strains belonging to Type I methanotrophs are at the same time halophiles (*Methylomicrobium alcaliphium* and *Methylomicrobium kenyense*; Kalyuzhnaya et al., 2008), as well as Type I methanotrophs isolated from marine habitats (*Methylomarinum vadi*, Hirayama et al., 2013, *Methylomarinovum caldicuralii*, 2014; *Methyloprofundus sedimenti*, Tavormina et al., 2015). Additionally, some Type I strains of the genus *Methylosoma* and *Methyloglobulus* have shown ability to live preferentially in environments with low oxygen availability (Rahalkar et al., 2007; Deutzmann et al., 2014). In general terms, gammaproteobacterial strains show higher versatility in terms of adaptation to different environmental conditions (e.g., high temperature, low and high pH, high salinity, low oxygen availability) as well as higher diversity, while Type II have less adaptability (e.g., low pH) and are less diverse (Knief, 2015).

Aerobic methanotrophs, as any other bacteria, produce various organic macromolecules, as for example 16S rRNA, amino acids and proteins, which are fulfilling specific functions in bacterial cells (Khmelenina et al., 2018). The composition of the macromolecular inventory, but especially the 16S rRNA composition allows an exact allocation in the bacterial phylogenetic tree (Bowman, 2006, 2014). Although information gained by 16S rRNA data is crucial, shortly after bacterial cell death most of the organic macromolecules are starting to degrade, imposing serious limitations on their preservation. An exception from this early lysis are microbial membrane lipids, which may survive biodegradation and diagenetic processes in the sediment, serving as molecular fossils (Summons et al., 2021). These lipids, termed biomarkers, can be monitored parallel with bacterial 16S rRNA data in recent sediments (Hanson & Hanson, 1996). In ancient sediments or rocks, the original lipid signature is modified to different degrees, but many lipid biomarker patterns still look alike patterns found in living bacteria or preserve their basic skeletons in recognizable form after diagenesis and early stages of catagenesis (Peters et al., 2004a; Killips & Killips, 2005).

1.1.2 Lipid biomarkers and aerobic methanotrophy

Lipids are ubiquitous in the environment and geological materials (e.g., sediments, rocks, and crude oils); however, only a small fraction of them has a high potential to be preserved, functioning as biomarkers (Summons et al., 2021). Biomarkers (used as a contraction of biological markers) are complex organic compounds composed of carbon, hydrogen, and other elements, which originated from formerly living organisms and show little or no change in their structure from parent biomolecules, revealing information regarding the source organisms (Fig. 1.3; Peters et al., 2004a).

Most bacterial lipids are components of cell membranes, which regulate membrane behavior (Summons et al., 2021). For example, acetogenic lipids (fatty acids and alcohols) are linked to glycerol, which is further modified with polar head groups forming the lipid bilayer of cell membranes (Fig. 1.3). Membranes contain polar, hydrophilic heads (e.g., sugars, phospholipids), which are mostly lost after cell death (Summons et al., 2021), but the non-polar fatty acid chains can be found even in Cretaceous rocks (e.g., Birgel et al., 2006a). Commonly found lipids (Fig. 1.4 and 1.5) with biomarker potential encompass cyclic terpenoids (i.e., sterols, and hopanols), biosynthesized by polymerization of several isoprene (C_5H_8) units. Cyclic terpenoids, which play an important role in membrane organization and dynamics in model membranes of bacteria (Fig 1.3; Mangiarotti et al., 2019) are also well preserved in sediments and the rock record (e.g., Birgel & Peckmann, 2008; Elvert & Niemann, 2008; Bouloubassi et al., 2009; Birgel et al., 2011; Sandy et al., 2012; Talbot et al., 2014; Himmler et al., 2015; Natalicchio et al., 2015; Rush et al., 2016). One special case are lipid biomarkers preserved in authigenic mineral phases, such as methane-seep carbonates or phosphorites (Arning et al., 2008; e.g., Birgel & Peckmann, 2008), where biomarkers of an environment favoring mineral formation can be preserved in situ. One of the most unique bacterial lipid biomarker patterns found in such deposits are produced by aerobic methanotrophic bacteria (Birgel & Peckmann, 2008). These unique lipid biomarker patterns are well known from inventories of cultured bacteria and can be transferred to environmental studies (Jahnke et al., 1999; Summons et al., 2021).

In addition to the characteristic lipid biomarker inventory, compound-specific stable carbon isotopes ($\delta^{13}C$) of biomarkers have been used as complementary information for tracing sources of organic matter in the environment. The carbon assimilation pathway is of special interest because the lipids in ancient rocks are at best carrying

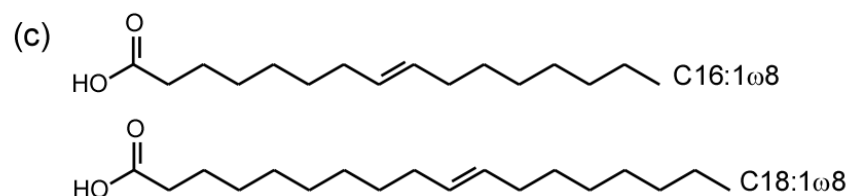
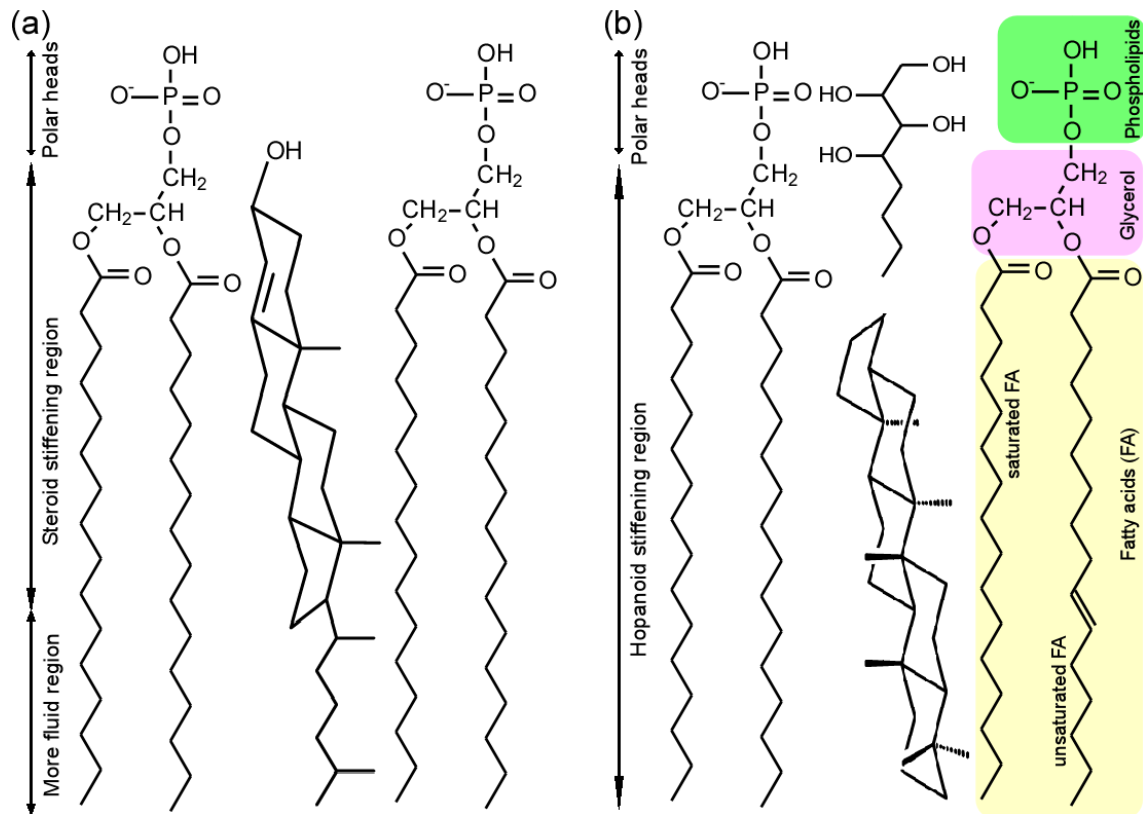
the isotopic fingerprint of the source organisms (Jahnke et al., 1999). This is especially true when source-characteristic and unique lipids are applied for this purpose. The signature of ^{13}C -depleted methane assimilated by aerobic methanotrophic bacteria is transferred to their lipids and facilitates the identification of lipid biomarkers of methanotrophic bacteria (Jahnke et al., 1999; Birgel & Peckmann, 2008; Himmler et al., 2015). Because Type I and Type II methanotrophs use different carbon assimilation pathways, their $\delta^{13}\text{C}$ values of lipid biomarkers can vary significantly (Summons et al., 1994; Jahnke et al., 1999). This peculiarity is also recorded in $\delta^{13}\text{C}$ values of lipid biomarkers of aerobic methanotrophic bacteria found in the environment (e.g., Birgel et al., 2011; Himmler et al., 2015).

FATTY ACIDS. Fatty acids are saturated or unsaturated alkyl chains containing a carboxylic acid group (COOH) (Fig. 1.3; Peters et al., 2004a). Among the numerous phospholipid fatty acids (PLFA) produced by aerobic methanotrophic Alpha- and Gammaproteobacteria, fatty acids with 16 or 18 carbon atoms and double bond position at $\omega 8$ are unique for aerobic methanotrophic bacteria and are valuable biomarkers in various modern environments (e.g., Hanson & Hanson, 1996; Knoblauch et al., 2008; Berndmeyer et al., 2013). The great disadvantage of unsaturated fatty acids in the study of ancient environments is the rapid loss of double bonds and consequently a loss of specificity (Killops & Killops, 2005). For that reason, they are no reliable biomarkers in ancient environments.

STEROIDS. In bacteria, steroids are formed from cyclization of squalene (Fig 1.4; Pearson, 2014). The first step in steroid biosynthesis is the oxygen-dependent epoxidation of squalene to 2,3-oxidosqualene. Subsequently, sterol cyclases yield the biosynthetic intermediate lanosterol (the first sterol formed in the biosynthesis; Pearson, 2014; Wei et al., 2016). The first steroids in aerobic methanotrophic bacteria were described in the 1970s in the Gammaproteobacterium *Methylococcus capsulatus* (Bird et al., 1971; Bouvier et al., 1976), probably the best characterized of the methanotrophic bacteria for over 40 years. At that time, sterols were only known from eukaryotes, and it was a novelty that bacteria produce sterols at all. Research on sterols in other cultured methanotrophic bacteria remained scarce, but some reports from bacterial cultures exist (*Methylosphaera hansonii*: Schouten et al., 2000; *Methylobacter luteus*, *Methylobacter whittenburyi*, *Methylococcus capsulatus*, *Methylosarcina lacus*: Wei et al., 2016). Remarkably among methanotrophic bacteria is the capacity to synthesize sterols with one or two methylations at C-4 (Fig. 1.4; Elvert & Niemann, 2008), which besides aerobic methanotrophs, are only produced by

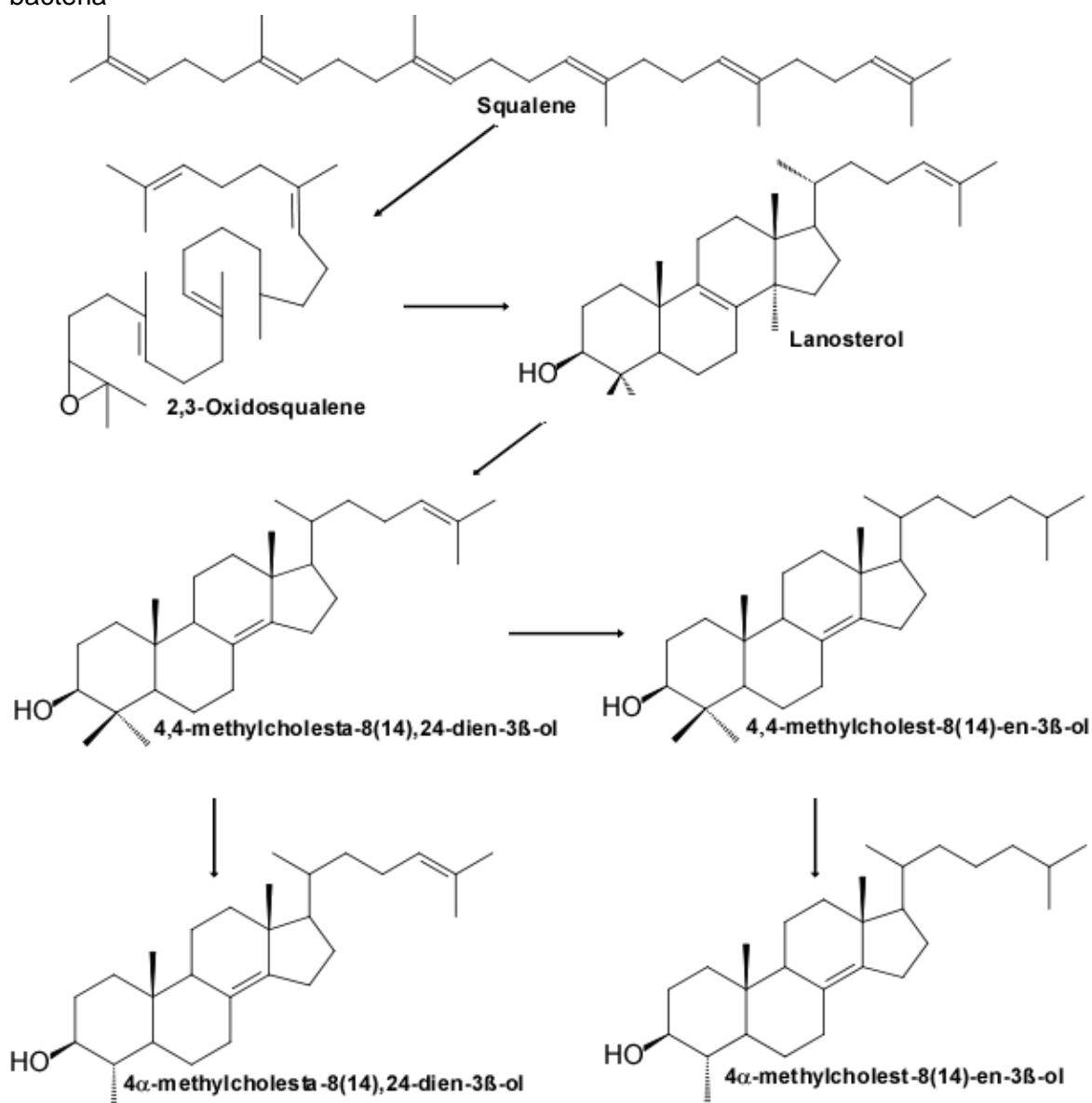
few myxobacterial strains of the genus *Nannocystis* (Wei et al., 2016). It is still unknown why bacteria produce sterols, and the potential significance of sterol-synthesizing bacteria in ancient environments is still a matter of debate (Pearson, 2014; Wei et al., 2016).

Figure 1.3 Cell lipid membranes with insertion of (a) sterols (eukaryotes) and (b) hopanols (bacteria). (c) Selected common fatty acids in methanotrophic bacteria



Source: adapted from Peters et al. (2004a)

Figure 1.4 Biosynthetic pathway for steroids from squalene in methanotrophic bacteria

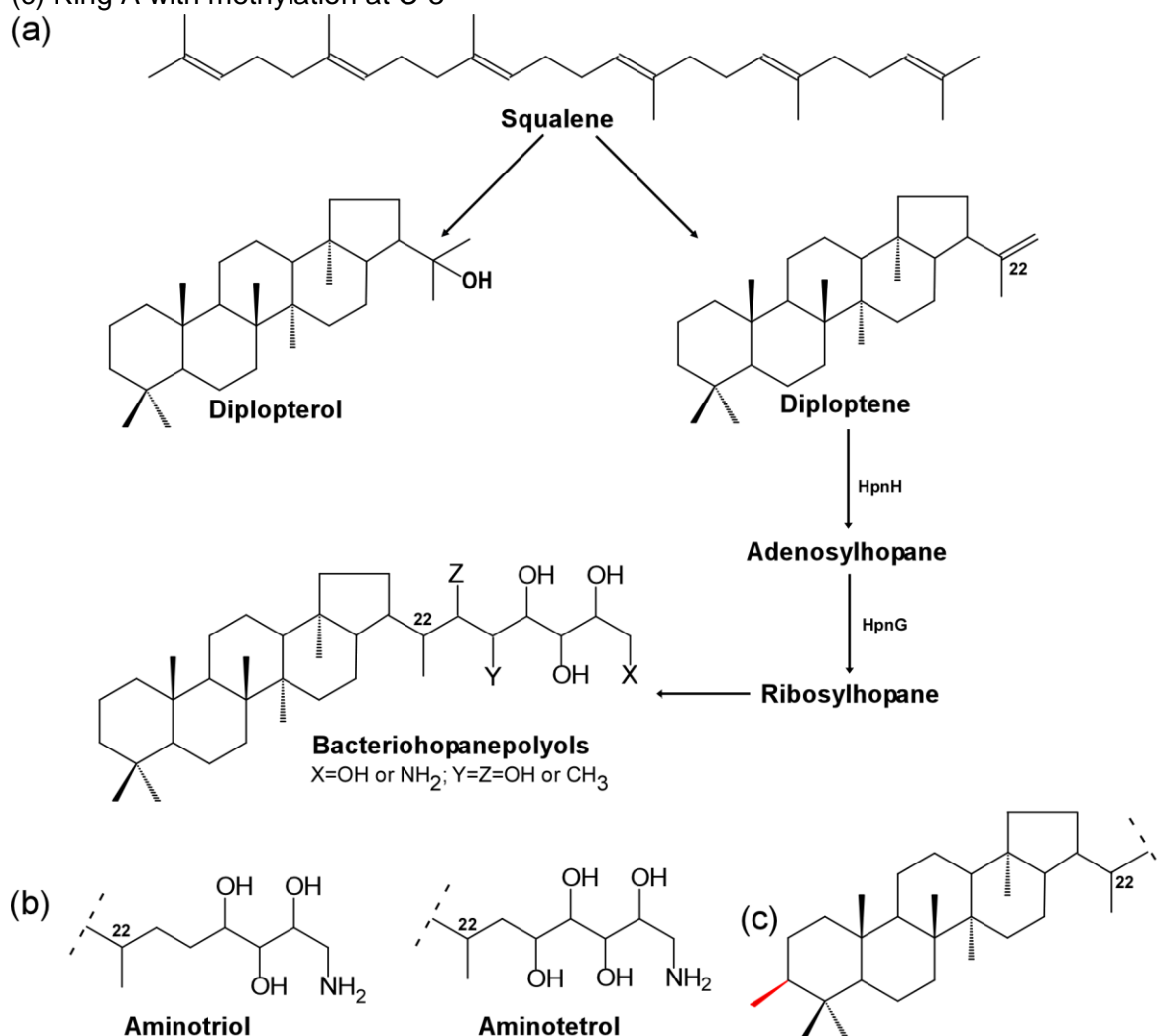


Source: Adapted from Elvert and Niemann (2008); Wei et al. (2016).

HOPANOIDS. Apart from sterols, also hopanoids, which were orphan lipids for many years (see Ourisson & Albrecht, 1992 for a review), were found to be produced by aerobic methanotrophic bacteria. Only in the 1970s it was shown that bacteria are the producers of hopanoids (see Pearson, 2014 for a review). Rohmer et al. (1984) systematically analyzed hopanoids in bacteria, including methanotrophic strains of Gammaproteobacteria (*Methylomonas albus*, *Methylomonas methanica*, *Methylococcus capsulatus*), and Alphaproteobacteria (*Methylocystis parvus* and *Methylosinus trichosporium*). In all five strains, bacteriohopanepolyols (BHPs) were identified. In the following years, the list of new BHPs was extended with compounds as for example 3-methylated BHPs (Zundel & Rohmer, 1985) and amino-BHPs

(Neunlist & Rohmer, 1985). In the 1990s, for the first time the stable isotope compositions of steroids and hopanoids of aerobic methanotrophic bacteria were studied, recognizing their characteristic ^{13}C depletion (Summons et al., 1994; Jahnke et al., 1999). Finally, new analytical methods were developed to improve BHP identification using high performance liquid chromatography-mass spectrometry (HPLC-MS Talbot et al., 2001, 2007b, 2007a), to analyze the same strains chosen by earlier workers. In recent years, more and more details were clarified. For example, the genes involved in hopanoid production like the gene *hpnR*, responsible for the C-3 methylation of hopanoids (Fig. 1.5c), have been described (Welander & Summons, 2012).

Figure 1.5 (a) Biosynthetic pathway for hopanoids from squalene. (b) Selected common hopanoids (side chain structures) synthesized by methanotrophic bacteria. (c) Ring A with methylation at C-3

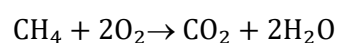


Source: Adapted from Elvert and Niemann (2008); Pearson (2014); Sato et al. (2020).

Like for the synthesis of sterols, hopanoid synthesis requires the isoprenoid precursor squalene (Fig. 1.5a). Squalene is cyclized in a single reaction by squalene–hopene cyclase to yield the pentacyclic backbone. The cyclization reaction yields the simple hopanoids diploptene or diplopterol (Fig 1.5a), or more commonly, is modified by addition of a polyfunctionalized side chain to yield the dominant bacteriohopanepolyols (Fig. 1.5b; Summons et al., 2006; Pearson, 2014). Due to their similar structures and amphiphilic character, it has been proposed that hopanoids are functional equivalents to sterols in eukaryotes (Fig. 1.; Rohmer et al., 1979).

1.1.3 Aerobic methanotrophs in marine cold seep systems

Cold seeps—or cold vents—are submarine fluid expulsions from the subsurface to the seafloor and into the water column (Ceramicola et al., 2018). The composition of fluids can vary, but the majority of cold seeps are characterized by venting fluids rich in methane (either of biogenic or thermogenic origin; Ceramicola et al., 2018). The high methane concentrations is the reason why cold seeps are often referred to as methane seeps, although a lesser proportion of other gases (e.g., hydrogen sulfide, carbon dioxide and C₂ to C₄ hydrocarbons) are expelled as well (Krause et al., 2017; Ceramicola et al., 2018). Methane seeps are the focus of intensive research because of the global warming potential of methane (Buffett & Archer, 2004; Archer et al., 2009; Suess, 2010; Biastoch et al., 2011; Howarth et al., 2011; Ceramicola et al., 2018). Cold seeps occur both along passive and active continental margins, where methane seepage is driven mainly by high pore pressures induced by fast burial and continuous accumulation of gases and fluids (Karstens et al., 2018; Ma et al., 2021). Further, they are associated with typical geological features, as for example, precipitation of authigenic carbonates, as well as the formation of gas hydrates, pockmarks, and mud volcanoes. Cold seeps have been documented at numerous prominent sites worldwide (e.g., the Gulf of Mexico, South China Sea, the Hydrate Ridge, the eastern Black Sea, the eastern Mediterranean, the Cascadia margin; see Ma et al., 2021 for a review). They are of major importance because of the potential impact of methane carbon transfer from long-term storage on the seafloor into the seawater and the atmosphere (Joseph, 2017). Also, the microbial oxidation of the released methane to carbon dioxide, leads to changes in the ocean chemistry, such as ocean acidification (Equation 1.1; Joseph, 2017).



Eq. 1.1

Cold seeps harbor a diversity of distinctive microbial communities that gain energy or carbon especially from methane (Fig. 1.6; Emil Ruff, 2020), oxidizing the gas in the sediment before it reaches the overlying water column and the atmosphere (Ciais et al., 2013). The major biogeochemical process removing methane at marine seeps is the sulfate-driven anaerobic oxidation of methane (AOM; Boetius et al., 2000), performed under anoxic conditions by a consortium of anaerobic methane-oxidizing archaea (ANME) and sulfate-reducing bacteria (Equation 1.2; Hinrichs et al., 1999; Thiel et al., 1999; Hinrichs & Boetius, 2002; Orphan et al., 2002; Niemann et al., 2006). This reaction produces bicarbonate (HCO_3^-), increasing alkalinity and favoring the precipitation of authigenic carbonates (Equation 1.3; Peckmann & Thiel, 2004), which typically preserve signatures of the microbial communities. The methane that is not oxidized by AOM continues its upward movement through the sediments, where methanotrophic bacteria oxidize it under aerobic conditions, contributing to different degrees to local methane consumption (Niemann et al., 2006; Lösekann et al., 2007; Tavormina et al., 2008).

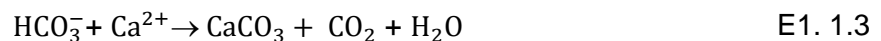
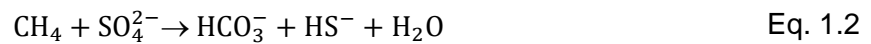
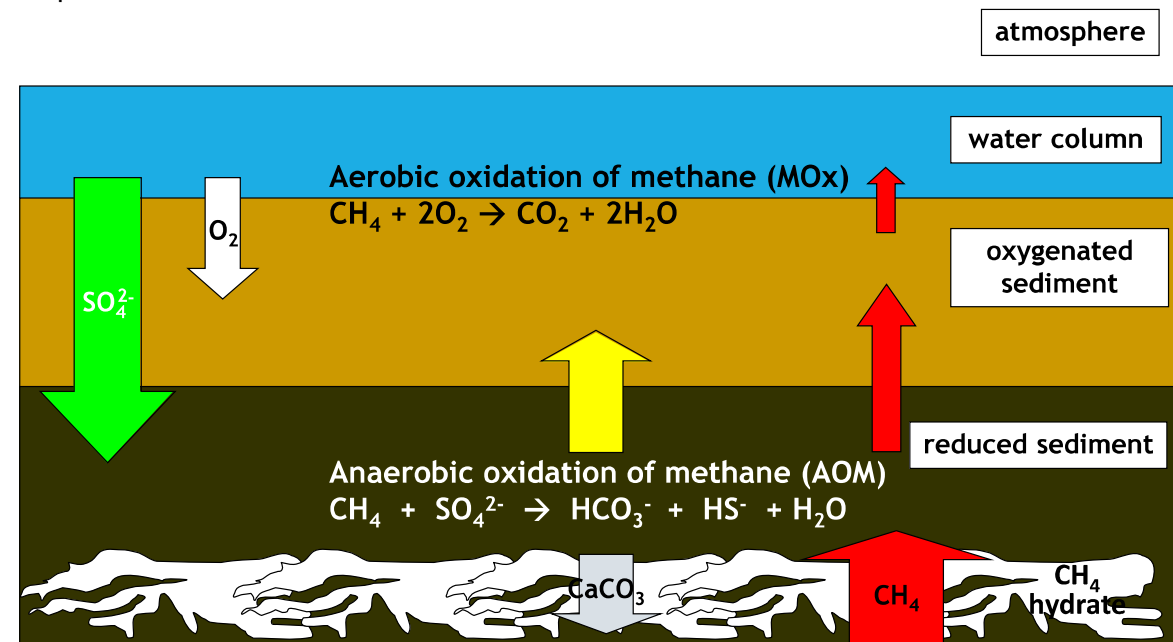


Figure 1.6 Schematic overview of the microbial metabolisms consuming methane at seeps



Source: IFM-GEOMAR.

Aerobic methanotrophs at methane seeps are found in the upper, mostly oxic sediment layers, often occurring in sediments not covered by microbial mats of sulfur-oxidizing bacteria—where the oxygen is consumed before it penetrates the sediment— (Sommer et al. 2010; Ruff et al. 2013; Thurber et al. 2013). Other settings where aerobic methanotrophy occurs are in sediments that are frequently disturbed, allowing oxygen penetration, such as the active centers of mud volcanoes (Niemann et al. 2006; Felden et al. 2010, 2013). However, the occurrence of aerobic methanotrophs has been reported also in hypoxic and anoxic/sulfidic layers at methane seeps (Lösekann et al. 2007; Pachiadaki et al. 2010; Roalkvam et al. 2011; Ruff et al. 2013), and even in the anoxic water column of the Black Sea (Blumenberg et al. 2007), indicating that these organisms can also adapt to low-oxygen and high-sulfide conditions. Seep ecosystems seem to harbor mainly Type I methanotrophs, although Type II methanotrophs have been reported in the Black Sea water column, accounting for up to 10% of the methanotrophic community (Durisch-Kaiser et al., 2005). Moreover, symbionts of mussels and sponges performing aerobic methane oxidation are also common in seep ecosystems (Kellermann et al., 2012; Rubin-Blum et al., 2019). In the symbiotic relationship, the animals harbor the methanotrophic bacteria in specialized tissues and provide them with oxygen and methane and, in return, the bacteria provide reduced organic carbon compounds for their hosts (Rubin-Blum et al., 2019).

1.2 Research questions and hypotheses

Aerobic methanotrophic bacteria are among the bacteria that produce characteristic patterns of lipid biomarkers. Not only they contain hopanoids, which are only produced by few bacteria, they also synthesize sterols (Summons et al., 2006). These two groups of cyclic terpenoids are stable and resistant against degradation and they have been identified even in very old rocks (Peters et al., 2004a). Some of them have been assigned to aerobic methanotrophs because of 4-methylations in sterols and 3-methylations in hopanoids (Welanders & Summons, 2012; Wei et al., 2016). Although a wealth of information has been gathered over the last centuries about steroids and hopanoids in aerobic methanotrophic bacteria, most of the studies have been done on the same few cultures. Besides hopanoids and sterols, diagnostic biomarkers of aerobic methanotrophs include a suit of unsaturated and monounsaturated fatty acids with double bond positions at $\omega 5$, $\omega 7$ and $\omega 8$, the last one being unique for aerobic methanotrophs (Hanson & Hanson, 1996).

Interestingly, lipid biomarkers of aerobic methanotrophs have been found in modern methane-seep carbonates (Birgel et al., 2011; Himmler et al., 2015), but their pattern suggests Type II methanotrophs as source organisms (e.g., Jahnke et al., 1999), although this group of bacteria is unknown from the marine realm. More recently, Rush et al. (2016) examined the BHPs inventory of five Type I methanotroph strains from marine and hypersaline environments (*Methylomarinum vadi* IT-4, *Methylomarinovum caldicuralii* IT-9, *Methylomarinovum* sp. IN45, *Methylomicrobium alcaliphilum* and *Methylomicrobium kenyense*) finding marked differences in their distribution of BHPs. Not all the strains produced aminopentol, until then a compound considered to be a characteristic biomarker of type I methanotrophs (cf. Talbot & Farrimond, 2007). Furthermore, marine sediments from methane-influenced environments were also analyzed and did not contain significant amounts of aminopentol, revealing important limitations in the use of this biomarker as tracer of marine aerobic methanotrophy (Rush et al., 2016). One of the major aims of this project was the cultivation of strains of aerobic methanotrophic bacteria at optimal and varying conditions, which might pose stress to the strains. The chosen strains (*Methylotuvimicrobium alcaliphilum* and *Methylotuvimicrobium kenyense*) are most likely closely related to marine strains regarding their phylogenetic positions or environmental tolerance. These strains can tolerate high salinity and alkalinity, such as the aerobic methanotrophs at marine methane seeps, but also in hypersaline environments. Do specific aerobic methanotrophic bacteria produce different hopanoid distribution at varying conditions? Can Type I methanotrophs produce signatures similar to those of Type II methanotrophs? This research helps to better understand the biomarker record of seep carbonates, which formed at high alkalinities and commonly contain unusual patterns of lipids of aerobic methanotrophs. Learning more about the abilities and tolerances of aerobic methanotrophs from cultures will help to interpret biomarker patterns in the rock record with more confidence and to understand the constraints for aerobic methanotrophy at marine methane seeps and other highly alkaline environments.

One further interesting detail of the lipid inventory of aerobic methanotrophs was recognized when tetrahymanol was found as a lipid biomarker in aerobic methanotrophic bacteria (Banta et al., 2015). This finding is of interest for two reasons. First, tetrahymanol or its degradation product gammacerane are commonly recognized in ancient and modern organic-rich sediments and were commonly assigned to ciliates (Werne et al., 2002 and references therein), which are feeding on

bacteria at oxic-anoxic interfaces. Later, anoxygenic phototrophic bacteria were also recognized as potential producers (Rashby et al., 2007). Interestingly, aerobic methanotrophic bacteria are also common at oxic-anoxic interfaces, revealing that in many instances aerobic methanotrophs may have been the producers of tetrahymanol too, not undermining the concept that tetrahymanol and gammacerane are biomarkers for water-column stratification (Sinninghe Damsté et al., 1995a). Moreover, tetrahymanol and gammacerane were also found at modern methane seeps (Werne et al., 2002; Birgel et al., 2011; Himmler et al., 2015) and in ancient methane-seeps carbonates (Sandy et al., 2012). In the latter environment, tetrahymanol revealed strong ^{13}C depletions, often similar to those of hopanoids and steroids in the same samples. Such a pattern may be still explained by the occurrence of bacterivorous ciliates, but aerobic methanotrophic bacteria have now to be considered as another potential source of tetrahymanol. This cultivation-based study tests if ^{13}C -depleted tetrahymanol and gammacerane can be used as proxies for aerobic methanotrophy and reveals the limitations of this concept.

Furthermore, the study of the carbon stable isotope signatures of cyclic terpenoids derived from aerobic methanotrophs helped to better understand signatures found in the environment. The current shortcomings in the concept of using carbon isotope signatures of cyclic terpenoids relies on few studies that examined only two strains of Type I (*M. capsulatus*) and II (*M. trichosporium*) methanotrophs, respectively (Summons et al., 1994; Jahnke et al., 1999). These strains have been the “workhorse” organisms for researchers studying carbon stable isotope signatures of methanotrophic bacteria. It is still common sense among many organic geochemists that methane oxidation is necessarily leading to strong ^{13}C depletions., except for Type II methanotrophs, as they take up not only methane but also carbon dioxide. Interestingly, there are many reports on pentacyclic terpenoids of aerobic methanotrophic bacteria with rather high $\delta^{13}\text{C}$ values (Birgel et al., 2011; Kellermann et al., 2012), although Type II methanotrophs are not known from marine environments. Either Type II methanotrophs after all exist in the marine realm or Type I methanotrophs are capable to produce less ^{13}C -depleted lipids than known. Thus, the consideration of carbon stable isotopes in this culturing-based study attempts to better understand the carbon isotope signatures found in modern environments and in the rock record.

Finally, the role of aerobic methanotrophs in the marine environment demands further research. Aerobic methanotrophy has been proposed as one of the mechanisms that

induce corrosion of authigenic carbonates in methane seeps due to its potential to lower the pH and promote carbonate dissolution (Matsumoto, 1990; Himmler et al., 2011). However, the influence of aerobic methanotrophy on carbonate dissolution has received little attention. Another focus of the thesis was a carbonate corrosion experiment at a modern marine cold seep (Congo deep sea channel, REGAB seep field). Carbonates exposed to seepage for 2.5 years were analyzed thoroughly for signatures of microbioerosion, using scanning electron microscopy and the dominant microbial community was assessed using a combination of 16S rRNA assays and lipid biomarker analyses. Do aerobic methanotrophs represent a relevant process in dissolution of carbonate at marine seeps? This carbonate experiment gives new insights on the role of aerobic methanotrophy and microbial processes in the corrosion of carbonate at marine methane seeps.

1.3 Objectives and structure

The aim of this research project is to increase the knowledge on the lipid biomarker inventory of aerobic methanotrophic bacteria regarding their lipid biomarker patterns and their carbon stable isotopic fingerprints, facilitating the recognition of aerobic methanotrophs in sediments and rocks and linking their occurrence with past environmental conditions and natural processes, such as microbioerosion.

To fulfil this objective and advance the biomarker concept for this important group of methane-consuming bacteria, the thesis has been structured in five chapters:

- Chapter I presents an examination of the most relevant aspects related to aerobic methanotrophy, the biomarker concept and marine methane seeps as host environments of aerobic methanotrophs, needed to understand the questions raised in the scientific topic.
- Chapter II analyzes the cyclic terpenoid inventory and compound-specific carbon isotopic composition of two strains of Type I methanotrophs (*Methylovimicrobium alcaliphilum* and *Methylovimicrobium kenyense*), which can tolerate alkalinity and salinity conditions similar to those typifying marine methane seeps. Furthermore, the range of compound-specific isotope compositions of various terpenoids is studied in modern and ancient seep deposits to use the fractionation between methane and aerobic methanotrophy biomarkers to help identify the type of aerobic methanotrophs that dwelled

seeps. This chapter corresponds to the first manuscript of the thesis entitled “Carbon stable isotope patterns of cyclic terpenoids: A comparison of cultured alkaliphilic aerobic methanotrophic bacteria and methane-seep environments” (published in *Organic Geochemistry* 139, 103940, 2020).

- Chapter III assesses the effect of changing conditions on the composition and abundance of pentacyclic triterpenoids synthesized by the Type I methanotroph *Methylotheobacterium alcaliphilum*, to better understand the scope and limitations of aerobic methanotrophy in haloalkaline environments and the significance of environmental factors for bacterial lipid production. This chapter corresponds to the second manuscript of the thesis entitled “Effect of varying conditions in the pentacyclic triterpenoid inventory of aerobic methanotrophic bacteria” (published in *Extremophiles* 25, 285-299, 2021).
- Chapter IV4 deals with a carbonate corrosion experiment at a modern marine cold seep (REGAB seep field, off Congo). Petrography of the extensive corrosion patterns documented for carbonates exposed to active methane seepage, combined with 16s rRNA and lipid biomarker analyses, helps to assess the microbial communities colonizing the surface of the corroded carbonates and gives new insights on the role of aerobic methanotrophy in the microbioerosion of carbonate at methane seeps. This chapter corresponds to the third manuscript of the thesis entitled “A carbonate corrosion experiment at a marine methane seep: The role of aerobic methanotrophic bacteria” (In preparation, to be submitted to *Geobiology*).
- Chapter V: presents the main outcomes and perspectives of the research work.
-

2. Chapter II

Carbon stable isotope patterns of cyclic terpenoids produced by aerobic methanotrophic bacteria

This chapter has been published as: Cordova-Gonzalez, A., Birgel, D., Kappler, A., & Peckmann, J., 2020. Carbon stable isotope patterns of cyclic terpenoids: A comparison of cultured alkaliphilic aerobic methanotrophic bacteria and methane-seep environments. *Organic Geochemistry*, 139, 103940. DOI: 10.1016/j.orggeochem.2019.103940

2.1 Abstract

Aerobic methanotrophic bacteria are known to synthesize a variety of cyclic terpenoids, which are typified by ^{13}C -depleted, methane-derived carbon. This peculiarity facilitates identification of methanotroph biomarkers in natural samples. However, the current biomarker database does not always allow biomarker patterns of marine samples to be assigned to the different types of aerobic methanotrophs. To overcome this shortcoming, the carbon stable isotope composition of cyclic terpenoids of two strains of the Type I methanotroph genus *Methylomicrobium* is analyzed herein. Other than aerobic methanotrophs used for biomarker studies in the past, these two strains deriving from soda lake environments are able to tolerate the conditions typifying marine environments including high alkalinity and salinity. The cyclic terpenoid inventory of the two strains comprises 4-methyl steroids, 3-methyl and desmethyl bacteriohopanepolyols (aminotetrol and aminotriol), and tetrahymanol, all of which are ^{13}C -depleted. The average carbon isotope fractionation between methane

and the respective lipid ($\Delta\delta^{13}\text{C}_{\text{terpenoid-methane}}$) is found to be -25‰ for *M. kenyense* and -16‰ for *M. alcaliphilum*. These data shed new light on the previously reported compound and carbon stable isotope patterns of cyclic terpenoids from methane-seep environments. Particularly, ^{13}C -depleted tetrahymanol and gammacerane are reinterpreted as biomarkers of aerobic methanotrophic bacteria based on their occurrence in methane-seep deposits in association with other biomarkers of aerobic methanotrophs. The use of $\delta^{13}\text{C}$ values of anaerobic methane-oxidizing archaea (ANME) lipids for the reconstruction of the isotopic composition of parent methane allows us to calculate the $\Delta\delta^{13}\text{C}_{\text{terpenoid-methane}}$ even for ancient seep environments. With this calculation, Type I and Type II methanotrophs can be discriminated, representing a new approach to better characterize past methanotrophy at seeps and possibly other marine environments.

2.2 Introduction

Methane is the simplest alkane and among the most abundant organic compounds in the atmosphere. Due to its radiative forcing, it is considered a major contributor to global warming (Myhre et al., 2013). Understanding the biogeochemistry of methane and the processes leading to its formation and consumption are consequently of major interest (Deppenmeier, 2002). Natural sources of methane are rice paddies, cattle, thawing of permafrost, as well as marine cold seeps (Reeburgh, 2007; Lupascu et al., 2014). Marine methane seepage occurs in a variety of geologic settings, including active and passive continental margins (Suess, 2010). Methane at marine seeps can be biogenic, thermogenic, or of a mixed source. Even though seeping methane can reach the atmosphere, a larger fraction of it is already microbially oxidized in the sediment before reaching the overlying water column and atmosphere (Ciais et al., 2013).

The major biogeochemical process removing methane at marine seeps is the sulfate-driven anaerobic oxidation of methane (AOM; Boetius et al., 2000). As methane-rich fluids move upward through sulfate-rich pore water, methane is oxidized under anoxic conditions by a consortium of anaerobic methane-oxidizing archaea (ANME) and sulfate-reducing bacteria (Hinrichs et al., 1999; Hinrichs & Boetius, 2002; Orphan et al., 2002; Birgel et al., 2006a; Niemann et al., 2006). Signatures of the AOM community are typically preserved in authigenic carbonates that form at seeps as a consequence of an increase in alkalinity caused by AOM (Peckmann & Thiel, 2004). Although AOM is the predominant biogeochemical process at seeps, aerobic methane

oxidation (MOx) performed by methanotrophic bacteria contributes to different degrees to local methane consumption (Birgel et al., 2006a; Niemann et al., 2006; Lösekann et al., 2007; Tavormina et al., 2008).

Molecular fossils (i.e., lipid biomarkers) of the microorganisms involved in AOM are typically preserved in seep carbonates as old as Paleozoic, revealing information on the affiliation of microorganisms (Peckmann et al., 1999; Thiel et al., 1999; Birgel et al., 2008). Biomarkers of both AOM-consortia and MOx, especially bacteriohopanepolyols (BHPs) for the latter, have been identified in sediments, authigenic carbonates, and mussel gills from recent seeps (e.g., Birgel et al., 2011; Kellermann et al., 2012; Himmler et al., 2015). In ancient seep deposits, BHPs have not been identified to date, but BHP degradation products including hopanoic acids and hopanes, together with tetrahymanol or gammacerane, and 4-methyl steranes (lanostanes) have been reported (Peckmann et al., 1999, 2004; Birgel et al., 2006b; Sandy et al., 2012; Natalicchio et al., 2015). The capacity of aerobic methanotrophic bacteria to synthesize a variety of cyclic triterpenoids – a group of lipids among the oldest and most ubiquitous compounds on Earth (Taylor, 1984) – facilitates their identification in the rock record. The biosynthesis of cyclic triterpenoids in aerobic methanotrophs is controlled by various cyclases, which catalyze the transformation of the acyclic triterpenoid squalene (C₃₀H₅₀) either to pentacyclic (i.e., chiefly hopanoids) triterpenoids (by squalene-hopene cyclase) or tetracyclic (i.e., steroids) triterpenoids (by oxidosqualene cyclase) (Welander et al., 2010; Wei et al., 2016). Among the pentacyclic triterpenoids, various BHPs have been reported to occur in some bacteria and are commonly accompanied by the C₃₀ hopanoids diploptene and diplopterol (Rohmer et al., 1984; Talbot & Farrimond, 2007).

Aerobic methanotrophic bacteria utilize methane as a sole carbon and energy source. The oxidation of methane by methanotrophs is catalyzed by enzymes known as methane monooxygenases (MMO), which occur, depending on the methanotroph species, either in a particulate membrane-bound form (pMMO) or a cytoplasmic soluble form (sMMO) (Hanson & Hanson, 1996; Bowman, 2006). Aerobic methanotrophs are classified into three groups based on the used carbon assimilation pathway (i.e., Type I, Type II, Type X; Hanson & Hanson, 1996). The lipid biomarker inventories of Type I and II methanotrophs have been detailed by (Talbot et al., 2001). These authors reported characteristic BHP patterns for Type I (dominated by aminopentol) and Type II methanotrophs (dominated by aminotetrol). Type I methanotrophs are known to show great versatility in terms of adaptation to different

environmental conditions and occur in terrestrial, aquatic, and marine ecosystems, whereas Type II methanotrophs are apparently less versatile and are believed to be restricted to terrestrial habitats (Knief, 2015). However, Birgel et al. (2011) and Himmler et al. (2015) reported BHP patterns of seep carbonates that rather point to Type II methanotrophs as source organisms. In contrast, the occurrence of 4-methyl steroids at some ancient (e.g., Peckmann et al., 1999, 2004; Birgel & Peckmann, 2008) and modern seeps (Elvert & Niemann, 2008; Bouloubassi et al., 2009) has been interpreted to reflect the former presence of Type I methanotrophs, because Type I and X methanotrophs are unique in synthesizing steroids among Bacteria (e.g., Bouvier et al., 1976; Schouten et al., 2000).

The putative occurrence of Type II methanotrophs at marine seeps is not the only inconsistency between reported biomarker patterns of cultures of aerobic methanotrophs and environmental samples. Rush et al. (2016) demonstrated that some Type I methanotrophs rather produce a BHP pattern typified by the dominance of aminotriol, while aminopentol, which is considered specific to Type I methanotrophs according to culture studies (e.g., Neunlist & Rohmer, 1985; Talbot et al., 2001), is absent. In methane-affected sediments and carbonates, aminotetrol and aminotriol are most common, but aminopentol has not been reported (Birgel et al., 2011; Himmler et al., 2015). In fact, the only known marine sediments with abundant aminopentol are characterized by high riverine input; in this case aminopentol is rather derived from soil methanotrophs (Wagner et al., 2014; Spencer-Jones et al., 2015).

The difficulties in assigning molecular fossils of aerobic methanotrophs from seep environments to the three types of methanotrophic bacteria do not end with molecular patterns but continue with compound-specific carbon stable isotope patterns. The different types of aerobic methanotrophs show significant variations in the $\delta^{13}\text{C}$ values of lipids and the fractionation between carbon source and respective lipid (Summons et al., 1994; Jahnke et al., 1999). Compound-specific isotope compositions provide insights into the origin of the carbon assimilated by microorganisms and can be used to constrain microbial populations and biosynthetic pathways (Hayes et al., 1990). Because the carbon source and predominant microbial populations are dependent on environmental conditions, carbon isotopic compositions can provide information on the biochemical processes occurring in the environment (Hayes, 1993). The carbon isotopic fractionation between methane and methanotroph biomass depends on the isotopic composition of the substrate (i.e., methane), the assimilation pathway, and methane and oxygen availability (Summons et al., 1994). For biomarker applications

on geologic material, the carbon assimilation pathway is particularly relevant, yet difficult to identify. Biomarkers from ancient seep limestones assigned to methanotrophic bacteria are commonly highly depleted in ^{13}C with values as low as -100‰ (e.g., 3-methyl-anhydrobacteriopanetetrol; Birgel & Peckmann, 2008), suggesting significant fractionation relative to the carbon source.

Type I and X methanotrophs terpenoids are typically more ^{13}C -depleted than Type II terpenoids. The fractionation between methane and terpenoids for Type X methanotrophs is approximately -23‰ on average, ranging from -31‰ to -18‰ (cf., Jahnke et al., 1999). Type II terpenoids are less ^{13}C -depleted and fractionation is smaller, ranging from -12‰ to 10‰ (avg.: -1‰ ; Jahnke et al., 1999). Due to ^{13}C depletion of thermogenic and, particularly, biogenic methane, low $\delta^{13}\text{C}$ values of terpenoids from environmental samples can be interpreted as biomarkers of aerobic methanotrophic bacteria (Collister et al., 1992; Himmler et al., 2015). Unfortunately, only very few and exclusively non-marine strains have been used for carbon isotope studies of aerobic methanotrophic bacteria in the past (Summons et al., 1994; Jahnke et al., 1999). As a consequence of this, it is uncertain whether or not the range of carbon isotope fractionations among Type I and Type II methanotrophs is as diverse as their BHP patterns.

Here, two alkaliphilic strains of Type I methanotrophs (*Methylomicrobium kenyense* and *Methylomicrobium alcaliphilum*) have been selected for a carbon stable isotope study, since BHP patterns of the two strains are similar to the patterns reported for recent seep carbonates. *Methylomicrobium kenyense* and *Methylomicrobium alcaliphilum* are non-marine strains, but tolerate high alkalinities and salinities, which are conditions under which seep carbonates are forming (see section 2.5.1). A comparison of the results of our culture experiments with environmental data from 13 seep deposits is provided to better understand the range of compound-specific isotope compositions of various terpenoids from methane-seep environments and to differentiate between Type I and II methanotrophs. We also provide new biomarker data for three seep deposits (Alaminos Canyon, Gulf of Mexico; Makran convergent margin, offshore Pakistan; Marmorito, Miocene, Italy). The 13 modern and ancient methane-seep deposits represent fully marine settings where both AOM and MOx occurred. Known stable isotope fractionations between methane and AOM-biomarkers are used to estimate the isotopic composition of the respective methane sources. The

latter is done to assess if fractionation between methane and MOx biomarkers may allow to identify the type of aerobic methanotrophs that dwelled at seeps.

2.3 Material and methods

2.3.1 Cultures of aerobic methanotrophs

Methylomicrobium kenyense and *Methylomicrobium alcaliphilum* are both Type I methanotrophs. The strains were isolated from surface sediments of highly alkaline soda lakes in Kenya and Russia, respectively (Kalyuzhnaya et al., 2008) and were obtained for this study from the Leibniz Institute DSMZ-German Collection of Microorganisms and Cell Cultures (DSMZ No. 19305 and 19304, respectively). The biomarker inventories of *Methylomicrobium kenyense* and *Methylomicrobium alcaliphilum* were previously described by Banta et al. (2015) and Rush et al. (2016). The cultivation of both strains was done at the Center for Applied Geosciences at the University of Tübingen. Strains were grown in serum bottles using a high salt NMS medium (nitrate mineral salts), containing 1.5% NaCl, 0.1% KNO₃, 0.1% MgSO₄, 0.02% CaCl₂ and trace elements. The gas phase to liquid ratio was 10:1. The pH was adjusted to 9.1 and cultures were incubated at 28 °C and shaken at 200 rpm. The initial gas-mixing ratio was adjusted at methane:air 1:1 (v/v), representing a O₂:CH₄ ratio of 0.21. The conditions of the batch culture provided a closed system, where new nutrients were not added, and waste products were not removed. Only new methane was supplied daily to the experiments to compensate for methane consumption. Cells were harvested by centrifugation as they entered the stationary phase and freeze-dried for posterior analyses. The growth stage was determined by measuring the optical density at 600 nm (OD₆₀₀).

2.3.2 Lipid extraction

Freeze-dried bacterial cells of *M. kenyense* and *M. alcaliphilum* as well as carbonate samples from three methane seep deposits (Alaminos Canyon, Makran convergent margin, Marmorito) available in house (Peckmann et al., 1999; Birgel et al., 2011; Himmler et al., 2015), were extracted and analyzed for their lipid biomarker contents. The samples were extracted with a mixture of dichloromethane/methanol (3:1 v/v) by ultrasonication until the solvents became colorless. An aliquot of the total lipid extract (TLE) was hydrolyzed with 6% KOH in methanol to cleave ester-bond lipids. The neutral lipids were separated by aminopropyl-bonded silica gel column chromatography into fractions using a sequence of solvents with increasing polarity:

(1) hydrocarbons were eluted with *n*-hexane; (2) ketones/esters with *n*-hexane/dichloromethane 3:1 (v/v); and (3) alcohols with dichloromethane /acetone 9:1 (v/v). Alcohols were analyzed as their trimethylsilyl ethers (TMS-derivatives) by reaction with N,O-bis(trimethylsilyl) trifluoroacetamide (BSTFA) in dichloromethane and pyridine (Birgel et al., 2006b) (Birgel et al., 2006b). A second aliquot of TLE was acetylated by reaction with acetic anhydride/pyridine (1:1 v/v) for analyses of BHPs.

2.3.3 Biomarker analysis

All fractions were analyzed via gas chromatography mass spectrometry (GC–MS) using an Agilent 7890 A GC system coupled to an Agilent 5975 C inert MSD mass spectrometer at the University of Vienna. Compounds were separated using a 30 m HP-5 MS UI fused silica capillary column (0.25 mm i.d., 0.25 µm film thickness) and He as a carrier gas. The GC temperature program was: 60 °C (1 min) to 150 °C at 10 °C/min, then 150 °C to 325 °C at 4 °C/min, 35 min isothermal. The identification by GC–MS was based on GC retention times and comparison of mass spectra with published data. Internal standards with known concentrations were added prior extraction for quantitation. Acetylated aliquots of TLE were analyzed by means of liquid chromatography–mass spectrometry (LC–MS) for identification and quantitation of BHPs, as described in Rush et al. (2016). The quantification was done using 5 α -cholestane as internal standard on the GC–FID for aminotriol and was correlated with non GC-amenable aminotetrol on the HPLC–MS (see Eickhoff et al., 2013a for details). For stable carbon isotope measurements of BHPs, an aliquot of underivatized TLE was treated with periodic acid and subsequently with sodium borohydride to cleave the C-C bonds between neighboring polyols and convert the BHPs in GC-amenable hopanols (Rohmer et al., 1984). The periodic acid cleavage procedure yield C₃₂ 17 β (H),21 β (H)-hopanol(bishomohopanol) from tetrafunctionalised BHPs (e.g., aminotriol and bacteriohopanetetrol), C₃₁ 17 β (H),21 β (H)-hopanol (homohopanol) from pentafunctionalised BHPs (e.g., aminotetrol and bacteriohopanepentol), and C₃₀ 17 β (H),21 β (H)-hopanol (hopanol) from hexafunctionalised BHPs (e.g., aminopentol). Finally, the hopanol products were derivatized with BSTFA and pyridine as described for the alcohols (see section 1.3.2).

The identified sterols, hopanoids, and hopanol products of BHPs, were analyzed for their compound-specific isotope compositions on a gas chromatograph (Agilent 6890) coupled with a Thermo Finnigan Combustion III interface to a Finnigan Delta Plus XL isotope ratio monitoring-mass spectrometer (GC–IRM–MS) at the University of

Hamburg. The GC conditions were identical to those mentioned above for GC–MS analyses. The $\delta^{13}\text{C}$ values have been corrected for the addition of carbon during preparation of TMS-derivatives. Each measurement was calibrated using several pulses of carbon dioxide with known isotopic composition at the beginning of the run. Instrument precision was checked with a mixture of *n*-alkanes (C_{15} to C_{29}) of known isotopic composition. The carbon isotope ratios are expressed as $\delta^{13}\text{C}$ values relative to the V-PDB standard. Standard deviation was less than 0.8‰.

2.3.4 Stable carbon isotopic composition of methane

The stable carbon isotopic signature of the methane supplied to the strains *M. kenyense* and *M. alcaliphilum* (–46‰ vs. V-PDB) was determined by means of GC–IRM–MS using a Thermo Fisher Scientific Trace GC connected to a Thermo Fisher Scientific MAT253 Isotope ratio mass spectrometer at the University of Duisburg-Essen.

2.4 Results and compilation of previous data

Results presented here are a combination of new data and published data. First, we present the carbon stable isotope values of lipids of cultured Type I methanotrophs *M. kenyense* and *M. alcaliphilum*. Second, carbon stable isotope values of lipids from ancient and modern methane-seep deposits (13 sites in total), as well as data for Type II (*Methylosinus trichosporium*) and Type X (*Methylococcus capsulatus*) methanotrophs are compiled from published work. We also provide some new data for three out of the 13 seep deposits (Alaminos Canyon, Gulf of Mexico; Makran convergent margin, offshore Pakistan; Marmorito, Miocene, Italy).

2.4.1 Results: Biomarker patterns of *Methylobacterium kenyense* and *M. alcaliphilum*

Contents of cyclic triterpenoids of the Type I methanotrophs *M. kenyense* and *M. alcaliphilum* are provided in Table 2.1 along with corresponding compound-specific $\delta^{13}\text{C}$ values. In cultures of both species, various 4-methyl sterols, (3-methyl) tetrahymanol, and (3-methyl) BHPs were present, whereas squalene and (3-methyl) C_{30} hopanes (diploptene, hop-21-ene) were detected in significant amounts only in *M. kenyense* strains. Tetrahymanol and BHPs are the most abundant compounds in cultures of *M. alcaliphilum*, with an average relative abundance of 44% for the former and 45% for the latter of all cyclic triterpenoids. In cultures of *M. kenyense*, 4-methyl

sterols and C₃₀ hopanols (diplopterol and 3-me-diplopterol) predominate, with relative amounts of 32% and 45%, respectively (Fig. 2.1a). Sterols with one and two methylations at the C-4 position of ring A were found in cultures of *M. kenyense*, while only sterols with two methylations at this position were present in *M. alcaliphilum*, more specifically 4,4-dimethylcholest-8(14)-en-3 β -ol and 4,4-dimethylcholesta-8(14),24-dien-3 β -ol. The former compound is also the most abundant sterol in *M. kenyense* (Fig. 2.1b). The full range of BHPs is not shown, since BHP patterns of the two strains were previously published in Rush et al. (2016). The BHP inventories obtained in this and in other studies (Banta et al., 2015; Rush et al., 2016) include aminotriol (bishomohopanol after periodic acid cleavage) as the most abundant BHP in both species, with 29% in *M. alcaliphilum* and 7% in *M. kenyense* (Fig. 1.1c), followed by minor contributions of 3-methyl aminotriol (3-methyl bishomohopanol after periodic acid cleavage) and aminotetrol (homohopanol after periodic acid cleavage).

In general, the proportion of 3-methyl compounds is low relative to their desmethyl homologues (3-me-diplopterol/diplopterol, 3-me-tetrahymanol/tetrahymanol, and 3-me-BHP/BHP below 1), except for diplopterol in *M. alcaliphilum*, where the 3-methyl homologues are more abundant than the desmethyl homologues (3-me-diplopterol/diplopterol above 1). The terpenoids of both methanotrophs are strongly ¹³C-depleted with $\delta^{13}\text{C}$ values ranging from -65‰ to -60‰ for *M. alcaliphilum* and -77‰ and -65‰ for *M. kenyense* (values relative to V-PDB; Table 2.1; Carbon isotopic composition of single experiments can be found in Table A.1, Appendix A). The $\delta^{13}\text{C}$ values of aminotetrol and aminotriol, measured as their cleavage products homohopanol and bishomohopanol, respectively, range between -63‰ to -60‰ for *M. alcaliphilum*, while BHPs produced by *M. kenyense* are more depleted with respect to the methane source, with ¹³C values ranging from -67‰ to -65‰ . Sterols with two methylations at position C-4 in *M. kenyense* are among the most ¹³C-depleted cyclic terpenoids (-75‰) for this strain. Unfortunately, contents of 4-methyl sterols in *M. kenyense* were too low to obtain isotope values. In *M. kenyense* cultures, the carbon isotope fractionation ($\Delta\delta^{13}\text{C}$) between methane and terpenoids is -25‰ on average, overall ranging from -29‰ (4,4-dimethylcholest-8(14)-en-3 β -ol) to -19‰ (3-me-aminotriol; measured as 3-methyl bishomohopanol); while in *M. alcaliphilum*, the average $\Delta\delta^{13}\text{C}_{\text{terpenoids-methane}}$ is -16‰ , ranging from -19‰ (tetrahymanol) to -14‰ (3-me-aminotriol; measured as 3-methyl bishomohopanol). Isotopic fractionation between methane and lipids is also expressed in terms of the ratio of isotopes using the epsilon (ϵ) notation (Equations 2.1 and 2.2) (Hayes, 1993).

$$\varepsilon = (\alpha_{A/B} - 1)10^3 \quad \text{Eq. 2.1}$$

where

$$\alpha_{A/B} = R_A/R_B = (1000 + \delta_A)/(1000 + \delta_B) \quad \text{Eq. 2.2}$$

$\alpha_{A/B}$ is the fractionation factor, δ_A is the isotopic composition of substrate (methane), and δ_B is the isotopic composition of the respective lipid.

Table 2.1 Contents and $\delta^{13}\text{C}$ values of lipid biomarkers from cultures of aerobic methanotrophs; n.d. = not detected; tr = traces.

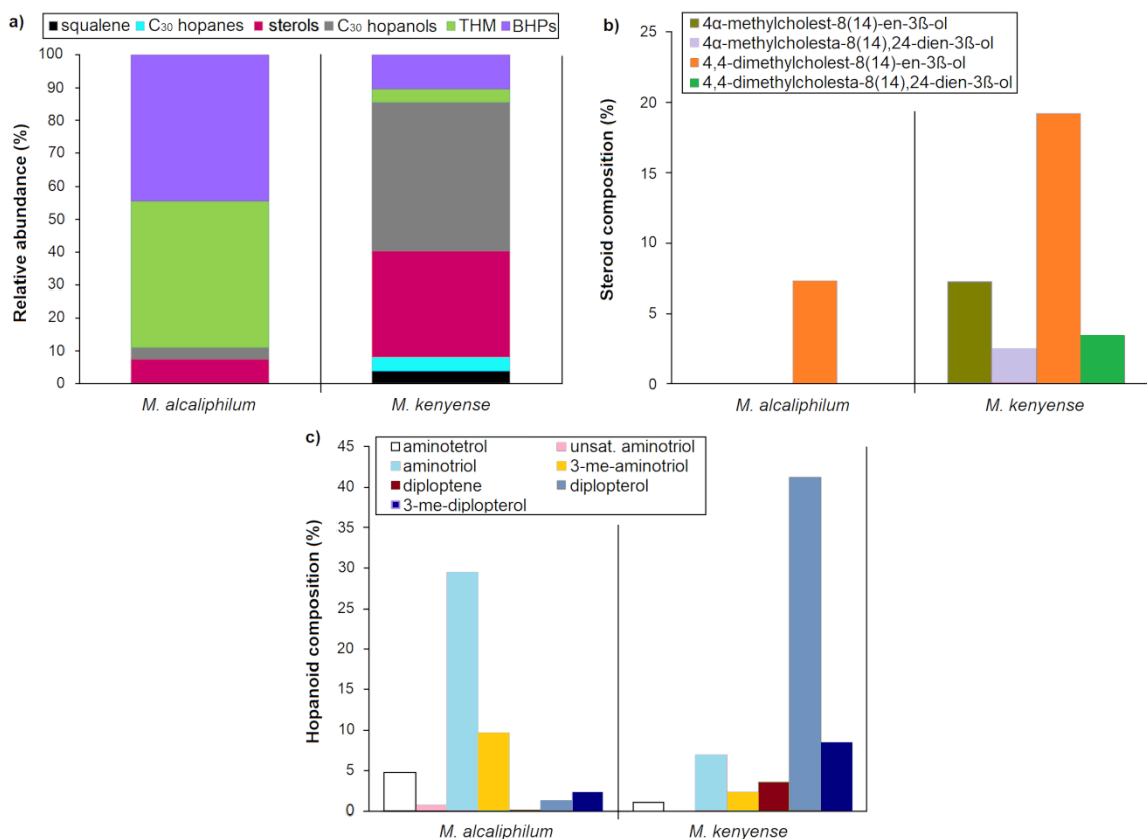
Compound	<i>M. alcaliphilum</i> (n = 3)				<i>M. kenyense</i> (n = 3)			
	Content ($\mu\text{g/g}$)	$\delta^{13}\text{C}$ (‰) V-PDB	$\Delta\delta^{13}\text{C}^*$ (‰)	ε^* (‰)	Content ($\mu\text{g/g}$)	$\delta^{13}\text{C}$ (‰) V-PDB	$\Delta\delta^{13}\text{C}^*$ (‰)	ε^* (‰)
Squalene	n.d.	n.d.			356	-73	-27	
Diploptene	19	tr			257	-71	-25	
Hop-21-ene	10	tr			33	tr		
3-me-diploptene	n.d.	n.d.			22	tr		
3-me-hop-21-ene	n.d.	n.d.			33	tr		
4 α -methylcholest-8(14)-en-3 β -ol	n.d.	n.d.			522	tr		
4 α -methylcholesta-8(14),24-dien-3 β -ol	n.d.	n.d.			179	tr		
4,4-dimethylcholest-8(14)-en-3 β -ol	500	tr			1332	-75	-29	31
4,4-dimethylcholesta-8(14),24-dien-3 β -ol	tr	tr			246	tr		
Diplopterol	85	tr			2934	-74	-28	30
Tetrahymanol	2376	-65	-19	20	291	tr		
3-me-diplopterol	164	tr			380	-77	-31	34
3-me-tetrahymanol	869	-62	-16	17	tr	tr		
C ₃₁ 17 β (H),21 β (H)-hopanol**	346	-62	-16	17	71	-67	-21	23
unsaturated C ₃₂ 17 β (H),21 β (H)-hopanol**	132	tr			n.d.	n.d.		
C ₃₂ 17 β (H),21 β (H)-hopanol**	2189	-63	-17	18	459	-66	-20	21
3-me-C ₃₂ 17 β (H),21 β (H)-hopanol**	723	-60	-14	15	228	-65	-19	20
Sum lipids of aerobic methanotrophy	7413				7343			
Average $\delta^{13}\text{C}$ value		-62	-16			-71	-25	
Average ε value				17				26
3-me-diplopterol/diplopterol	1.9				0.1			
3-me-tetrahymanol/tetrahymanol	0.4				0			
3-me-BHP/BHP	0.3				0.5			

* Values calculated relative to methane source. $\delta^{13}\text{C}_{\text{methane}} = -46\text{‰}$ vs. V-PDB (n=5).

** Products of periodic acid cleavage procedure; C₃₁ 17 β (H),21 β (H)-hopanol (homohopanol) is derived from aminotetrol, and C₃₂ 17 β (H),21 β (H)-hopanol (bishomohopanol) and 3-methyl C₃₂ 17 β (H),21 β (H)-hopanol (bishomohopanol) are derived from aminotriol and 3-methyl aminotriol, respectively. Lipid structures are shown in Fig. A.1, Appendix A

The differences in fractionations expressed as ε (17 for *M. alcaliphilum* and 26 for *M. kenyense*) and Δ (as absolute values) are only minor (Table 2.1). The ε values provide information on the nature and the environment of bacterial strains, while Δ values reflect isotopic shifts associated with the reworking of organic matter prior to burial and trophic structure, i.e., secondary isotopic fractionations (Hayes, 1993), which makes Δ values more suitable to express carbon isotopic fractionation observed for the various seep sites studied herein. For the above reasons, we have chosen the $\Delta\delta^{13}\text{C}$ notation throughout the discussion for both, culture experiments and methane-seep deposits.

Figure 2.1 Relative contents (in relation to all extracted lipids) of a) lipid biomarkers, b) 4-methylated sterols and c) hopanoids in *M. alcaliphilum* and *M. kenyense*



Notes: TMH = tetrahymanol; BHP = bacteriohopanepolyols. BHPs in 1c) were measured as products of periodic acid cleavage products (aminotetrol yielded homohopanol, aminotriol yielded all bishomohopanol, and 3-me-aminotriol yielded 3-me-bishomohopanol). See also Table 2.1 for details.

2.4.2 New results and compilation of previous data: Biomarker patterns and compound-specific $\delta^{13}\text{C}$ values of aerobic methanotrophs in modern and ancient seep deposits

For a comparison with the cyclic triterpenoid inventories of *M. kenyense* and *M. alcaliphilum*, data from samples of 13 seep provinces are examined, including modern sediments (Haakon Mosby; Niemann et al., 2006; Elvert & Niemann, 2008), subrecent carbonates (Alaminos Canyon 645; Birgel et al., 2011; oxygenated zone of the Makran convergent margin; Himmler et al., 2015), mussel symbionts (*Bathymodiolus brooksi* and *Bathymodiolus childressi*; Jahnke et al., 1995; Kellermann et al., 2012), and various ancient seep deposits spanning in age from Miocene to Jurassic (Marmorito; Peckmann et al., 1999, Pietralunga; 2004; Cold Fork of Cottonwood Creek, Wilbur Springs and Paskenta; Birgel et al., 2006b, Tepee Buttes; 2006a; Zizin; Sandy et al., 2012; Buje; Natalicchio et al., 2015). For all deposits, information on carbon isotope compositions of MOx biomarkers and ANME biomarkers is provided in Table 2.2. For

comparison, this table also includes compound-specific $\delta^{13}\text{C}$ values previously obtained from cultures of Type X (*Methylococcus capsulatus*) and II (*Methylosinus trichosporium*) methanotrophs (Jahnke et al., 1999). For Type X and II methanotrophs, values are calculated considering the expression of the soluble methane monooxygenase enzyme (sMMO), expressed under copper limited conditions, considering that these strains require low levels of copper for growth (Hanson & Hanson, 1996). Molecular probe studies have also shown that sMMO may be the prevalent enzyme form in a wide range of natural environments (McDonald et al., 1995).

4-Methyl steroids

4-Methyl sterols are possibly the most specific biomarkers of aerobic methanotrophic bacteria, because no other organisms are known to synthesize these compounds (Wei et al., 2016). Their characteristic ^{13}C depletion is typically further evidence of methane consumption. Seep environments yielded 4-methyl sterols with average $\delta^{13}\text{C}$ values of -75‰ for sediments of the Haakon Mosby mud volcano (Elvert & Niemann, 2008) and mussel symbionts of *Bathymodiolus childressi* and *B. brooksi* with values of -44‰ and -60‰ , respectively (Kellermann et al., 2012). ^{13}C -depleted 4-methyl sterols were also reported for sediments of Ace Lake, Antarctica (Coolen et al., 2008) and in surface sediments from the REGAB pockmark, an active seep area on the Angola-Congo margin, accompanied by ^{13}C -depleted diploptene, also indicative of aerobic methanotrophy (Bouloubassi et al., 2009). In modern seep carbonates, 4-methyl sterols were only reported for Alaminos Canyon of the Gulf of Mexico with a $\delta^{13}\text{C}$ value of -57‰ (Birgel et al., 2011). Even though 4-methyl sterols seem to be scarce in seep carbonates, they have been found in traces in a Miocene seep carbonate (Marmorito, Italy), but unfortunately $\delta^{13}\text{C}$ values were not obtained due to too low contents (Peckmann et al., 1999). Other than for the Marmorito limestone, 4-methyl sterols were not reported from ancient seep deposits to date. Instead, 4-methyl and 4,4-dimethyl steranes, so-called lanostane and nor-lanostane have been found with isotope values ranging from -86‰ to -73‰ in a Miocene seep carbonate (Pietralunga, Italy) and with values from -47‰ to -46‰ in an Eocene seep carbonate (Buje, Croatia). Lanostanes are considered to represent diagenetic products of C-4 monomethylated and C-4 dimethylated sterols; when found in seep deposits, they are typically accompanied by ^{13}C -depleted hopanoids (Peckmann et al., 2004; Birgel & Peckmann, 2008; Natalicchio et al., 2015). Lanostanes were also detected in Cretaceous seep carbonates from Zizin, Romania, but their contents were too low to

measure isotopic compositions. Since the occurrence of 4-methyl sterols in methane-seep deposits seems to be limited to young deposits, the preservation potential of these compounds is apparently low. Yet, their derivatives (i.e., lanostanes) enable recognition of aerobic methanotrophy in ancient seep environments.

Hopanoids and 3-methyl hopanoids

Although hopanoids, including BHPs and geohopanoids, have commonly been encountered in modern and ancient seep carbonates, it is often unclear if they were synthesized by methanotrophic bacteria. Specific hopanoids including aminotetrol and 3-methyl hopanoids are thought to be produced mainly by Type I methanotrophs; in particular when exhibiting significant ^{13}C depletion, such compounds can be assigned to aerobic methanotrophic bacteria (Welander & Summons, 2012). Aminotetrol and aminotriol have been found in methane-seep carbonates from the oxygenated zone of the Makran accretionary wedge, exhibiting $\delta^{13}\text{C}$ values as low as -75‰ (Himmler et al., 2015) and -70‰ , respectively. A similar pattern was found for seep carbonates from Alaminos Canyon of the Gulf of Mexico, but there aminotetrol (-58‰) and aminotriol (-49‰) were less ^{13}C -depleted. Similarly, aminotetrol ($\delta^{13}\text{C}$: -51‰) and aminotriol (trace amounts) have been observed in the gills of *B. childressi* and only aminotriol ($\delta^{13}\text{C}$: -56‰) in *B. brooksi*. Although the $\delta^{13}\text{C}$ values of BHPs from Alaminos Canyon carbonates and bacterial symbionts are not as low as cyclic terpenoids in some methane-seep deposits, the values are still in accordance with isotope fractionation determined for methanotrophic cultures in this and previous studies (Jahnke et al., 1999). Even less ^{13}C -depleted BHPs (-41‰) supposedly produced by aerobic methanotrophs have been found in recent marine sediments of the Congo deep-sea fan (Talbot et al., 2014). However, in this case accompanying evidence indicated a terrestrial source of BHPs. Sediments of permanently stratified Ace Lake yielded a suite of ^{13}C -depleted BHPs (-73‰ to -31‰ ; Coolen et al., 2008), some of which were interpreted to have been derived from Type I methanotroph endosymbionts of seep mussels.

BHPs are absent in methane-seep carbonates older than Neogene or are present in trace amounts only. They tend to be transformed during diagenesis and burial (Sinninghe Damsté et al., 1995b). Nevertheless, anhydrobacteriohopanetetrol (anhydroBHT), which is considered to represent a diagenetic product of bacteriohopanetetrol (BHT) via dehydration of the side chain (Bednarczyk et al., 2005; Saito & Suzuki, 2007), and its 3-methyl homologue were found in a Miocene seep

limestone (Marmorito limestone), revealing $\delta^{13}\text{C}$ values of -42‰ and -100‰ , respectively (Birgel & Peckmann, 2008). From the same deposit, C_{32} hopanoic acid, 3-me C_{32} hopanoic acid, and C_{32} hopanol were reported (-75‰ , -100‰ and -47‰ , respectively). These compounds are considered to represent oxidative degradation products of BHPs, specifically those of tetrafunctionalised BHPs such as aminotriol and BHT (Innes et al., 1997; Farrimond et al., 2002). Although, anhydroBHT and C_{32} hopanol may principally derive from aerobic methanotrophs, their only moderate ^{13}C depletion in comparison to other methanotroph biomarkers found in the Marmorito limestone, did not allow assignment to this group of bacteria. In contrast, ^{13}C -depleted hopanoic acids (-74‰) as well as minute amounts of a 3-methyl homologue (no $\delta^{13}\text{C}$ data) from another Miocene seep limestone (Pietralunga) have been assigned to aerobic methanotrophic bacteria based on the low $\delta^{13}\text{C}$ values of hopanoic acids (Peckmann et al., 2004; Birgel & Peckmann, 2008).

In Cretaceous and Jurassic seep carbonates from California only hopanoids without C_3 methylations, yet with low $\delta^{13}\text{C}$ values from -65‰ to -55‰ were found. Since no 4-methyl sterols or their degradation products were found in the Californian carbonates, the biomarkers have not been considered as unequivocal evidence of aerobic methanotrophy since these compounds could have been derived from anaerobic bacteria too (Birgel et al., 2006b). Cretaceous seep limestones from the Western Interior Seaway yielded a series of unusual 8,14- C_{34} -secohexahydrobenzohopanes with extremely low $\delta^{13}\text{C}$ values (averaging -109‰ ; Table 2.2) and 8,14- C_{35} -secohexahydrobenzohopanes (no $\delta^{13}\text{C}$ data; Birgel et al., 2006a). These compounds have previously only been reported from oils and sediments of evaporitic, carbonate-rich, and anoxic environments (Connan & Dessort, 1987). 8,14- C_{35} -secohopanes series are believed to derive from BHT via a sequence of dehydration and cyclisation reactions, with subsequent degradation of the side chain involved in the formation of the lower homologs (Hussler et al., 1984).

Tetrahymanol and gammacerane

Tetrahymanol has been reported to occur in many seep carbonates where also other biomarkers of aerobic methanotrophic bacteria have been recognized (Peckmann et al., 1999, 2004; Birgel et al., 2011; Himmler et al., 2015). Gammacerane, the diagenetic product of tetrahymanol, has also been found in a number of seep deposits (Peckmann et al., 2004; Birgel et al., 2006b; Sandy et al., 2012; Natalicchio et al., 2015). For all sites, tetrahymanol and gammacerane are strongly ^{13}C -depleted,

exhibiting $\delta^{13}\text{C}$ values similar to the associated hopanoids and sterols (Table 2.2). With the recognition of the presence of tetrahymanol in aerobic methanotrophic bacteria (Banta et al., 2015), the occurrence of tetrahymanol and gammacerane at seeps and in ancient seep deposits needs to be re-evaluated (see Discussion).

Table 2.2 Average compound-specific $\delta^{13}\text{C}$ values (‰ V-PDB) of lipids from four species of aerobic methanotrophs bacteria, two mussel symbionts, one sediment sample from Haakon Mosby (H.M.), two subrecent carbonates (A.C. = Alaminos Canyon 645, Makr = Makran) and eight ancient seep carbonates; Pietr = Pietralunga (Miocene), Marm = Marmorito (Miocene), Buje (Eocene), Tepee Buttes (Late Cretaceous), C.C. = Cold Fork of Cottonwood Creek (Early Cretaceous), W.S. = Wilbur Springs (Early Cretaceous), Zizin (Early Cretaceous), PSK = Paskenta (Late Jurassic); tr = traces

	Type I/X			Type II	Sub-recent to recent methane-seep deposits					Ancient methane-seep deposits (n=1)				^k C.C.	^h W.S.	^l Zizin	^k PSK				
	<i>M. alcaliphilum</i>	<i>M. kenyense</i>	<i>M. capsulatus</i> [^]	<i>M. trichosporium</i> [^]	<i>B. childressi</i>	<i>B. brooksi</i>	H.M.	A.C. (n=3)	Makr (n=5)	Pietr	Marm	Buje	Tepee Buttes								
<i>Aerobic methanotrophs (MOx)</i>																					
Tetrahymanol	-65	tr						-59	-72	-87 ^g	-92										
3-me-THM	-62	tr																			
Gammacerane										-81 ^g		tr ^l		-68 ^m	tr ^m	-90 ^{###}	tr ^m				
Lanostane										-73 ^{a,h}		-46 ^l									
Nor-lanostane										-86 ^{a,h}		-47 ^l					tr ^l				
4-methyl sterol*					-44 ^b	-60 ^b	-75 ^c	-57 ^e			tr ^j										
4,4-dimethylsterol**	tr	-75																			
Diplopterol	tr	-74							-75 ^c	-53 ^e	-70 ^f										
3-me-diplopterol		-77																			
Hop-17(21)-ene																					
C ₃₂ 17 β (H),21 β (H)-hopanol										-59	-78 ^f										
C ₃₂ 17 β (H),21 β (H)-hopanoic acid										-57 ^e	-82 ^f										
3-me-C ₃₂ 17 β (H),21 β (H)-hopanoic acid																					
Anyhydrobacteriohopanetetrol																					
3-me-anhydro bacteriohopanetetrol																					
C ₃₀ 17 β (H),21 β (H)-hopanol****			-58 ^a																		
3-me-C ₃₀ 17 β (H),21 β (H)-hopanol****			-54 ^a																		
C ₃₁ 17 β (H),21 β (H)-hopanol***	-62	-67		-37 ^a		-51 ^b			-58 ^e	-75 ^f											
3-me-C ₃₁ 17 β (H),21 β (H)-hopanol***			-51 ^a																		
C ₃₂ 17 β (H),21 β (H)-hopanol****	-63	-66		-37 ^a		-56 ^b			-49 ^e	-70											
3-me-C ₃₂ 17 β (H),21 β (H)-hopanol****	-60	-65																			
Hopane														-49 ^{###}	-55 ^m	-64 ^m	-60 ⁿ	-60 ^m			
Homohopanes														-44 ^{###}	-65 ^m	-65		tr ^m			
C ₃₄ -secohexahydrobenzohopane														-109 ^k							
MOx average	-62	-71	-56	-37	-48	-58	-75	-56	-75	-80	-90	-52	-109	-63	-65	-60	-60				
<i>Anaerobic methanotrophs (AOM)</i>																					
Crocetane/phytane										-83 ^{o+}	-106 ^f			-50 ^{a,h}	-33 ^{h#}	-98 ^l	-82 ^h	-85 ^m	-98 ^m	-86 ⁿ	-47 ^{m+}
Pentamethylsane (PMI)										-105 ^d	-92 ^e	-120 ^f		-105 ^{g,h}	-82 ⁱ	-111 ^l	-118 ^h	-94 ^m	-101 ^m	-61 ^{##}	-122 ^m
Biphytane														-94 ^h	-109 ^j	-102 ^h	-81 ^m	-105 ^m	-92 ⁿ	-101 ^m	
Acyclic biphytanic diacid														-110 ^j	-96 ⁱ						
Monocyclic biphytanic diacid														-110 ^j	-109 ^j						
Bicyclic biphytanic diacid														-109 ^j	-115 ^j						
Archaeol										-98 ^d	-107 ^e	-119 ^f		-52 ^{##}	-90 ⁱ						
sn2-hydroxyarchaeol										-107 ^d	-108 ^e	-118 ^f		-108 ^h	tr ^h						
AOM average										-103	-102	-116		-108	-98	-106	-101	-87	-101	-89	-112

Notes: tr = traces.

^aJahnke et al. (1999); ^bKellermann et al. (2012); ^cElvert and Niemann (2008); ^dNiemann and Elvert (2008); ^eBirgel et al. (2011); ^fHimmler et al. (2015); ^gPeckmann et al. (2004); ^hBirgel and Peckmann (2008); ⁱBirgel et al. (2008a) ^jPeckmann et al. (1999); ^kBirgel et al. (2006a); ^lNatalicchio et al. (2015); ^mBirgel et al. (2006b); ⁿSandy et al. (2012). *Comprise 4- α -methylcholest-8(14)-en-3 β -ol and 4- α -methylcholesta-8(14),24-dien-3 β -ol. **Comprise 4,4-dimethylcholest-8(14)-en-3 β -ol and 4,4-dimethylcholesta-8(14),24-dien-3 β -ol. ***Products of periodic acid cleavage procedure; C₃₀ 17 β (H),21 β (H)-hopanol (hopanol) and 3-me-C₃₀ 17 β (H),21 β (H)-hopanol (3-methyl hopanol) are derived from aminopentol and 3-methyl aminopentol, respectively; C₃₁ 17 β (H),21 β (H)-hopanol (homohopanol) and 3-me-C₃₁ 17 β (H),21 β (H)-hopanol (3-methyl homohopanol) are derived from aminotetrol and 3-methyl aminotetrol, respectively; and C₃₂ 17 β (H),21 β (H)-hopanol (bishomohopanol) and 3-me-C₃₂ 17 β (H),21 β (H)-hopanol (3-methyl bishomohopanol) are derived from aminotriol and 3-methyl aminotriol, respectively. ⁺Values excluded (coelution with phytane). [#]Values excluded (mixed with non-AOM sources). ^{##}Values excluded (non-MOx sources). [^]values for expression of sMMO; *M. capsulatus* was grown at 37 °C and high methane concentration; *M. trichosporium* was grown at 30 °C and high and low methane and carbon dioxide concentrations. Lipid structures are shown in Fig. A.1, Appendix A

Tetrahymanol and gammacerane

Tetrahymanol has been reported to occur in many seep carbonates where also other biomarkers of aerobic methanotrophic bacteria have been recognized (Peckmann et al., 1999, 2004; Birgel et al., 2011; Himmler et al., 2015). Gammacerane, the diagenetic product of tetrahymanol, has also been found in a number of seep deposits (Peckmann et al., 2004; Birgel et al., 2006b; Sandy et al., 2012; Natalicchio et al., 2015). For all sites, tetrahymanol and gammacerane are strongly ^{13}C -depleted, exhibiting $\delta^{13}\text{C}$ values similar to the associated hopanoids and sterols (Table 2.2). With the recognition of the presence of tetrahymanol in aerobic methanotrophic bacteria (Banta et al., 2015), the occurrence of tetrahymanol and gammacerane at seeps and in ancient seep deposits needs to be re-evaluated (see Discussion).

2.5 Discussion

2.5.1 Cyclic triterpenoids of Type I methanotrophs and their carbon stable isotope composition

The Type I methanotrophs *Methylomicrobium kenyense* and *Methylomicrobium alcaliphilum* are non-marine strains. They are, however, of interest for the study of marine environments, because they are adapted to environmental conditions that are close to those found at marine methane seeps (high alkalinity, high salinity; see Kalyuzhnaya et al., 2008). This makes them good candidates for the reconstruction of environmental conditions – normal marine or higher salinities and high alkalinity – under which carbonate minerals precipitate at methane seeps. The analysis of cultures of the two strains revealed the presence of aminotetrol, aminotriol, and 3-me-aminotriol (Table 2.1), as well as the absence of aminopentol – typically the most abundant BHP in Type I methanotrophs (Neunlist & Rohmer, 1985). It has previously been assumed that aminotriol and aminotetrol are predominantly synthesized by Type II methanotrophs (e.g., *Methylosinus trichosporium*), while BHP distributions in Type I and X methanotrophs had been found to be dominated by aminopentol or 3-me-aminopentol with minor contributions of aminotetrol, 3-me-aminotetrol, and aminotriol (Talbot et al., 2001); as for example reported for *Methylococcus capsulatus* (Type X; Jahnke et al., 1999). Talbot et al. (2001) had already found aminotriol and aminotetrol in the Type I methanotroph *Methylomicrobium album*. However, at that time, the results were attributed to a contamination. More recently, Banta et al. (2015) and Rush et al. (2016) studied the lipid inventories of *M. alcaliphilum* and *M. kenyense*, revealing a BHP distribution more typical of Type II methanotrophs. The samples from Rush et

al. (2016) are identical to the samples studied herein. The capability of Type I methanotrophs to produce aminotriol and aminotetrol is of importance to interpret some lipid signatures found in environmental samples, since Type I methanotrophs are consequently possible source organisms when similar biomarker patterns are found in marine environments including methane-seep deposits (cf. Birgel et al., 2011; Kellermann et al., 2012; Himmler et al., 2015).

The sterol inventories of *M. alcaliphilum* and *kenyense* comprise 4,4-dimethyl sterols, confirming the ability of *M. alcaliphilum* (cf. Banta et al., 2015) to produce 4,4-dimethyl sterols with and without unsaturation at the C-24 position. The inventory of sterols of *M. kenyense* also includes 4-dimethyl sterols (Table 2.1). To date, the only species known to produce these sterols in significant amounts other than the strains studied herein are *Methylococcus capsulatus* (Bouvier et al., 1976), *Methylosphaera hansonii* (Schouten et al., 2000), and *Methylobacter whittenbury* (Wei et al., 2016). Jahnke and Nichols (1986) identified 4 α -methyl sterol as the predominant sterol of Type X *M. capsulatus*, and 4,4-dimethyl sterol as the less abundant sterol. However, at low oxygen concentrations, the production of 4,4-dimethyl sterols was found to increase with respect to the total amount of sterols (Jahnke & Nichols, 1986). The authors explained this observation with a higher oxygen requirement for the second demethylation step of lanosterol. This suggests that the production of 4,4-dimethyl sterols as most abundant sterol in our cultures of *M. kenyense* and *M. alcaliphilum* might reflect oxygen limitation. Oxygen limitation may indeed have occurred during the experiments, since oxygen was not replenished. The findings of Banta et al. (2015) and our findings help to expand the knowledge on sterol production in aerobic methanotrophs and allow for a better interpretation of biomarker signatures found in sediments and rocks.

Another interesting outcome of the experiments is the production of tetrahymanol by *M. kenyense* and *M. alcaliphilum* (Table 2.1). Tetrahymanol synthesis by *M. alcaliphilum* has already been reported by Banta et al. (2015). Tetrahymanol and its degradation product gammacerane are pentacyclic triterpenoids commonly used as biomarkers for water-column stratification (Sinninghe Damsté et al., 1995a). In modern methane-seep deposits (Werne et al., 2002; Birgel et al., 2011; Himmler et al., 2015) and at ancient methane-seep carbonates (Sandy et al., 2012) tetrahymanol and gammacerane have been found to show similar $\delta^{13}\text{C}$ values like ANME and MOx biomarkers. Since aerobic methanotrophic bacteria had not been known to produce

tetrahymanol at the time of these studies, it had been suggested these molecular fossils represent input from ciliates. Ciliates are known to inhabit oxic-anoxic interfaces, feeding on bacteria (Werne et al., 2002). Low $\delta^{13}\text{C}$ values of tetrahymanol from seep environments were consequently previously explained by ciliates feeding on methanotrophic bacteria or archaea or AOM-associated sulfate-reducing bacteria, inheriting the isotopic fingerprint of the seep-dwelling prokaryotes. With the recognition of aerobic methanotrophic bacteria as producers of tetrahymanol (Banta et al., 2015; this study), findings of ^{13}C -depleted tetrahymanol in seep environments need to be re-evaluated. Many of the reported occurrences of tetrahymanol and its diagenetic product gammacerane are likely to reflect input from aerobic methanotrophs (e.g., Peckmann et al., 2004; Birgel et al., 2006b, 2011).

The cyclic terpenoids synthesized by *M. kenyense* and *M. alcaliphilum* are found to be strongly ^{13}C -depleted, averaging -69‰ and -62‰ , respectively (Table 2.2). Carbon isotopic fractionation from substrate to lipid for cultures of *M. kenyense* ($\Delta\delta^{13}\text{C}$: -25‰ ; Table 2.3) and *M. alcaliphilum* ($\Delta\delta^{13}\text{C}$: -16‰ ; Table 2.3) is similar to that of the Type X methanotroph *M. capsulatus* ($\Delta\delta^{13}\text{C}$: -21‰ ; Jahnke et al., 1999). Fractionation for Type II *M. trichosporium* ($\Delta\delta^{13}\text{C}$: -2‰) is considerably lower than for Type I and X methanotrophs, varying between -8‰ under high methane conditions and $+5\text{‰}$ at low methane availability (Jahnke et al., 1999). Interestingly, the expression of pMMO (favored under high copper conditions) in both Type X and II methanotrophs seems to produce stronger fractionation; *M. capsulatus* exhibits offsets of up to -31‰ and *M. trichosporium* up to -12‰ at high methane concentrations (Jahnke et al., 1999). At low methane concentrations, *M. trichosporium* expressing pMMO produces cyclic terpenoids that are ^{13}C -enriched relative to the methane source ($\Delta\delta^{13}\text{C}$: $+10\text{‰}$; Jahnke et al., 1999). Various types of aerobic methanotrophs use different carbon assimilation pathways. Type I methanotrophs (Gammaproteobacteria) utilize ribulose monophosphate (RuMP) as primary pathway for formaldehyde assimilation, while Type II methanotrophs (Alphaproteobacteria) use the serine pathway. Type X methanotrophs (Gammaproteobacteria) assimilate formaldehyde using the RuMP pathway like Type I methanotrophs, but also possess enzymes of the serine pathway (Taylor et al., 1981; Hanson & Hanson, 1996; Chistoserdova et al., 2009). The different assimilation pathways result in differences in carbon isotopic fractionation relative to the substrate (i.e., methane), with Type I and X methanotrophs showing greater fractionation (Jahnke et al., 1999).

Table 2.3 Offset of $\delta^{13}\text{C}$ values ($\Delta\delta^{13}\text{C}$) between methane and lipid biomarkers

	Type I/X			Type II	Recent methane-seep deposits					Ancient methane-seep deposits							
	<i>M. alcaliphilum</i>	<i>M. kenyense</i>	^a <i>M. capsulatus</i> [^]	^a <i>M. trichosporium</i> [^]	^b <i>B. childressi</i>	^b <i>B. brooksi</i>	^c H.M.	^d A.C.	^e Makr	^{f,g} Pietr	^{g,h} Marm	ⁱ Buje	ⁱ Tepee Buttes	^k C.C.	^k W.S.	^l Zizin	^k PSK
$\delta^{13}\text{C}_{\text{methane}}$ (measured)	-46	-46	-35	-35	-45**	-45**	-61	-56	-67								
$\delta^{13}\text{C}_{\text{methane}}$ (ANME)*								-52	-66	-58	-68 to -58	-76	-71	-47 to -37	-61 to -51	-59	-72 to -62
$\Delta\delta^{13}\text{C}_{\text{ANME-methane}}$ (measured)								-46	-49								
$\Delta\delta^{13}\text{C}_{\text{ANME-methane}}$ *								-50	-50	-50	-40 to -30	-30	-30	-50 to -40	-50 to -40	-30	-50 to -40
$\Delta\delta^{13}\text{C}_{\text{terpenoid-methane}}$ (measured)	-16	-25	-21	-2	-3	-13	-14	0	-8								
$\Delta\delta^{13}\text{C}_{\text{terpenoid-methane}}$	n.a.	n.a.	n.a.	n.a.	n.a.	n.a.	n.a.			-22	-32 to -22	24	-38	-26 to -16	-14 to -4	-1	2 to 12
$\delta^{13}\text{C}_{\text{lipid biomarkers}}$																	
$\delta^{13}\text{C}_{\text{ANME}}$ (avg.)	n.a.	n.a.	n.a.	n.a.	n.a.	n.a.	-103	-102	-116	-108	-98	-106	-101	-87	-101	-89	-112
$\delta^{13}\text{C}_{\text{terpenoids}}$ (avg.)	-62	-71	-56	-37	-48	-58	-75	-56	-75	-80	-90	-52	-109	-63	-65	-60	-60
ANME							<u>ANME-3</u>	<u>ANME-2</u>	<u>ANME-2</u> ANME-1	<u>ANME-2</u>	<u>ANME-1</u> ANME-2	<u>ANME-1</u>	<u>ANME-1</u>	<u>ANME-2</u> ANME-1	<u>ANME-2</u> ANME-1	<u>ANME-1</u>	<u>ANME-2</u> ANME-1
Aerobic methanotrophy	Type I	Type I	Type X	Type II		Type I	Type I			Type I/X	Type I/X	?	Type I/X	Type I/X			

Notes: H.M. = Haakon Mosby, A.C. = Alaminos Canyon 645, Makr = Makran, Pietr = Pietralunga (Miocene), Marm = Marmorito (Miocene), Buje (Eocene), Tepee Buttes (Late Cretaceous), C.C. = Cold Fork of Cottonwood Creek (Early Cretaceous), W.S. = Wilbur Springs (Early Cretaceous), Zizin (Early Cretaceous), PSK = Paskenta (Late Jurassic). ^aJahnke et al. (1999); ^bKellermann et al. (2012); ^cElvert and Niemann (2008); ^dBirgel et al. (2011); ^eHimmeler et al. (2015); ^fPeckmann et al. (2004); ^gBirgel and Peckmann (2008); ^hPeckmann et al. (1999); ⁱBirgel et al. (2006a); ^jNatalicchio et al. (2015); ^kBirgel et al. (2006b); ^lSandy et al. (2012).

[^] Values for expression of sMMO.

* $\delta^{13}\text{C}_{\text{methane}}$ values were back-calculated using $\delta^{13}\text{C}$ values of AOM biomarkers ($\Delta\delta^{13}\text{C}_{\text{ANME-methane}}$) (Niemann and Elvert, 2008). For deposits with mixed ANME-1 and ANME-2 communities (Marmorito, Cold Fork of Cottonwood Creek, Wilbur Springs, and Paskenta), a range of $\Delta\delta^{13}\text{C}_{\text{ANME-methane}}$ values between -40‰ (average $\Delta\delta^{13}\text{C}$ of ANME-1 and ANME-2 biomarkers) and the $\Delta\delta^{13}\text{C}$ of the predominant ANME community (underlined) was used for calculations. ** Lanoil et al. (2001).

Despite *M. kenyense* and *M. alcaliphilum* strains being phylogenetically closely related (Banta et al., 2015), there are significant differences in the cyclic terpenoid distribution between the strains. *M. alcaliphilum* is dominated by tetrahymanol and BHPs, while 4-methyl sterols and C₃₀ hopanols predominate in *M. kenyense*. The differences in distribution may be related to the presence and length of specific proteins involved in the biosynthesis of these compounds (e.g., Pearson et al., 2007; Banta et al., 2015; Wei et al., 2016). Even though the lipid inventories, especially the BHP patterns, seem to vary among Type I methanotrophic bacteria, their $\Delta\delta^{13}\text{C}$ values appear to be more constant and are consequently a useful tool for differentiation. With tools being developed that allow for the reconstruction of the carbon stable isotope composition of methane in ancient and inactive subrecent seep environments using ANME lipids (Himmler et al., 2015), $\delta^{13}\text{C}$ values evolve as new approach to distinguish biomarkers of Type I and Type II methanotrophs.

2.5.2 Comparison of carbon isotope fractionation patterns

Cultures and methane-seep deposits

The culture experiments conducted herein revealed an average $\Delta\delta^{13}\text{C}_{\text{terpenoids-methane}}$ of -25‰ with an overall range from -31‰ to -19‰ for *M. kenyense*, and an average $\Delta\delta^{13}\text{C}_{\text{terpenoids-methane}}$ of -16‰ with an overall range from -19‰ to -14‰ for *M. alcaliphilum*. Culture experiments of Jahnke et al. (1999) yielded fractionations corresponding to $\Delta\delta^{13}\text{C}_{\text{terpenoids-methane}}$ of -25‰ to -16‰ (avg.: -21‰ , for sMMO; Table 2.3) for Type X *M. capsulatus*, and of -8‰ (high methane) to $+5\text{‰}$ (low methane) (avg.: -2‰ , for sMMO; Table 2.3) for Type II *M. trichosporium*. The same authors showed that fractionation associated with pMMO is higher, varying from -31‰ to -27‰ for *M. capsulatus* and -12‰ (high methane) to $+10\text{‰}$ (low methane) for *M. trichosporium*. The differences in isotopic fractionation ($\Delta\delta^{13}\text{C}$) between terpenoids and the methane source are the result of different carbon assimilation pathways and can therefore be used to differentiate between Type I/X and II methanotrophs.

BHPs and 4-methyl sterols extracted from the gills of *B. childressi* and *B. brooksi* revealed the presence of methanotrophic symbionts (Kellermann et al., 2012). Based on the average $\delta^{13}\text{C}$ value of -58‰ of these terpenoid biomarkers, the $\Delta\delta^{13}\text{C}_{\text{terpenoids-methane}}$ for the *B. brooksi* symbionts was -13‰ given a $\delta^{13}\text{C}$ value of -45‰ of seeping methane (Table 1.3; Lanoil et al., 2001). Although the high abundance of aminotriol agreed with Type II methanotrophs in that case, the $\Delta\delta^{13}\text{C}_{\text{terpenoids-methane}}$ values for the

B. brooksi symbiont lipids rather pointed to Type I/X methanotrophs. Such interpretation is consistent with the new finding that some strains of Type I methanotrophs, such as *M. kenyense* and *M. alcaliphilum*, also produce tetrafunctionalised BHPs, and, therefore, cannot be excluded as possible source organisms. In addition, comparative 16S rRNA sequence analysis confirmed that the gill symbionts in the Gulf of Mexico bathymodiolin bivalves are exclusively Type I/X methanotrophs (Duperron et al., 2007). In the case of the *B. childressi* symbionts, the $\Delta\delta^{13}\text{C}_{\text{terpenoids-methane}}$ value was found to only amount to -3‰ (Kellermann et al., 2012). Such isotope offset suggested the dominance of Type II methanotrophs, an inference supported by the abundance of aminotetrol and the lower amounts of aminotriol, which is typical of Alphaproteobacteria. The fatty acid profile of *B. childressi* was found to contain abundant $\text{C}_{16:1\omega8}$ and significant amounts of $\text{C}_{18:1\omega8}$ (Kellermann et al., 2012), compounds typical of Type I and Type II methanotrophs, respectively (Bowman, 2006). However, 16S rRNA analysis of Duperron et al. (2007) contradicted the hypothesis of a presence of Type II methanotrophic symbionts in *B. childressi*, yielding only sequences of Gammaproteobacteria. Based on such contradictory evidence, the presence of both types of methanotrophs in the *B. childressi* symbionts should not be ruled out at this point.

Abundant 4-methyl sterols found in the sediments of Haakon Mosby Mud Volcano yielded a $\Delta\delta^{13}\text{C}_{\text{terpenoid-s-methane}}$ of -14‰ (Table 2.3), agreeing with the dominance of Type I/X methanotrophs. A suite of 4-methyl sterols and hopanoids from recent seep carbonates of Alaminos Canyon revealed a $\Delta\delta^{13}\text{C}_{\text{terpenoids-methane}}$ of 0‰ (Table 2.3), falling in the range of values diagnostic for Type II methanotrophs. In the latter case, however, evidence was contradictory since the presence of 4-methyl sterols together with BHPs more typical of Gammaproteobacteria disagree with Type II methanotrophs as source organisms. Another possible source in this case are Type X methanotrophs, which are capable to assimilate small amounts of CO_2 using the ribulose biphosphate carboxylase oxygenase (Rubisco) pathway and possibly the serine pathway (Taylor et al., 1981; Baxter et al., 2002; Chistoserdova et al., 2009), which can result in different carbon isotope fractionation (Summons et al., 1994). In the case of seep carbonates from the oxygenated zone of the Makran accretionary prism, cyclic triterpenoids yielded a $\Delta\delta^{13}\text{C}_{\text{terpenoids-methane}}$ of -8‰ (Table 2.3; Himmler et al., 2015), suggesting the dominance of Type II methanotrophs. Interestingly, the BHP patterns of Makran and Alaminos Canyon seep carbonates resembled those of *M. kenyense* and *M.*

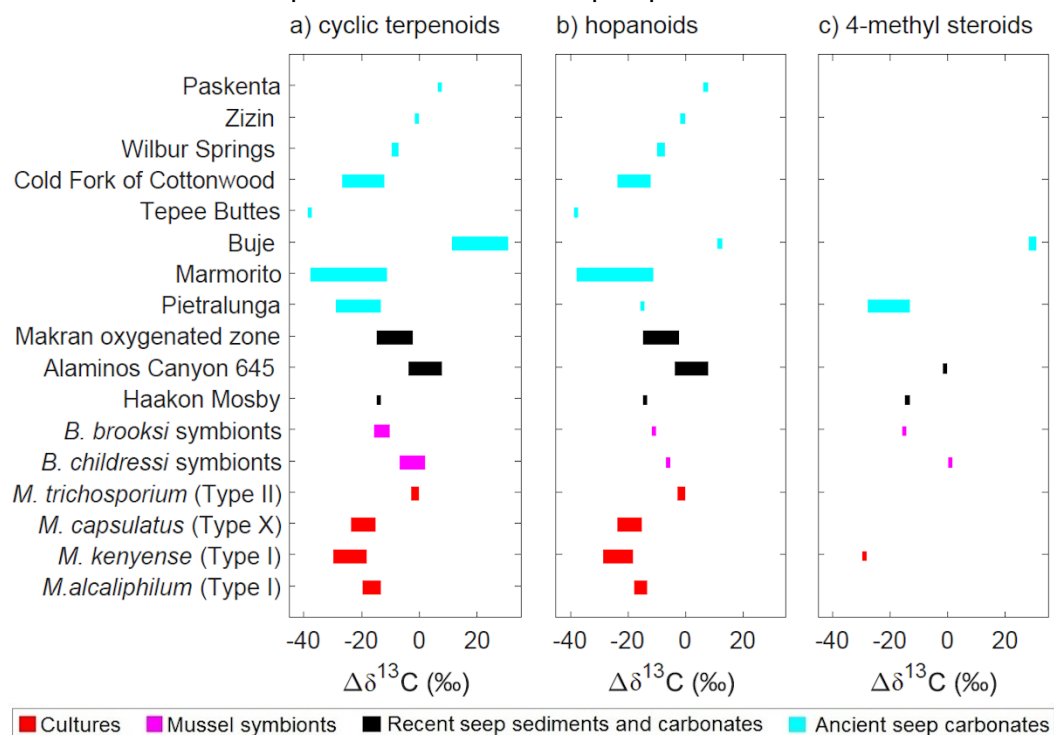
alcaliphilum. Moreover, in case of Alaminos Canyon seep carbonates, the presence of 3 β -methyl hopanoids, 4-methyl sterols and steroids, and tetrahymanol is strong evidence for Type I methanotrophs, particularly because type I methanotrophs are the only organisms known to synthesize 4-methyl sterols (Bouvier et al., 1976; Schouten et al., 2000; Wei et al., 2016). Another aspect that needs to be considered is the circumstance that Type II methanotrophs have never been discovered in the marine realm to date (Knief, 2015). Although the chain of arguments is anything but straightforward and the $\Delta\delta^{13}\text{C}_{\text{terpenoids-methane}}$ of the Makran seep carbonates is rather pointing to Type II methanotrophs, it seems more likely that Type I methanotrophs are the BHP source even in this case. We might just still be lacking the appropriate cultures of Type I methanotrophs with little carbon isotope fractionation involved in terpenoid synthesis. Taken together, current evidence suggests that Type I methanotrophs are exclusively responsible for aerobic methane oxidation at marine methane seeps.

How to constrain the carbon isotope composition of methane at ancient seeps

A comparison of $\delta^{13}\text{C}$ values of ANME biomarkers and the respective methane sources ($\Delta\delta^{13}\text{C}_{\text{ANME-methane}}$) originally put forward by Niemann and Elvert (2008) has been applied to sediments, mats, and carbonates of modern seeps to develop a proxy for $\delta^{13}\text{C}_{\text{methane}}$ values when seeping methane is not available anymore (Himmeler et al., 2015). It has been found that the isotopic offset ($\Delta\delta^{13}\text{C}_{\text{ANME-methane}}$) is approximately -50‰ in ANME-2 dominated systems and approximately -30‰ in ANME-1 dominated systems (Elvert & Niemann, 2008). For the Alaminos Canyon carbonates, which contained mostly lipids typical of the ANME-2/DSS consortium, a $\Delta\delta^{13}\text{C}_{\text{ANME-methane}}$ of -50‰ can be expected, resulting in an estimate for the $\delta^{13}\text{C}_{\text{methane}}$ value of -52‰ . These values are close to the measured $\delta^{13}\text{C}_{\text{methane}}$ value (-56‰) and the correspondingly calculated $\Delta\delta^{13}\text{C}_{\text{ANME-methane}}$ (-46‰) for this site, supporting the applicability of the approach. Based on the wide range of carbon isotope fractionation during terpenoid synthesis in aerobic methanotrophic bacteria, such an approach to constrain the isotopic composition of parent methane cannot be easily adopted for MOx biomarkers. However, if one estimates the isotopic composition of parent methane with ANME biomarkers, $\Delta\delta^{13}\text{C}_{\text{terpenoids-methane}}$ will help with the assignment of terpenoid biomarkers to either Type I methanotrophs or Type II methanotrophs (Table 2.3; Fig. 2.2). For some of the sites, especially some of the ancient sites, an exclusive assignment to ANME-1 or ANME-2 is not possible. For those samples, which show

signatures of both types of ANMEs, we report ranges rather than single values (see Table 2.3).

Figure 2.2 Offset of $\delta^{13}\text{C}$ values ($\Delta\delta^{13}\text{C}$) between methane and terpenoid biomarkers of aerobic methanotrophs in cultures and seep deposits



Note: See Table 2.1 for isotope values of compounds.

The Miocene Pietralunga seep deposit contains abundant *sn2*-hydroxyarchaeol ($\delta^{13}\text{C}$: -108‰ , Table 2.2), suggesting the dominance of ANME-2/DSS and resulting in an estimated $\delta^{13}\text{C}_{\text{methane}}$ value of -58‰ . Using the average Pietralunga $\delta^{13}\text{C}_{\text{terpenoid}}$ value of -80‰ , the $\Delta\delta^{13}\text{C}_{\text{terpenoids-methane}}$ was -22‰ and suggests the dominance of Type I/X methanotrophs at the Miocene seep. Such interpretation is supported by the occurrence of abundant 4-methyl steranes and accessory 3-methyl hopanoic acids (Table 2.3; Peckmann et al., 2004; Birgel & Peckmann, 2008), both only known to be produced by Type I/X methanotrophs. For the Marmorito seep limestone, the low abundance of *sn2*-hydroxyarchaeol and crocetane indicate the dominance of ANME-1 over ANME-2, and assuming that ANME-1/DSS predominated, a range of $\delta^{13}\text{C}_{\text{methane}}$ values between -68 and -58‰ and a $\Delta\delta^{13}\text{C}_{\text{terpenoids-methane}}$ value between -32‰ and -22‰ is calculated. Such high fractionation agrees with the presence of a 4-methyl sterol and 3-methyl BHP (Peckmann et al., 1999; Birgel & Peckmann, 2008) and, accordingly, the dominance of Type I/X methanotrophs. Similarly, the presence of 4-

methyl steranes in the Buje seep deposit is pointing to Type I methanotrophic bacteria (Table 2.3; Natalicchio et al., 2015). However, the calculated average $\Delta\delta^{13}\text{C}_{\text{terpenoids-methane}}$ value of +24‰ is not in accord with isotope fractionation in any aerobic methanotroph reported to date. Based on such uncertainty, the affiliation of the Buje aerobic methanotrophs cannot be constrained.

The absence of crocetane and the abundance of ^{13}C -depleted phytane and phytanic acid (Table 2.2) – most likely originating from cleavage of archaeol – in the Cretaceous Tepee Buttes point towards the dominance of ANME-1. Based on the correspondingly calculated $\delta^{13}\text{C}_{\text{methane}}$ value of -71‰ and the resultant $\Delta\delta^{13}\text{C}_{\text{terpenoids-methane}}$ of -38‰, Type I methanotrophs apparently produced the precursor lipids of a suite of uncommon C_{34} - and C_{35} -8,14-secohexahydrobenzohopanes. Interestingly, as for the Marmorito limestone, such large $\Delta\delta^{13}\text{C}_{\text{terpenoid-methane}}$ values exceed all fractionation that has been observed in culture to date (Fig. 2.2). The Cretaceous seep carbonates of Cold Fork of Cottonwood Creek and Wilbur Springs and the Jurassic seep carbonates of Paskenta contain ^{13}C -depleted PMI, crocetane, and only small amounts of biphytanes (Table 2.2). The presence of crocetane is diagnostic for ANME-2 archaea, while biphytane, derived from GDGTs, is indicative of ANME-1. Assuming a predominance of ANME-2 over ANME-1, $\delta^{13}\text{C}_{\text{methane}}$ values ranging from -47‰ to -37‰, -61‰ to -51‰, and -72‰ to -62‰, as well as $\Delta\delta^{13}\text{C}_{\text{terpenoids-methane}}$ values from -26‰ to -16‰, -14‰ to -4‰, and +2‰ to +12‰, are obtained for Cold Fork of Cottonwood Creek, Wilbur Springs, and Paskenta, respectively. According to these calculations that are admittedly based on the uncertain assumption of an ANME-2 dominance, the former presence of Type I/X methanotrophs can be inferred for Cold Fork of Cottonwood Creek, while for Wilbur Springs and Paskenta the isotope signatures are again rather in accord with Type II methanotrophs. Unfortunately, diagnostic lipids that would help with such assignment are absent. Lastly, ^{13}C -depleted phytane ($\delta^{13}\text{C}$: -86‰, Table 2.2) and high contents of biphytane ($\delta^{13}\text{C}$: -92‰) in the Cretaceous Zizin seep carbonates most likely represent predominant input from ANME-1. Based on this assumption, a $\delta^{13}\text{C}_{\text{methane}}$ value of -59‰ and a $\Delta\delta^{13}\text{C}_{\text{terpenoids-methane}}$ value of -1‰ would indicate Type II methanotrophs, but the occurrence of trace amounts of nor-lanostanes (Table 2.3; Sandy et al., 2012) rather point to Type I methanotrophs, very similar to the inconclusive patterns found for the Alaminos Canyon seep carbonates of the Gulf of Mexico.

It is commonly assumed that all marine strains of aerobic methanotrophic bacteria are Type I methanotrophs (Knief, 2015). Fractionation patterns derived from cultured aerobic methanotrophs and compound-specific $\delta^{13}\text{C}$ values of MOx biomarkers from marine methane seeps suggest that fractionation in the course of lipid synthesis can be stronger among Type I methanotrophs in the environment under certain environmental conditions than what is known from culture experiments. The $\Delta\delta^{13}\text{C}_{\text{terpenoids-methane}}$ values calculated herein vary widely from seep locality to seep locality, also suggesting a strong dependence of the degree of fractionation on local environmental conditions. For most seep provinces, biomarker evidence agrees with the presence of Type I/X methanotrophs, whereas for some examples the calculated isotope fractionation seems at odds with this interpretation (Fig. 2.2). Interestingly, the fractionation calculated for the cyclic terpenoids of the Tepee Buttes seep deposits exceeds all fractionation documented for cultures. Our study indicates that terpenoid biomarkers and their carbon stable isotope patterns have great potential to constrain the affiliation of aerobic methanotrophs that dwelled in ancient environments. But it also becomes obvious that more work on cultures and environmental samples is needed to use the full potential of this approach.

2.6 Conclusions

The suite of cyclic terpenoids of the Type I methanotrophs *Methylobacterium kenyense* and *Methylobacterium alcaliphilum* comprises 4-methyl sterols, C_{30} hopanols, tetrahymanol, and BHPs, namely aminotetrol and aminotriol (cf. Banta et al., 2015), which are strongly depleted in ^{13}C . The average carbon stable isotope fractionation relative to the methane source in *M. kenyense* and *M. alcaliphilum* are -25‰ and -16‰ , respectively, considerably higher than isotope fractionation in Type II methanotrophs. Aerobic methanotrophs are likely source organisms of ^{13}C -depleted tetrahymanol and its degradation product ^{13}C -depleted gammacerane when present along with other biomarkers of aerobic methanotrophs, as discussed for examples from methane-seep environments. 4-methyl sterols represent reliable biomarkers of Type I aerobic methanotrophs in young sediments and sedimentary rocks. However, the preservation potential of these compounds is apparently low. Lanostanes are interpreted to represent derivatives of 4-methyl sterols and are sometimes preserved in ancient methane-seep deposits. BHPs occur in recent and subrecent samples, but are absent in older rocks, where only their degradation products such as anhydroBHT

and secohexahydrobenzohopanes are found. Some ancient seep deposits have been shown to contain 3-methyl hopanoids, allowing Type I methanotrophs to be traced into the rock record. The biomarker data base for aerobic methanotrophy reveals great variability of $\delta^{13}\text{C}$ patterns. While ANME biomarkers can be used to calculate the $\delta^{13}\text{C}$ values of the methane source, this approach is hampered for MOx biomarkers by the observed great variability of $\delta^{13}\text{C}_{\text{terpenoid}}$ values. Fractionation between methane and terpenoids of aerobic methanotrophs seems to vary greatly as a function of environmental conditions, and in some instances the extent of fractionation cannot be used to unequivocally discriminate Type I and Type II methanotrophs.

3. Chapter III

Effect of varying conditions in the pentacyclic triterpenoid inventory of aerobic methanotrophic bacteria

This chapter has been published as: Cordova-Gonzalez, A., Birgel, D., Kappler, A., & Peckmann, J., 2021. Variation of salinity and nitrogen concentration affects the pentacyclic triterpenoid inventory of the haloalkaliphilic aerobic methanotrophic bacterium *Methylovumicrobium alcaliphilum*. *Extremophiles* 25(3):285-299. DOI: 10.1007/s00792-021-01228-x.

3.1 Abstract

The occurrence and activity of aerobic methanotrophs are influenced by environmental conditions, including pH, temperature, salinity, methane and oxygen concentrations, and nutrient availability. Aerobic methanotrophs synthesize a variety of lipids important for cell functions. However, culture-based experiments studying the influence of environmental parameters on lipid production by aerobic methanotrophs are scarce. Such information is crucial to interpret lipid patterns of methanotrophic bacteria in the environment. In this study, the alkaliphilic strain *Methylovumicrobium alcaliphilum* was cultivated under different salinities and different nitrate concentrations to assess the effect of changing conditions on the inventory of pentacyclic triterpenoids. The results indicate that hopanoid abundance is enhanced at lower salinity and higher nitrate concentration. The production of most pentacyclic triterpenoids was favored at low salinity, especially for aminotriol. Interestingly, 3-methyl-aminotetrol and tetrahymanol were favored at higher salinity. Bacteriohopanepolyols (BHPs), particularly aminotriol and 3-methyl-aminotriol,

increased considerably at higher nitrate concentration. Four novel N-containing BHPs – aminodiol, 3-methyl-aminodiol, and isomers of aminotriol and 3-methyl-aminotriol – were identified. This study highlights the significance of environmental factors for bacterial lipid production and documents the need for cultivation studies under variable conditions to utilize the full potential of the biomarker concept.

3.2 Introduction

Aerobic methanotrophic bacteria are an important methane sink due to their ability to utilize methane as sole carbon and energy source, using the key enzyme monooxygenase (Hanson & Hanson, 1996; Semrau et al., 2010). Bacterial aerobic methane oxidation (MOx) contributes significantly to the withdrawal of methane released from anoxic sediments and soils, which otherwise could accumulate in the atmosphere as severe greenhouse gas. Therefore, MOx is essential for methane consumption (Hanson & Hanson, 1996; Sherry et al., 2016). Aerobic methanotrophs occur in terrestrial, freshwater, and marine ecosystems, preferably at oxic-anoxic interfaces. Aerobic methanotrophic bacteria are microaerophilic, using oxygen as electron acceptor and methane as carbon and energy source (Boetius & Wenzhoefer, 2013; Bessette et al., 2017). Generally, aerobic methanotrophs are divided in two major groups, belonging to the Gammaproteobacteria (Type I and Type X methanotrophs) and Alphaproteobacteria (Type II methanotrophs), which differ in physiology, chemotaxonomy, internal ultrastructure, carbon assimilation pathways, and other biochemical aspects (Bowman, 2006).

Type II methanotrophic bacteria are restricted to terrestrial environments such as peats, soils, and lakes. Type I methanotrophic bacteria are more versatile, also dwelling in the marine realm (e.g., Knief, 2015). Generally, the occurrence and activity of aerobic methanotrophic bacteria is influenced by environmental conditions, including pH, temperature, salinity, methane and oxygen concentrations, and nutrient availability (Semrau et al., 2010; Knief, 2015; Sherry et al., 2016). Among these factors, the effect of inorganic nitrogen on aerobic methanotrophs has been widely studied, particularly for agricultural soils, where ammonium- or nitrate-based fertilizers may influence methane oxidation and affect the global methane budget (Noll et al., 2008). Unfortunately, results of culture studies on the effect of inorganic nitrogen addition on methanotrophic activity are not in agreement with reports demonstrating either inhibition (Dunfield & Knowles, 1995) or stimulation (Bodelier et al., 2000; Bodelier & Laanbroek, 2004) of methane oxidation. Although the link between nitrogen

availability and methane consumption is still unclear, it is assumed that the effect of nitrogen is dependent on the structure of the *in situ* methanotrophic community (Hoefman et al., 2014), since aerobic methanotrophs have shown metabolic variability regarding nitrogen assimilation on both genus and species level. The nitrogen metabolism of various aerobic methanotrophs strains is diverse, including cometabolic oxidation of ammonia (Nyerges & Stein, 2009), nitrate reduction to nitrite (Bowman et al., 1993), detoxification of hydroxylamine and nitrite (Nyerges & Stein, 2009; Nyerges et al., 2010), and fixation of atmospheric nitrogen, the latter known from few strains only (Hoefman et al., 2014; Tays et al., 2018). Among the various genera of aerobic methanotrophs, the nitrogen metabolism seems to be strain specific (Hoefman et al., 2014). Nonetheless, gammaproteobacterial methanotrophs are preferentially stimulated by nitrogen amendments (Bodelier et al., 2000) and alphaproteobacterial methanotrophs cope better with nitrogen limitation than Gammaproteobacteria, perhaps due to their ability to fix dinitrogen (Nyerges & Stein, 2009).

Another important factor influencing the activity of aerobic methanotrophs is salinity. Sherry et al. (2016) analyzed the response of a methanotroph community in estuarine sediments to salinity change and documented an inverse correlation of decreasing methane oxidation rates with increasing salinity. MOx communities at salinities higher than 35 g/l were dominated by Type I *Methylobacterium* species, closely related to the halo-/alkalitolerant methanotroph *Methylobacterium alcaliphilum*, which lives at normal marine and higher salinities (Orata et al., 2018). Intriguingly, none of the sequences identified were affiliated with known marine methanotrophs (Sherry et al., 2016).

Among the most specific capabilities of aerobic methanotrophs is their ability to synthesize a unique lipid biomarker inventory. Apart from fatty acids with characteristic double bond positions (e.g., Hanson & Hanson, 1996), this group of bacteria is known as producer of a variety of source-specific pentacyclic (hopanoids) and tetracyclic triterpenoids (steroids) (e.g., Bouvier et al., 1976; Rohmer et al., 1984; Talbot & Farrimond, 2007; Banta et al., 2015; Rush et al., 2016; Wei et al., 2016; Cordova-Gonzalez et al., 2020). The cyclic triterpenoids are known to be crucial for cell functions such as cell growth and survival (Kannenberg & Poralla, 1999; Welander et al., 2009; Welander & Summons, 2012). Aerobic methanotrophs are among the few bacteria capable to express their ability to produce significant amounts of 3-methyl hopanoids (Welander & Summons, 2012) and bacteriohopanepolyols (BHPs) with

terminal amino groups and three to five hydroxyl groups (amino BHPs), or a combination of both (Zundel & Rohmer, 1985; Talbot et al., 2003). Amino BHPs are used by aerobic methanotrophs to cope with environmental stress (Welander & Summons, 2012; Kulkarni et al., 2013). Previous studies have investigated the influence of temperature, pH, and nitrogen metabolism on bacterial hopanoid production. For example, contents of BHPs in *Bacillus acidocaldarius*, a thermoacidophilic bacterium, increased with increasing temperature, but only moderately with decreasing pH (Poralla et al., 1984), while a psychrotolerant strain of the aerobic methanotroph *Methylomonas methanica* revealed an opposite trend with respect to temperature, showing a decrease of hopanoid contents with increasing temperature (Jahnke et al., 1999). Strains of *Methylovulum psychrotolerans*, an aerobic psychrotolerant methanotroph, also showed a decrease in hopanol contents, specifically tetrafunctionalized BHPs and diplopterol, with increasing temperature, along with an increase in penta- and hexafunctionalized BHPs (Bale et al., 2019). Osborne et al. (2017) have studied the effect of varying temperatures on BHP production in a sedimentary methanotrophic community from the environment. These authors demonstrated a temperature dependence of aminopentol production, but not for aminotetrol or aminotriol. Nalin et al. (2000) have reported slightly increased hopanoid contents under nitrogen-replete (NH_4^+) conditions for several nitrogen-fixing actinomycete *Frankia* strains. Even though some studies exist, our knowledge on the influence of environmental parameters on lipid production by methanotrophic bacteria is still limited, being based on only few culture experiments (Jahnke et al., 1999; Talbot et al., 2001; Cordova-Gonzalez et al., 2020). Often the interpretation of environmental samples is still challenging due to the lack of culture experiments under conditions close to those of the respective environments. More cultivation experiments are needed to evaluate possible unknown adaptations of aerobic methanotrophs strains in response to changing environmental conditions. Complementarily, experiments using uncultured strains in micro- and mesocosms (Sherry et al., 2016; Osborne et al., 2017) need to be performed to close the gap between the biomarker patterns of cultures and environmental samples.

Here, we use cultivation experiments to assess whether changes in nitrate availability and salinity affect the composition and abundance of pentacyclic triterpenoids produced by the Type I methanotroph *Methylotheobacterium alcaliphilum*, a haloalkaliphilic strain, which has been studied previously for its triterpenoid inventory (Banta et al., 2015; Rush et al., 2016; Cordova-Gonzalez et al., 2020). We report the occurrence of novel BHPs in *M. alcaliphilum* and modifications of its lipid inventory at

varying salinities and nitrate concentrations. This approach will help to understand the limitations of aerobic methanotrophy in haloalkaline environments and will foster interpretation of biomarker patterns observed in the environment and the rock record.

3.3 Materials and methods

Methylobacterium alcaliphilum 20Z (now *Methylotuvimicrobium alcaliphilum*; Orata et al., 2018) strain was obtained from the Leibniz Institute DSMZ–German Collection of Microorganisms and Cell Cultures. The cultivation experiments were performed in the Geomicrobiology group at the University of Tübingen, Germany. *M. alcaliphilum* was first isolated from surface sediments of highly alkaline soda lakes in Russia (Kalyuzhnaya et al., 2008).

3.3.1 Culture conditions

M. alcaliphilum strains were grown in 100 ml serum bottles filled with 10 ml of the DSMZ recommended *Methylobacterium* medium (DSMZ 1180) containing 30 g NaCl, 0.20 g MgSO₄ × 7 H₂O, 0.02 g CaCl₂ × 2 H₂O and 1 g KNO₃, in 1000 ml distilled water. The pH was adjusted to 8.5 and cultures were incubated at 28°C and shaken at 200 rpm. The initial gas-mixing ratio was adjusted at methane:air 1:1 (v/v). Four different culture conditions were applied: standard growth conditions (3% NaCl, 0.1% or 10 mM KNO₃), low salinity (1% NaCl), high salinity (8.7% NaCl), and high nitrate concentration (1% or 100 mM KNO₃). Cells were harvested by centrifugation at 4,000 rpm for 10 min when entering the stationary phase and freeze-dried for further analyses. Cell growth was monitored by measuring the optical density at 600 nm on a Thermo Scientific Multiskan Go spectrophotometer.

3.3.2 Extraction and derivatization

Harvested cells were freeze-dried and gently ground, then extracted with dichloromethane (DCM)/methanol (MeOH) (3:1, v/v) by successive ultrasonication to produce the total lipid extract (TLE) according to Cordova-Gonzalez et al. (2020). An aliquot of the TLE was acetylated by adding acetic acid anhydride/pyridine (1:1 v/v) to the dried TLE at 60°C for one hour and left at room temperature overnight. The solvent mixture was carefully dried with a gentle stream of N₂. Hopanoids with ≤30 carbons and tetrahymanol were measured by gas chromatography–flame ionization detector (GC–FID) and coupled gas chromatography–mass spectrometry (GC–MS). For analysis of BHPs, the acetylated aliquots of TLE were measured by means of

high-performance liquid chromatography–mass spectrometry (HPLC–MS). Tetrafunctionalized BHPs (aminotriols) were additionally measured on GC–MS with a high temperature column (see section 2.3.3). A second aliquot of the underivatized TLE was treated with periodic acid and sodium boron hydride to transform BHPs in GC-amenable hopanols (Rohmer et al., 1984). Briefly, after periodic acid cleavage, tetrafunctionalized BHPs (e.g., aminotriol and bacteriohopanetetrol) were converted to C₃₂ 17 β (H),21 β (H)-hopanol (bishomohopanol), pentafunctionalized BHPs (e.g., aminotetrol and bacteriohopanepentol) produce C₃₁ 17 β (H),21 β (H)-hopanol (homohopanol), and hexafunctionalized BHPs (e.g., aminopentol) yield C₃₀ 17 β (H),21 β (H)-hopanol (hopanol). The resulting hopanols were acetylated as described above.

3.3.3 Gas chromatography and high-performance liquid chromatography

The acetylated TLEs were analyzed by GC–FID for quantification, using a Thermo Scientific Trace 1300 Series, and by GC–MS for identification, using a Thermo Scientific Trace GC Ultra coupled to a Thermo Scientific DSQ II mass spectrometer at the University of Hamburg, Germany. A programmed temperature vaporizer (PTV) was used for injection in both devices, the carrier gases were hydrogen for GC–FID and helium for GC–MS. Compounds were separated using an Agilent HP-5 MS UI fused silica capillary column (30 m length, 0.25 mm i.d., 0.25 μ m film thickness). The GC temperature program was 50°C (3 min) to 230°C at 15°C/min (2 min), 230°C to 325°C at 6°C/min, 25 min isothermal. The identification by GC–MS was based on GC retention times and comparison of mass spectra with published data. Internal standards (1-nonadecanol and 5 α -cholestane) with known concentrations were added prior to extraction for quantification. BHPs were analyzed as their BHP-cleaved hopanols under the same conditions. High temperature gas chromatography coupled with mass spectrometry (HTGC–MS) was performed on the same machines using a Zebron ZB-5HT capillary column (15 m length, 0.32 mm i.d., 0.10 μ m film thickness). The GC temperature program was 50°C (3 min) to 260°C at 15 °C/min (0 min), 260°C to 350°C at 10°C/min, 30 min isothermal.

High-performance liquid chromatography–mass spectrometry (HPLC–MS) analyses were performed using a Varian MS Workstation 6.91 HPLC system coupled to a Varian 1200L triple quadrupole mass spectrometer, equipped with a reversed-phase Phenomenex Kinetex® EVO C₁₈ 100Å column (150 mm length, 2.1 mm i.d., 2.6 μ m

particle size) and a security guard column cartridge of the same material. The program used was 0.14 ml/min at 35°C with 100% A (0-3 min) to 100% B (at 30 min); isocratic (to 40 min), returning to starting conditions over 5 min and stabilizing for 5 min (where A = 90% MeOH/10% water and B = 59% MeOH/40% propan-2-ol/1% water). The MS instrument was equipped with an atmospheric pressure chemical ionization (APCI) source operated in positive ion mode. The detection was achieved at a peak width of 1.0 amu (scan time 2.5 s) and the mass scan range was set to m/z 200–1200. The acetylated extracts were injected in MeOH/propan-2-ol (3:2 v/v) and a known amount of internal standard (5 α -pregnane-3 β ,17 β ,20 β -triol) was added prior to analysis for a semi-quantitative estimate of the concentration of BHPs. Compounds were identified by comparison with published data and relative retention time. To verify the elution time of the regular aminotriol, peaks in the samples were compared with those in samples of *Desulfovibrio* strains (Blumenberg et al., 2006), run at the same conditions.

BHPs were measured as intact BHPs by means of HPLC–MS and as periodic acid cleavage products (Fig. 3.1a-b). GC–MS analyses of periodic acid cleavage products (Fig. 3.1) showed a considerably higher contribution of aminotetrol (**V**) and 3-methyl-aminotetrol (**VI**) than in HPLC–MS, suggesting an underestimation in the latter technique. In general, tetrafunctionalized BHPs (aminotriols **III** and 3-methyl-aminotriols **IV**) were more abundant in LC–MS measurements than in GC–FID measurements of the respective hopanol products. Pentafunctionalized BHPs (aminotetrol **V** and 3-methyl-aminotetrol **VI**) were less abundant in LC–MS measurements than their corresponding hopanol products measured by GC–FID. Similar discrepancies have been reported for tetrafunctionalized BHPs by van Winden (2011) and were attributed either to underestimation of pentafunctionalized compounds due to LC–MS response factors or to oversight of unknown pentafunctionalized BHPs in the LC–MS analyses. Other studies have shown that BHP contents measured with HPLC–MS are 50–100% higher than those measured with GC–FID (Sessions et al., 2013), although the reasons remain unclear. In view of these discrepancies, the BHP contents are reported herein as their periodic acid cleavage products only. Moreover, since standards were not available for each functionalized hopanoid, quantification of BHPs with HPLC–MS could introduce a large error, while GC–FID provides the most accurate quantitation assuming a uniform response factor (Jorgensen et al., 1990), particularly for compounds within the same class.

3.4 Results and discussion

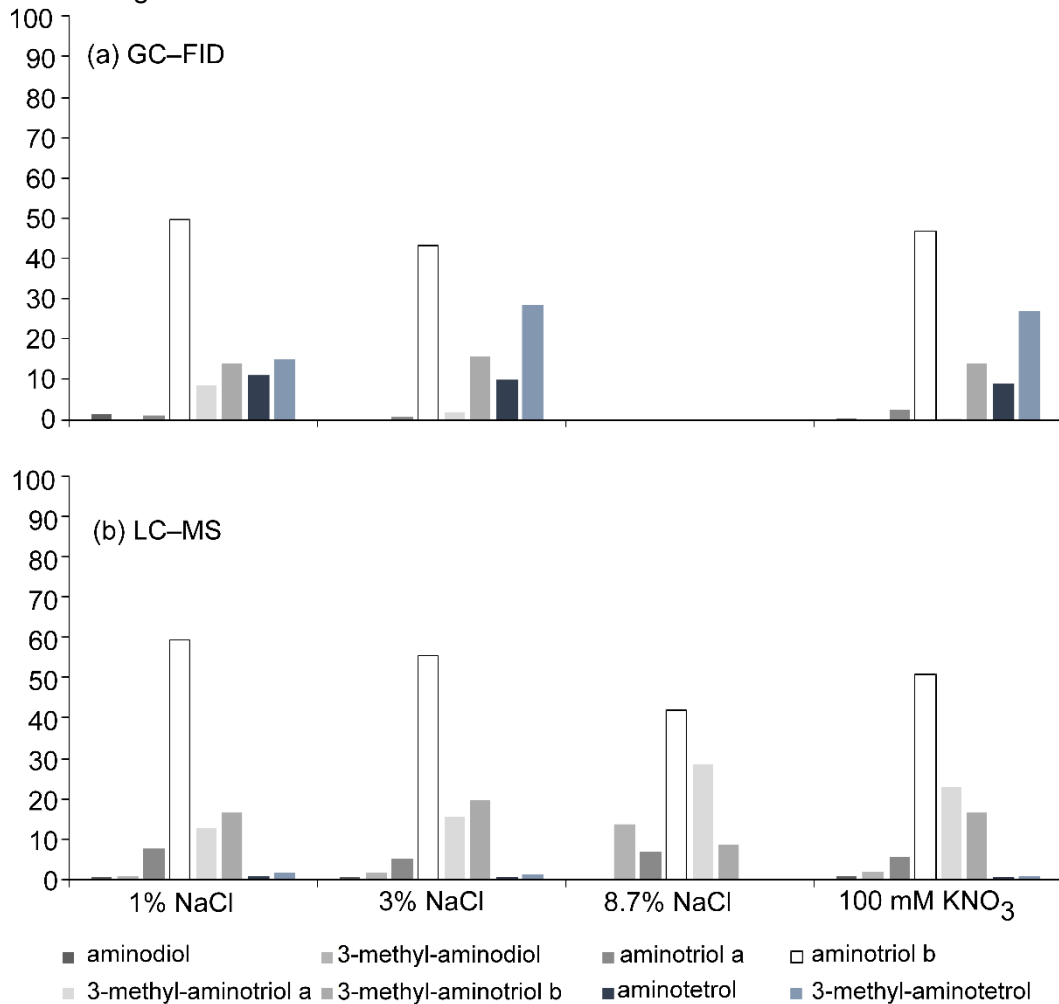
3.4.1 Novel N-containing BHPs

The inventory of lipid biomarkers of the Type I methanotroph *M. alcaliphilum* has been previously described by Banta et al. (2015), Rush et al. (2016), and Cordova-Gonzalez et al. (2020), although under different culturing conditions than those chosen in this study. Most abundant BHPs in *M. alcaliphilum* cultures are aminotriol (**IIIb**), 3-methyl-aminotriol (**IVb**), aminotetrol (**V**), and 3-methyl-aminotetrol (**VI**; Figs. 3.2, 3.3).

In addition to the amino-BHPs previously reported for *M. alcaliphilum* (**IIIb**, **IVb**, **V**, and **VI**; Figs. 3.2, 3.3), the HPLC–MS analysis revealed the presence of four novel components with base peaks at m/z 656 (acetylated; BHP-656 **I**), m/z 670 (acetylated; BHP-670 **II**), m/z 714 (**IIIa**) and m/z 728 (**IVa**), respectively ($[M+H]^+$; Figs. 3.2, 3.3). These compounds are tentatively identified as novel N-containing BHPs on the basis of the even m/z value of the base peak ion (cf. Talbot et al., 2016).

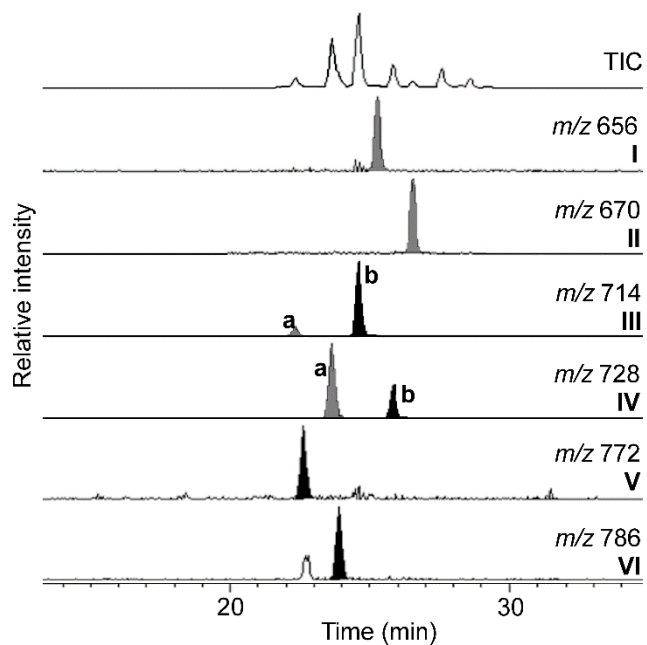
The LC mass spectrum of BHP-656 (**I**; Fig. 3.3a) includes a minor peak at m/z 596, indicating a loss of 60 Da (i.e., acetylated OH group, CH_3COOH). Compound BHP-656 **I** elutes later than aminotriol **IIIb**, suggesting a less polar compound on the reversed phase HPLC column (see section ‘Gas chromatography and high-performance liquid chromatography’). The peak in question was tentatively identified as aminodiol. Directly after BHP-656 **I** elutes the compound BHP-670 **II**. The mass spectrum of BHP-670 **II** (Fig. 3.3b) includes other minor peaks at m/z 610 and m/z 568, indicating a neutral loss of 60 Da (i.e., acetylated OH group, CH_3COOH) followed by a neutral loss of 42 Da (i.e., partial loss of acetylated OH group, COCH_2), respectively. The 14 Da difference suggests non-methylated (**I**) and methylated (**II**) homologues, with the presence of a methyl group at C-3 in the latter, since methylation at this position is typical of Type I methanotrophs (Talbot et al., 2003).

Figure 3.1 Comparison of quantification of BHPs of *M. alcaliphilum* as (a) hopanol products after periodic acid cleavage using GC–FID and (b) intact hopanols using LC–MS reflecting different salinities and nitrate concentration



Note: GC–FID data for experiments at 8.7% NaCl are not shown.

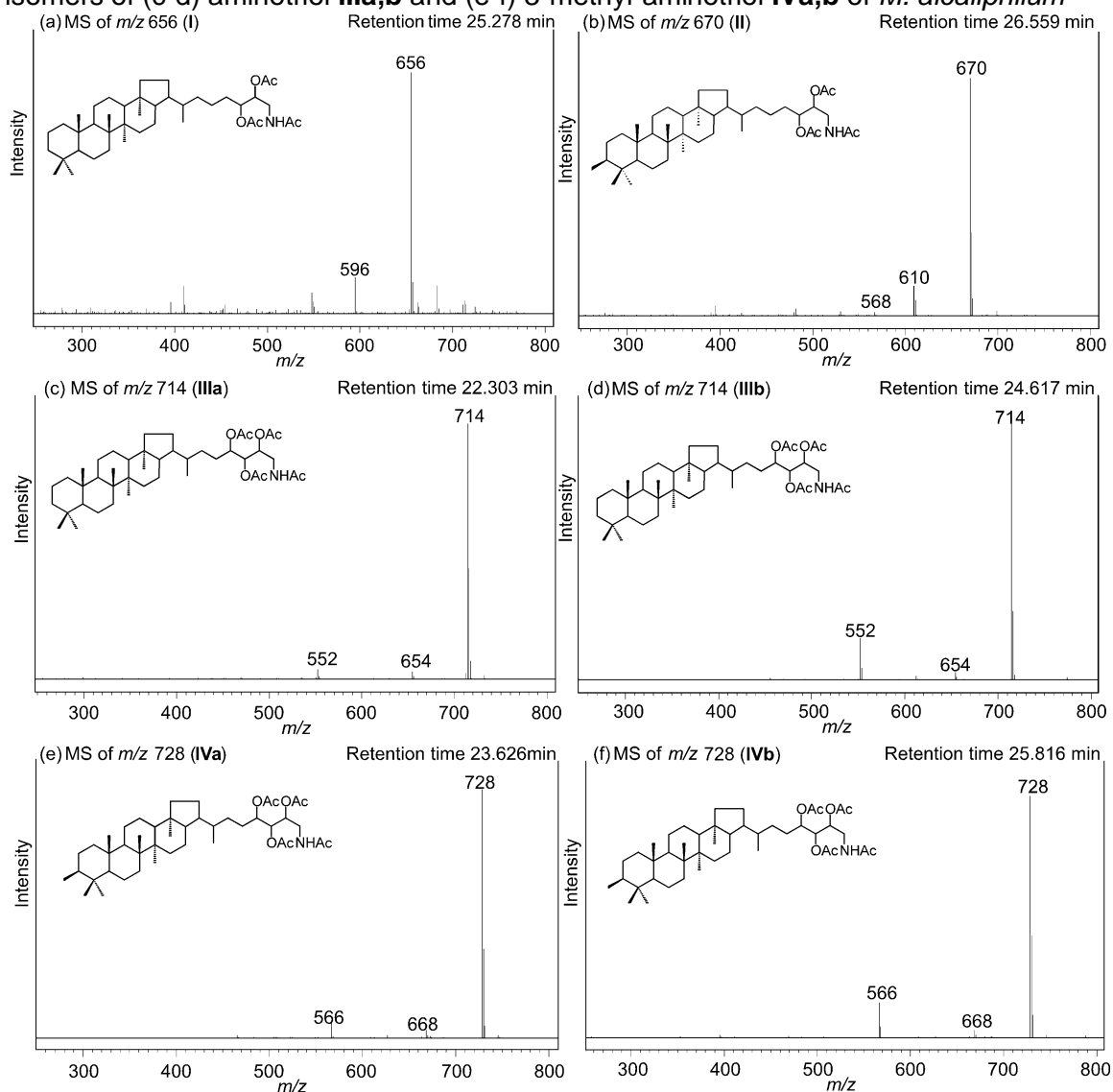
Figure 3.2 Partial HPLC–MS chromatograms showing BHPs in the acetylated total lipid extract of *M. alcaliphilum* grown at 3% salinity and 100 mM KNO₃.



Note: Novel BHPs are indicated in gray.

As mentioned above, two new peaks with m/z 714 (**IIIa**) and m/z 728 (**IVa**) were identified, respectively. Both peaks **IIIa** and **IVa** were eluting earlier than the commonly found BHPs aminotriol **IIIb** and 3-methyl-aminotriol **IVb**, respectively (see Fig. 3.2). The mass spectrum of m/z 714 **IIIa** (Fig. 3.3c) is almost identical to the mass spectrum of regular aminotriol **IIIb** (Fig. 3d) with $([M+H]^+ = m/z$ 714 and minor peaks at m/z 654, m/z 612 and m/z 552 representing neutral losses of 60 Da (i.e., acetylated OH group) followed by losses of 42 Da (i.e., loss of partial fragment of acetylated OH group) and 60 Da, respectively. However, the peak at m/z 552 ($[M+H-2CH_3COOH-COCH_2]^+$) in the MS spectrum of compound **IIIa** is less prominent than in the MS spectrum of regular aminotriol **IIIb** and the association ion at m/z 774 ($[M+H+60]^+$) (sensu Talbot et al., 2001) is absent.

Figure 3.3 HPLC–MS spectra of acetylated (a) aminodiol **I**, (b) 3-methyl-aminodiol **II**, isomers of (c-d) aminotriol **IIIa,b** and (e-f) 3-methyl-aminotriol **IVa,b** of *M. alcaliphilum*

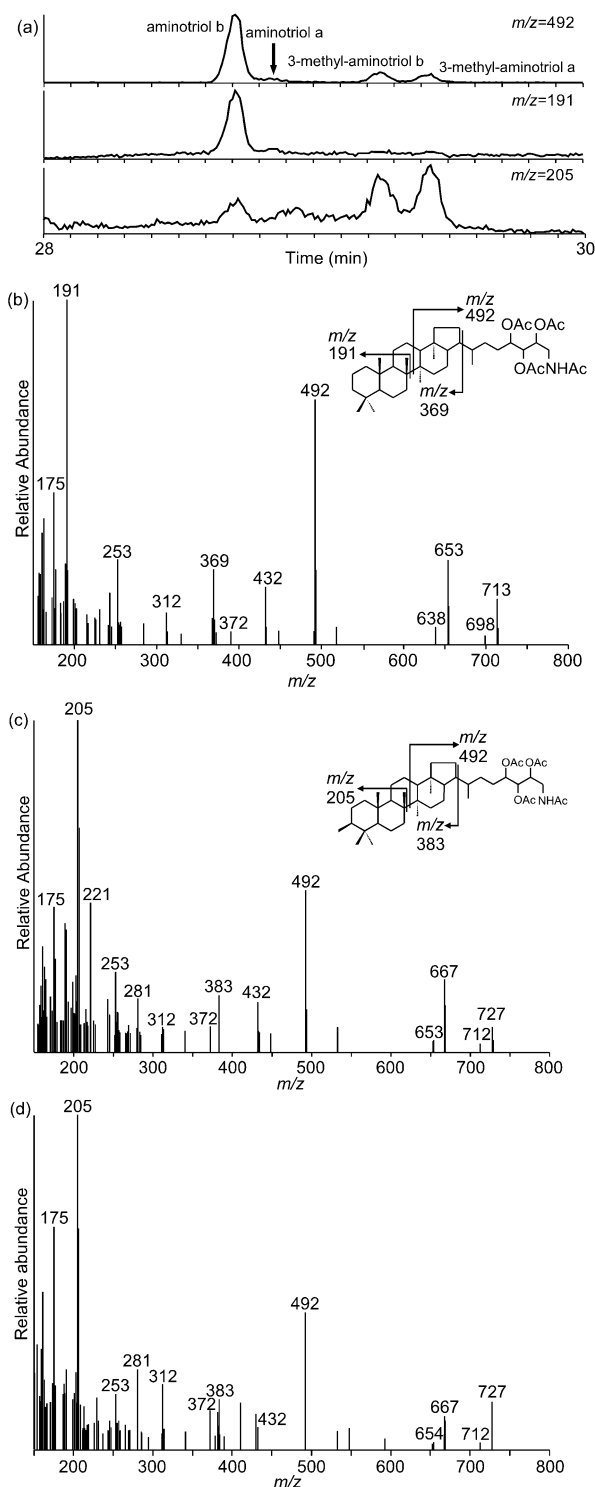


Analogous to m/z 714 peaks, the spectrum of m/z 728 **IVa** (Fig. 3.3e) is similar to the mass spectrum of regular 3-methyl-aminotriol **IVb** (Fig. 3f) with $([M+H]^+ = m/z$ 728) and minor peaks at m/z 668 (loss of 60 Da; i.e., acetylated OH group), m/z 626 (loss of 42 Da; i.e., loss of a partial fragment of an acetylated OH group) and m/z 566 (neutral loss of 60 Da). In the MS spectrum of **IVa**, the peak at m/z 566 is less prominent than in the MS spectrum of regular 3-methyl-aminotriol **IVb** and the association ion at m/z 788 ($[M+H+60]^+$) is absent. Compounds **IIIa** and **IVa** have been tentatively assigned as stereoisomers of aminotriol **IIIb** and 3-methyl-aminotriol **IVb**, respectively. Unfortunately, the similarity between MS spectra of the respective isomers did not allow discrimination of the stereochemistry of the compounds. The relative abundances of compounds **IIIa** and **IVa** of all measured BHPs are 5% and 16%, respectively (relative abundance in the HPLC runs for experiments with *M. alcaliphilum* run at standard conditions). However, co-elution of compounds **IIIa** with aminotetrol **V** and compound **IVa** with 3-methyl-aminotetrol **VI** complicated the assessment of the peak areas. The production of compounds **IIIa** and **IVa** as a consequence of fragmentation in the source of the HPLC–MS from the known aminotriol **IIIb** and 3-methyl-aminotriol **IVb** was discarded as two isomers of aminotriol and 3-methyl-aminotriol were also found in HTGC–MS analyses (Fig. 3.4a). The order of elution on HTGC–MS is reversed compared to HPLC analyses due to measurement on a reversed phase column on the HPLC–MS.

HTGC–MS analyses of intact BHPs were used to further confirm the presence and possible structure of compounds **IIIa** and **IVa**. The tentative identification of aminotriol stereoisomers using HTGC–MS was based on their molecular masses and expected fragmentation patterns from Sessions et al. (2013) and comparison with retention time and mass spectra of aminotriol **IIIb** from a co-injected extract of *Desulfovibrio* strain BSS (cf. Blumenberg et al. 2006). The extracted m/z 191 chromatogram showed two peaks, eluting at slightly different retention times (Fig. 3.4a), with M^+ at m/z 713 (Fig. 3.4b; corresponding to $[M+H]^+$ at m/z 714 in HPLC–MS). Diagnostic ions include m/z 713 (M^+), m/z 492 (ring D + E + side chain), m/z 369 (ring A–E), m/z 191 (ring A + B), and other fragments representing losses of acetylated groups such as m/z 432 ($492 - 60$), m/z 372 ($492 - 60 \times 2$), m/z 312 ($492 - 60 \times 3$), and m/z 653 ($713 - 60$). The full GC–MS spectrum for the novel aminotriol **IIIa** is not displayed, due to low concentration of the compound. BHP-656 **I** and BHP-670 **II** were not found in HTGC–MS analyses, most likely due to the even lower concentrations of these compounds, since sensitivity of measurements with HPLC–MS are 50 to 100% higher than those

measured with GC–MS. This phenomenon is possibly caused by more severe analyte loss during GC–MS analyses (cf. Sessions et al., 2013). Peaks at m/z 653 and m/z 668 were observed in HTGC–MS analyses and interpreted as degradation products of aminotriol **III** and 3-methyl-aminotriol **IV**, when injected on a PTV or split/splitless injector and run on the ZB-5HT column (see Sessions et al., 2013; Eickhoff et al., 2014).

Figure 3.4 (a) HTGC–MS partial chromatograms (m/z 492; m/z 191; m/z 205) of acetylated total lipid extract of *M. alcaliphilum*. (b) EI mass spectrum of acetylated isomer of aminotriol b **IIIb**. (c) EI mass spectra of acetylated 3-methyl-aminotriol b **IVb**. (d) EI mass spectra of acetylated 3-methyl-aminotriol a **IVa**



The identification of 3-methylhomologs of

aminotriol is based on molecular mass and changes in major MS fragmentation from m/z 191 to m/z 205. The m/z 205 chromatogram showed two peaks, similar as for desmethylated aminotriol (Fig. 3.4a). The GC–MS spectra of the two stereoisomers of 3-methyl-aminotriol (**IVa** and **IVb**) showed fragments characteristic of the hopanoid rings (m/z 205 and m/z 383; Fig. 3.4c-d), and a major peak at m/z 492 (ring D + E + side chain). Diagnostic fragments resulting from the loss of one or more acetic acid groups, as described above for aminotriol **IIIb**, were apparent in the mass spectrum of 3-methyl-aminotriols **IVa,b** (m/z 667, 432, 372, 312). The identification of the proposed stereoisomers of aminotriol and 3-methyl-aminotriol in both analyses, HTGC–MS and HPLC–MS, helps to exclude an artificial production of the novel described amino-BHPs. Moreover, HTGC–MS spectra confirmed the structure of aminotriol **III** and 3-methyl-aminotriol **IV** under EI conditions.

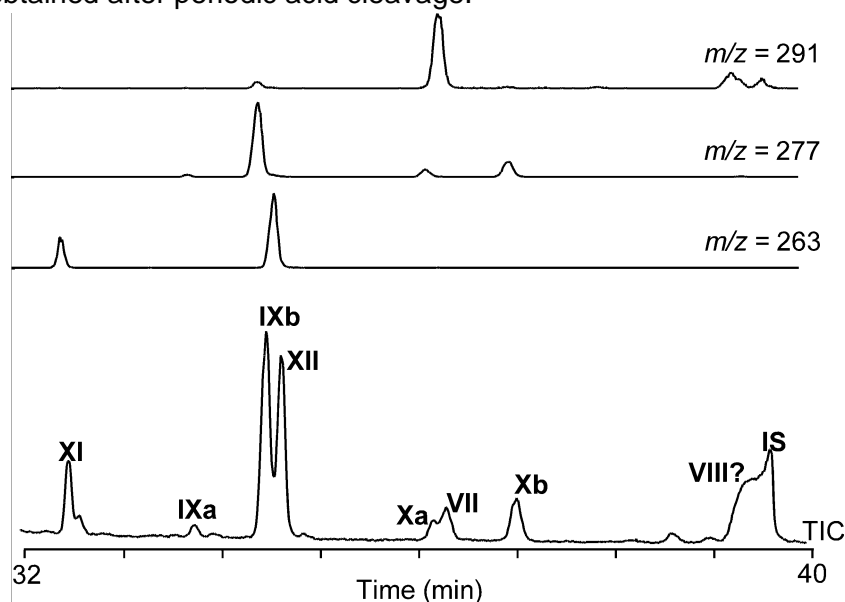
The stereochemistry of both identified isomers of aminotriol **IIIa,b** and 3-methyl-aminotriol **IVa,b** could not be clarified with HTGC–MS and HPLC–MS either, due to low contents. Typically, the spectra of the biological stereoisomers 17 β (H),21 β (H) of common hopanes exhibit a stronger response for the ring D + E + side chain fragment (m/z 492) than for the ring A + B fragment (m/z 191 for aminotriol or m/z 205 for 3-methyl-aminotriol), although this reasoning does not necessarily extend to all related hopanoids (Peters et al., 2004b). In this study, all isomers identified in HTGC–MS showed a ring A + B fragment dominating over the D + E + side chain fragment, however no evidence was found for the presence of isomers with another configuration than the biological 17 β (H),21 β (H) stereoisomer.

In the cultures of *M. alcaliphilum*, the two isomers of aminotriol **IIIa,b** and 3-methyl-aminotriol **IVa,b** are probably best explained by isomerization at the chiral centers of the side chain. The isomers are most likely C-32 epimers, since the two isomers of aminotriol and two isomers of 3-methyl-aminotriol were present in most samples after periodic acid cleavage (Fig. 3.5). Periodic acid cleavage of aminotriol produces C₃₂ 17 β (H),21 β (H)-hopanol **IX** (bishomohopanol). Consequently, isomers at positions C-33, C-34, and C-35 would have been lost after cleavage, resulting in one single isomer of C₃₂ 17 β (H),21 β (H)-hopanol. The same holds true for 3-methyl-aminotriol. The formation of $\beta\beta$ isomers of aminotriol and methylated homologues (at C-2 position) have been previously described in cultures of the purple non-sulfur bacterium *Rhodospseudomonas palustris* TIE-1, although only after artificial maturation (170°C, 120 MPa; see Eickhoff et al., 2014). In great contrast to the artificial production of

isomers in experiments with *R. palustris* TIE-1, the stereoisomers in cultures of *M. alcaliphilum* were produced at optimum temperature and pressure conditions and not as product of degradation experiments.

The production of BHP isomers in bacteria is common. Isomers of bacteriohopanetetrol (aminotriol equivalent N-free BHP) have been previously reported in a variety of bacterial cultures (e.g., *Komagataeibacter xylinus*, *Frankia sp.*, *Methylocella palustris*, '*Ca. Brocadia sp.*', '*Ca. Scalindua profunda*' and '*Ca. Scalindua brodeae*'; Rush et al., 2014; Schwartz-Narbonne et al., 2020).

Figure 3.5 Partial GC–MS chromatograms (m/z 291; m/z 277; m/z 263) of hopanol products obtained after periodic acid cleavage.



Notes: Aminotetrol yielded homohopanol **XI**, 3-methyl-aminotetrol yielded 3-methyl-homohopanol **XII**, aminotriols yielded bishomohopanol **IX**, 3-methyl-aminotriols yielded 3-methyl-bishomohopanol **X**, and aminodiols yielded tentatively identified trishomohopanol **VII**. **VIII** = tentatively identified 3-methyl-trishomohopanol (hopanol product of 3-methyl-aminodiols) coeluted with the internal standard (IS)

3.4.2 Effect of salinity and nitrate concentration on growth rates

M. alcaliphilum is a haloalkaliphilic aerobic methanotrophic bacterium belonging to the Type I methanotrophs. *M. alcaliphilum* strains grow optimally at NaCl concentration of 3% (Kalyuzhnaya et al., 2019), and a nitrogen source (KNO_3) concentration of 10 mM (0.1%) is recommended. Here, *M. alcaliphilum* was grown under four different conditions, standard conditions (3% salinity, 10 mM KNO_3), high nitrate concentration (100 mM KNO_3), low salinity (1%) and high salinity (8.7%). All conditions were chosen arbitrarily considering the range of conditions tolerated by the strain (Kalyuzhnaya et

al., 2008). Growth rates (Table 3.1, Equation 3.1) were highest for the experiments with low salinity and high nitrate concentration, while the experiment at high salinity yielded the slowest growth rate. Lag phases (See growth curves in Fig. B.1, Appendix B) were also shorter for experiments grown at low salinity, high nitrate concentrations, and standard conditions, while they were longer for the experiment with high salinity, suggesting poor growth or a long period of adaptation to the condition (Tays et al., 2018). Growth rates (α) were calculated from two data points on the growth curve (covering an interval of logarithmic growth) using the equation 3.1.

$$\alpha = \frac{\ln\left(\frac{N_T}{N_0}\right)}{(t_T - t_0)} \quad \text{Eq. 3.1}$$

where t is time, and N is the cell number (defined by $\text{OD}_{600\text{nm}}$) at time t (Tays et al., 2018).

Table 3.1 Growth rates for each condition tested

Experiment	Growth rate (1/h)
3% NaCl, 100 mM KNO ₃	3.90E-02
1% NaCl, 10 mM KNO ₃	3.17E-02
8.7% NaCl, 10 mM KNO ₃	1.32E-02
3% NaCl, 10 mM KNO ₃	2.08E-02

3.4.3 Effect of salinity and nitrate concentration on the pentacyclic triterpenoid inventory

Pentacyclic triterpenoids synthesized by *M. alcaliphilum* comprise (3-methyl **IV**) aminotriol **III**, (3-methyl **VI**) aminotetrol **V**, (3-methyl **XX**) tetrahymanol **XIX**, and minor amounts of (3-methyl **XVIII**) diplopterol **XVII**, (3-methyl **XV**) diploptene **XIII**, and (3-methyl **XVI**) hop-21-ene **XIV** (Table 3.2 and 2.3; Contents of pentacyclic triterpenoids of single experiments can be found in Tables B.1 and B.2, Appendix B). However, hop-21-ene **XIV** (and its 3-methylhomologue **XVI**), as well as other hopenes such as, hop-17(21)-ene, and neohop-13(18)-ene (Eickhoff et al., 2013a), apparently formed by dehydration of diplopterol **XVII** during injection on the GC-MS via PTV or split/splitless injection and are not produced by the bacteria (Sessions et al., 2013). Given the natural variation typical for culture experiments and the fact that the experiments of this study were prepared from different batches of freshly prepared starter cultures, a certain variability in the data is to be expected. Still, the standard deviation for some of the compounds is too high, precluding a meaningful comparison. Furthermore, cell

numbers (OD_{600}) were determined for one replicate under each culture condition only; it is therefore possibly that samples were harvested during different growth phases.

Table 3.2 Contents of pentacyclic triterpenoids in cultures of *M. alcaliphilum* grown at different salinities

Compound	1% NaCl (n=3)		3% NaCl (n=3)	
	Content ($\mu\text{g/g dw}$)	SD	Content ($\mu\text{g/g dw}$)	SD
diploptene XIII	28	12	21	6
hop-21-ene XIV	16	6	10	3
3-me-diploptene XV	6	3	5	2
3-me-hop-21-ene XVI	2	0	3	1
diplopterol XVII	72	39	40	22
3-me-diplopterol XVIII	15	1	12	5
tetrahymanol XIX	55	2	50	14
3-me-tetrahymanol XX	2	1	4	2
Aminodiol I *	12	4	0	0
aminotriol a IIIa *	9	1	3	5
aminotriol b IIIb *	420	243	172	34
3-me-aminotriol a IVa *	71	28	8	6
3-me-aminotriol b IVb *	117	70	63	20
aminotetrol V *	93	49	40	8
3-me-aminotetrol VI *	127	52	114	26
Sum pentacyclic triterpenoids	1045	413	544	88
3-me-diploptene/diploptene	0.20	0.03	0.23	0.04
3-me-diplopterol/diplopterol	0.18	0.04	0.29	0.04
3-me-tetrahymanol/tetrahymanol	0.03	0.01	0.09	0.01
3-me-aminotriol/aminotriol b	0.28	0.04	0.37	0.04
3-me-aminotetrol/aminotetrol	1.35	0.49	2.87	0.13
3-methylhopanoids/hopanoids	0.43	0.10	0.77	0.03

* BHPs were measured as products of periodic acid cleavage (aminotetrol yielded homohopanol, aminotriols yielded bishomohopanols, aminodiol yielded trishomohopanol). Bold values show statistically significant difference with respect to standard growing conditions (3% NaCl) using unpaired *t*-test ($\alpha < 0.05$). SD = standard deviation; dw = dry weight. Lipid structures are shown in Table B.2, Appendix B

For consistency with the section 'Novel N-containing BHPs', BHPs are referred to by the name of the intact compounds, even if the reported contents correspond to the measurement of hopanol cleavage products (see also section 3.3.3). The periodic acid cleavage procedure yielded C_{32} $17\beta(H),21\beta(H)$ -hopanol (bishomohopanol **IX**) from tetrafunctionalized BHPs and C_{31} $17\beta(H),21\beta(H)$ -hopanol (homohopanol **XI**) from pentafunctionalized BHPs. Since the only tetrafunctionalized and pentafunctionalized BHPs produced by *M. alcaliphilum* are aminotriol **III** and aminotetrol **V**, respectively, the bishomohopanol **IX** and homohopanol **XI** (and their respective methyl

homologues) derived exclusively from these compounds (Fig. 3.5). Minor amounts of 17 β (H),21 β (H)-33-hopanol (trishomohopanol **VII**) in samples grown at high nitrate and low salinity are interpreted as cleavage product of aminodiol (BHP-560 **I**).

Table 3.3 Contents of pentacyclic triterpenoids in cultures of *M. alcaliphilum* grown with varying amounts of nitrate

Compound	10 mM KNO ₃ (n=3)		100 mM KNO ₃ (n=3)	
	Content (µg/g dw)	SD	Content (µg/g dw)	SD
diploptene XIII	21	6	18	7
hop-21-ene XIV	10	3	9	3
3-me-diploptene XV	5	2	8	7
3-me-hop-21-ene XVI	3	1	2	0
diplopterol XVII	40	22	47	0
3-me-diplopterol XVIII	12	5	23	21
tetrahymanol XIX	50	14	136	92
3-me-tetrahymanol XX	4	2	19	19
aminodiol I *	0	0	2 [#]	1
aminotriol a IIIa *	3	5	27	14
aminotriol b IIIb *	172	34	467	159
3-me-aminotriol a IVa *	8	6	4 [#]	2
3-me-aminotriol b IVb *	63	20	140	30
aminotetrol V *	40	8	90	69
3-me-aminotetrol VI *	114	26	267	200
sum pentacyclic triterpenoids	544	88	1239	608
3-me-diploptene/diploptene	0.23	0.04	0.43	0.25
3-me-diplopterol/diplopterol	0.29	0.04	0.49	0.36
3-me-tetrahymanol/tetrahymanol	0.09	0.01	0.14	0.05
3-me-aminotriol/aminotriol b	0.37	0.04	0.30	0.05
3-me-aminotetrol/aminotetrol	2.87	0.13	2.97	0.14
3-methyhopanoids/hopanoids	0.77	0.03	0.87	0.11

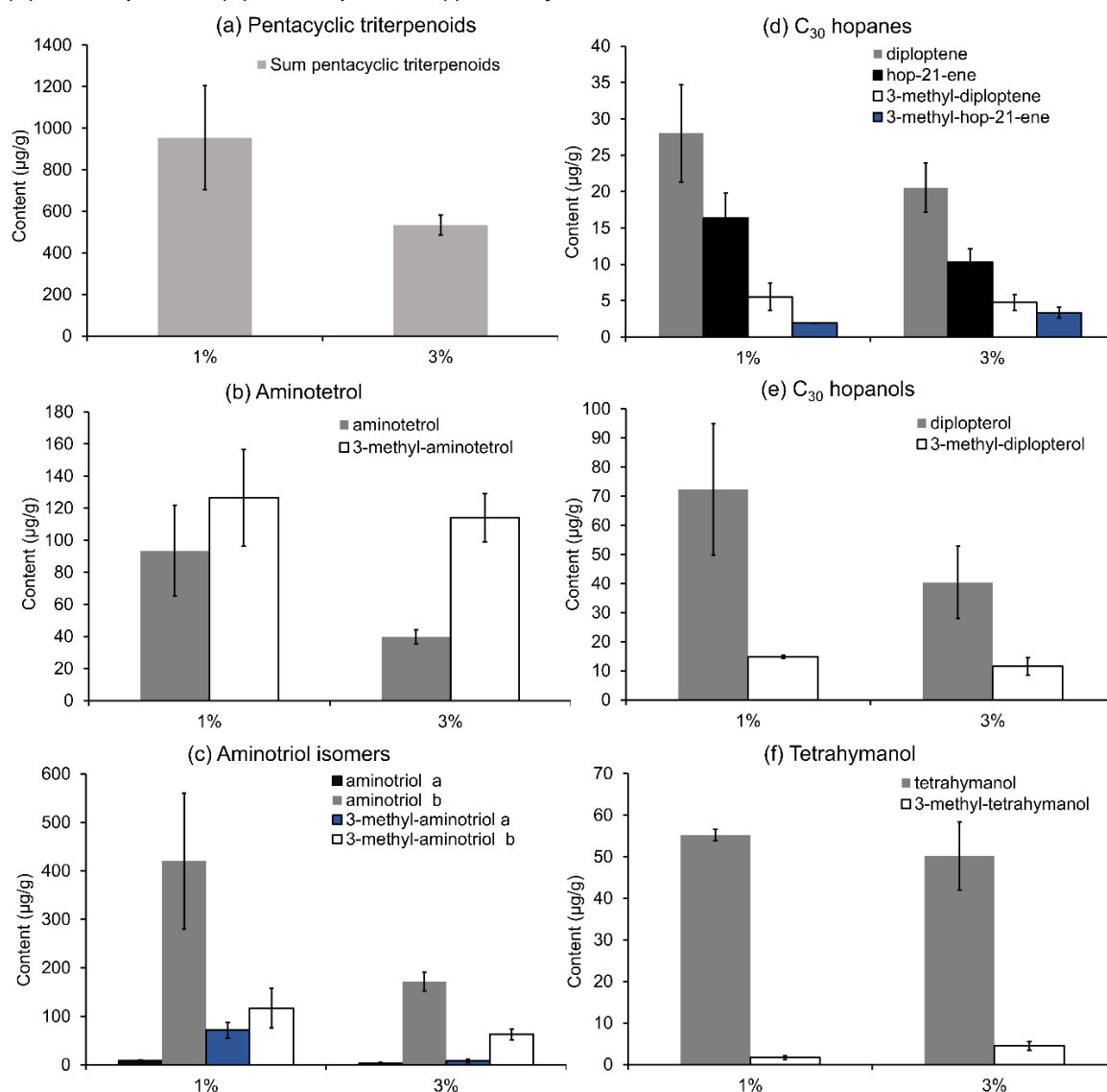
* BHPs were measured as products of periodic acid cleavage (aminotetrol yielded homohopanol, aminotriols yielded bishomohopanols, aminodiol yielded trishomohopanol). Bold numbers indicate statistically significant differences to standard growth conditions (10 mM KNO₃) using unpaired *t*-test ($\alpha < 0.05$). SD = standard deviation; dw = dry weight. Lipid structures are shown in Table B.2, Appendix B

Average of 2 samples

In experiments at different salinities, the total amount of pentacyclic triterpenoids decreased with increasing salinity (Fig. 3.6a, Table 3.2), suggesting that hopanoid production in *M. alcaliphilum* is higher at lower salinities. The overall contents of pentacyclic triterpenoids produced at 8.7% NaCl (maximum salinity tolerance, Kalyuzhnaya et al., 2008) could not be determined since contents were too low (no measurements on the GC-FID were possible). However, measurement of BHPs on the

HPLC–MS (Fig. 3.1) revealed that under high salinity conditions *M. alcaliphilum* produced less hopanoids than under standard (3%) and low salinity (1%) conditions. Experiments at 8.7% NaCl also gave the slowest growth rates (Table 3.1), indicating reduced activity of *M. alcaliphilum* under such conditions. Reduced activity of *M. alcaliphilum* at higher salinity is consistent with experiments performed by Sherry et al. (2016) on sediments from the River Tyne estuary, UK, hosting a diverse community of methanotrophic bacteria, where methanotrophic activity and methane oxidation rates decreased with increasing salinity.

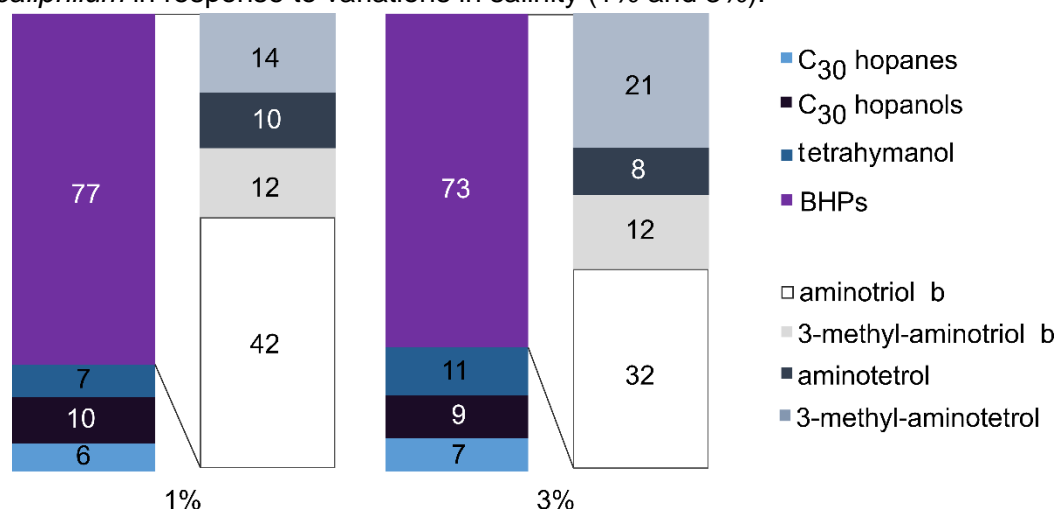
Figure 3.6 Distribution of pentacyclic triterpenoids in response to variations in salinity (1% and 3%): (a) total pentacyclic triterpenoids, (b) aminotetrol, (c) aminotriol isomers, (d) C₃₀ hopanes, (e) C₃₀ hopanols, (f) tetrahymanol.



Notes: BHPs were measured as products of periodic acid cleavage (aminotetrol yielded homohopanol, aminotriols yielded bishomohopanol). Error bars represent standard errors for n = 3 replicates.

In our experiments most hopanoids were produced at the lowest salinity (1% NaCl; Fig. 3.6), with highest contents of aminotriols **IIIa,b** and the corresponding 3-methylhomologues **IVa,b** (Fig. 3.6c), and 3-methyl-aminotetrol **VI**, and tetrahymanol **XIX** with lowest contents (Fig. 2.6b,f). According to statistical analysis (unpaired *t*-test; *p* values from *t*-tests can be found in Table B.3, Appendix B), only 3-methyl-aminotriol **a IIIa** varied significantly between different culture conditions. More relevant than changes of the absolute content of a specific hopanoid are changes of the proportion of this molecule to the considered class of compounds at varying salinities (Fig. 3.7); i.e., the relative abundance of a compound. The relative abundances of C₃₀ hopanoids and C₃₀ hopanols were similar under the two conditions tested. Tetrahymanol **XIX** showed an increase of 4% in experiments with 3% NaCl, while the proportion of BHPs decreased by 3%. Tetrahymanol – and its degradation product gammacerane – are commonly used as biomarkers for stratification of the water column; these compounds were also suggested to indicate hypersaline conditions in stratified water bodies (Sinninghe Damsté et al., 1995a; Peters et al., 2004b; Banta et al., 2015). Our results confirm that an increase of salinity indeed favors the synthesis of tetrahymanol **XIX** at the expense of hopanoids. Even though aerobic methanotrophic bacteria are not the only known producers of tetrahymanol (Werne et al., 2002; Rashby et al., 2007; Eickhoff et al., 2013b), all tetrahymanol producers seem to have in common that they live at oxic-anoxic interfaces or high salinities.

Figure 3.7 Relative abundance in percent of main pentacyclic triterpenoids of *M. alcaliphilum* in response to variations in salinity (1% and 3%).



Notes: BHPs were measured as products of periodic acid cleavage (aminotetrol yielded homohopanol, aminotriol yielded bishomohopanol). Novel compounds (aminodiol, aminotriol a, and 3-methyl-aminotriol a) were excluded from calculations due to low contents

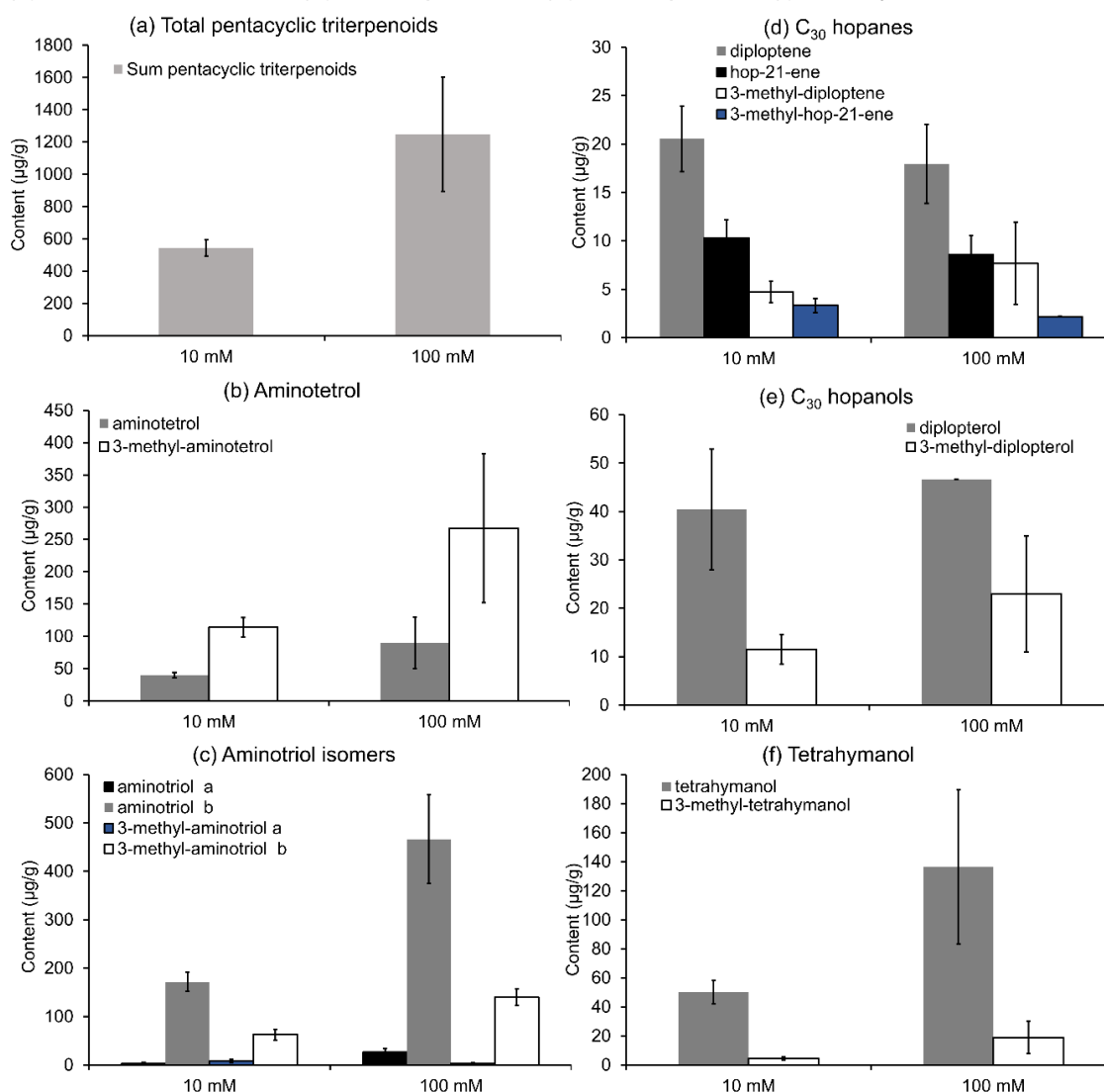
The results of this study indicate that low salinities favor the formation of BHPs (Fig. 3.7), especially formation of the regular aminotriol **IIIb**, which showed a relative increase of 10% at 1% NaCl. Interestingly, 3-methyl-aminotetrol **VI**, which is among the most specific biomarkers of aerobic methanotrophic bacteria (Talbot et al., 2014), showed a relative increase of 7% in the 3% NaCl experiments, consistent with an increase of the 3-methyl to desmethylated homologues ratio at 3% salinity (Table 3.2). Such increased production of 3-methyl compounds is possibly an adaptive response to more extreme conditions, since 3-methylhopanoids were shown to play an important role in maintaining the cell membrane integrity under unfavorable conditions in mesocosm experiments (Osborne et al., 2017).

In experiments with high nitrate level, total contents of pentacyclic triterpenoids increased (Fig. 3.8a, Table 3.3). Particularly BHP contents increased (Fig. 3.8b-c), especially the aminotriol isomers **IIIa** and **b**, as well as 3-methyl-aminotriol **IVb** (Fig. 3.8c). Contents of these compounds were more than doubled compared to standard culture conditions (Table 3.3, unpaired *t*-test; *p* values from *t*-tests can be found in Table B.3, Appendix B). For some compounds (namely hopanoids, hopanols, tetrahymanol, and aminotetrol), the standard deviation is unfortunately too high – even considering the natural variability typically associated to culture experiments – to make robust interpretations regarding the behavior of these lipids at different nitrate concentrations.

Considering the relative percentages of compounds, all BHPs showed an increase of 7%, regular aminotriol **IIIb** increased by 8%, while relative contents of aminotetrol **V**, 3-methyl-aminotetrol **VI**, and 3-methyl-aminotriol **IVb** remained similar at higher nitrate concentrations (not shown). This may suggest that higher BHP contents at higher nitrate concentration are especially related to an increased production of aminotriol. To date, few studies have been undertaken to understand the role of nitrate in hopanoid production, specifically in hopanoid-producing bacteria capable of nitrogen fixation (*Frankia sp.* Nalin et al., 2000; *Nostoc punctiforme* Doughty et al., 2009; *Desulfovibrio bastinii* Blumenberg et al., 2012). For instance, experiments with strains of *Frankia sp.*, under nitrogen-enriched (NH₄⁺) and nitrogen-depleted (nitrogen fixation) conditions, revealed that BHP contents in most of the strains were slightly higher under nitrogen-enriched conditions (Nalin et al., 2000). In the cyanobacterium *N. punctiforme*, nitrogen limitation enhanced BHP production as a survival mechanism during the first two weeks of incubation, returning afterwards to the starting levels encountered during standard conditions (Doughty et al., 2009). A similar study with the

sulfate-reducing bacterium *D. bastinii*, grown with NH_4^+ or N_2 as sole nitrogen source, found that nitrogen conditions do not much affect hopanoid composition, although the growth yield was higher with NH_4 as nitrogen source (Blumenberg et al., 2012). The conflicting results of these studies argue against a direct link between hopanoid production and nitrogen uptake. Instead hopanoid production is more likely related to physiological processes reflecting adaptation. Although we are only able to use some of the data of the nitrate experiments for a statistically sound comparison, the results of this study are in line with some of the earlier studies, documenting a strong positive response in BHP production to increased nitrate concentrations.

Figure 3.8 Distribution of pentacyclic triterpenoids in response to variations in nitrate concentration (10 mM and 100 mM): (a) total pentacyclic triterpenoids, (b) aminotetrol, (c) aminotriol isomers, (d) C_{30} hopanoids, (e) C_{30} hopanols, (f) tetrahymanol.



Notes: BHPs were measured as products of periodic acid cleavage (aminotetrol yielded homohopanols, aminotriols yielded bishomohopanols). Error bars represent standard errors for n = 3 replicates per condition.

The ratio of 3-methyl to desmethyl homologues tended to increase slightly in high nitrate experiments too. This applies to C₃₀ hopanoids, tetrahymanol, and aminotetrol as well, but this ratio decreased for aminotriol b (Table 3.3). The effect of the culture conditions on hopanoid methylation seems to have been a minor variable under the chosen conditions, although it has been shown that the degree of methylation influences membrane stability as well (Doughty et al., 2009; Welander et al., 2009). Future experiments on the factors governing lipid production by aerobic methanotrophs should expand the range of environmental conditions to better constrain the patterns in the response of methanotrophs to changing conditions.

3.5 Conclusions

Besides previously reported BHPs, *M. alcaliphilum* was shown to synthesize four novel N-containing BHPs identified as aminodiol, 3-methyl-aminodiol, and early eluting isomers of aminotriol and 3-methyl-aminotriol. When grown at different salinities and nitrate concentrations, *M. alcaliphilum* strains revealed higher growth rates and shorter lag phases at lower salinity (1% NaCl) and higher nitrate concentration (100 mM). Our results also demonstrate an effect of salinity and nitrate concentration on the abundance and composition of pentacyclic triterpenoids. Hopanoid abundance was found to be higher in low salinity experiments (1% NaCl). Likewise, low salinity settings favored the production of BHPs, especially that of regular aminotriol b, while higher salinity (3% NaCl) favored the synthesis of tetrahymanol and 3-methyl-aminotetrol. Production of 3-methyl compounds was favored at higher salinity as well, reflected in an increase in the ratio of methylated to desmethylated compounds. In experiments with varying nitrate concentrations, higher concentrations correlated with more production of BHPs (aminotriol and 3-methyl-aminotriol).

4. Chapter IV

Carbonate corrosion at marine methane seeps induced by aerobic methanotrophy

Cordova-Gonzalez A., Birgel D., Wisshak M., Urich T., Brinkmann F., Marcon Y., Bohrmann G. & Peckmann J. A carbonate corrosion experiment at a marine methane seep: The role of aerobic methanotrophic bacteria. (Ready for submission to Geobiology)

4.1 Abstract

Methane seeps are typified by the formation of authigenic carbonates, many of which exhibit corrosion surfaces and secondary porosity believed to be caused by microbial carbonate dissolution. Aerobic methane oxidation and sulfur oxidation are two processes capable of inducing carbonate corrosion at methane seeps. Although the potential of aerobic methanotrophy to dissolve carbonate was confirmed in laboratory experiments, this process has not been studied in the environment to date. Here, we report on a carbonate corrosion experiment carried out in the REGAB Pockmark, Gabon-Congo-Angola passive margin, in which marble cubes were deployed for 2.5 years at locations with and without methane seepage. Marble cubes exposed to active seepage (experiment CAB-C) were found to be affected by a new type of microbioerosion. Based on 16S rRNA assays, the biofilms adhering to the bioeroded marble mostly consisted of aerobic methanotrophic bacteria, predominantly belonging to the uncultured Hyd24-01 clade. The presence of abundant ¹³C-depleted lipid biomarkers including fatty acids (*n*-C_{16:1ω8c}, *n*-C_{18:1ω8c}, *n*-C_{16:1ω5t}), 4-methyl sterols, and diplopterol agrees with the dominance of aerobic methanotrophs in the CAB-C biofilms. Among the lipids of aerobic methanotrophs, the uncommon 4α-

methylcholest-8(14)-en-3 β ,25-diol is interpreted to be a specific biomarker for the Hyd24-01 clade. The combination of textural, genetic, and organic geochemical evidence suggests that aerobic methanotrophs are the main drivers of carbonate dissolution above the seabed at the REGAB seeps. This study highlights the importance of biogeochemical processes for the marine carbon cycle and calls for more studies aiming to quantify the carbon flux from marine sediment to the water column at seeps.

4.2 Introduction

The dynamics of methane seeps have been studied in great detail since this carbon pool may play an important role in global climate change (Kennett et al., 2003) and potentially as energy source (Sloan, 2003). Methane seeps occur along passive and active continental margins, associated with geological features, as for example, gas hydrates, pockmarks and mud volcanoes (Suess, 2014). It has been shown that many seeps are related to gas hydrate dynamics (Elvert et al., 1999; Suess et al., 1999). The stability of gas hydrate depends on the conditions at the seafloor and in the subsurface, such as temperature, pressure, and the availability of water and gas, predominantly methane (Bohrmann & Torres, 2006). If bottom water temperature increases, gas hydrates may dissociate rapidly and gas bubbles escape from the seafloor to the water column—the so-called clathrate gun hypothesis introduced by Kennett et al. (2003)—forming methane seeps. Methane seeps, which are active over long time, are further characterized by the formation of authigenic methane-derived carbonate (e.g., Bohrmann et al., 1998; Peckmann et al., 2001; Greinert et al., 2013), commonly precipitating in anoxic sediments affected by seepage. Seep carbonate is the result of an increase in alkalinity induced by the anaerobic oxidation of methane (AOM; Peckmann & Thiel, 2004), a process mediated by a consortium of methane-oxidizing archaea and sulfate-reducing bacteria (Boetius et al., 2000). Seep carbonates have a global distribution, including numerous recent and ancient deposits (Campbell, 2006 for a review). Although AOM is favoring carbonate precipitation, many seep carbonates exhibit corrosion surfaces and secondary porosity, likely caused by microbially induced carbonate dissolution (e.g., Matsumoto, 1990; Campbell et al., 2002; Birgel et al., 2006a; Himmler et al., 2011; Cr mi re et al., 2012; Natalicchio et al., 2015).

Carbonate dissolution in the marine realm has received much attention because it is a key process in global carbon cycling (Subhas et al., 2017; Naviaux et al., 2019).

However, the role of microbes in carbonate dissolution has received little attention to date (Krause et al., 2014). The two biological processes that have been put forward to induce carbonate corrosion at seeps are aerobic methane oxidation (Matsumoto, 1990; Cai et al., 2006; Himmler et al., 2011; Crémière et al., 2012; Natalicchio et al., 2015) and hydrogen sulfide oxidation (Crémière et al., 2012; Leprich et al., 2021). Both processes can locally lower pH, resulting in carbonate dissolution (Crémière et al., 2012). In particular, aerobic methane oxidation leads to the production of carbon dioxide, with a subsequent increase of $p\text{CO}_2$, favoring the dissolution of carbonate (Equation 4.1; Aloisi et al., 2000). The influence of aerobic methanotrophy on carbonate dissolution has already been confirmed in closed-system experiments with the Type II methanotrophic bacterial strain *Methylosinus trichosporium* OB3b, demonstrating that aerobic methanotrophs have the potential to enhance carbonate dissolution and induce corrosion (Krause et al., 2014).



Lipid biomarkers are a powerful tool to identify and classify aerobic methanotrophic bacteria in modern environments and in the rock record (Cordova-Gonzalez et al., 2020 and references therein). Biomarkers of aerobic methanotrophic bacteria are typically ^{13}C -depleted to different degrees (Jahnke et al., 1999), providing additional evidence for an assignment to this group of source organisms. One example of seep carbonates with the coincidence of extensive corrosion features and abundant lipids of aerobic methanotrophic bacteria stems from northern Istria, Croatia (Natalicchio et al., 2015). The Istrian Eocene carbonates were found to contain characteristic ^{13}C -depleted lanostanes ($\delta^{13}\text{C}$: -47‰), degradation products of 4-methyl sterols of methanotrophic bacteria (Bouvier et al., 1976; Schouten et al., 2000; Cordova-Gonzalez et al., 2020). Another example with the same coincidence of rock fabric and biomarker inventory are the Cretaceous Tepee Buttes of the Western Interior Seaway (Birgel et al., 2006a), which were found to contain rearranged ^{13}C -depleted hopanoids produced by thermal alteration (e.g. C34-8 α (H),14 α (H)-secohexahydrobenzohopane, $\delta^{13}\text{C}$: -110‰) of bacteriohopanepolyols of aerobic methanotrophs ((Talbot et al., 2001). Besides hopanoids and regular sterols, diagnostic biomarkers of aerobic methanotrophs include a suit of unsaturated and monounsaturated fatty acids with double bond positions at $\omega 5$, $\omega 7$, and $\omega 8$ (Hanson & Hanson, 1996). The common occurrence of characteristic lipids of aerobic methanotrophs in seep carbonates and sediments (Birgel et al., 2006b, 2011; Birgel & Peckmann, 2008; Elvert & Niemann,

2008; Kellermann et al., 2012; Himmler et al., 2015) confirms that aerobic methanotrophy is a prominent process in methane seep environments. However, the effect of aerobic methanotrophy on carbonate dissolution in natural environments is currently only based on circumstantial evidence.

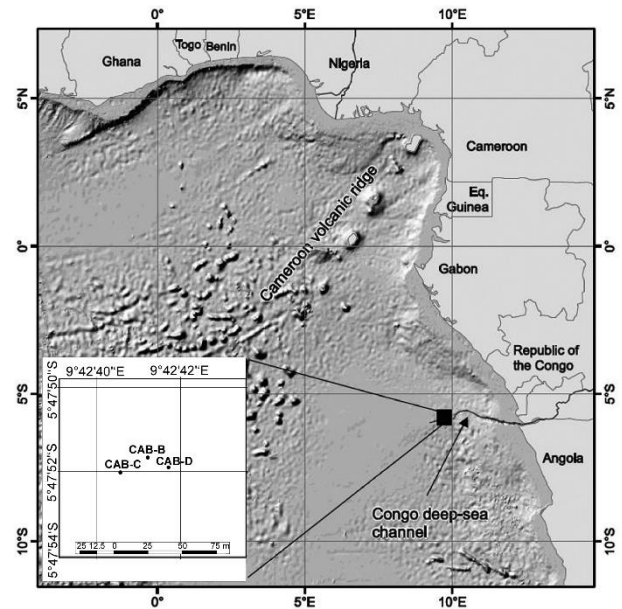
Here we report on a corrosion and bioerosion experiment using limestone cubes deployed for 2.5 years at three locations within the REGAB seep field of the Gabon-Congo-Angola passive margin, including a mussel bed, a site with outcropping methane hydrate and active seepage, and a site with no apparent seepage for comparison. After sample recovery, adhering biofilms were scraped off the cubes, and were analyzed by 16S rRNA sequencing and for their lipid biomarker inventories. The surfaces of cubes were inspected for carbonate corrosion and bioerosion, by identifying traces of microbioerosion on the limestone surfaces and in epoxy casts thereof using scanning electron microscopy. The combination of obtained data allows us to make a case for carbonate corrosion caused by aerobic methanotrophic bacteria, supporting the hypothesis of aerobic methanotrophy as one of the triggers of carbonate corrosion at marine methane seeps.

4.3 Geological setting

The giant REGAB Pockmark is an active seep field located at approximately 3160 m water depth on the Gabon-Congo-Angola passive margin, about 10 km to the north of the Congo deep-sea channel (Fig. 4.1; Ondréas et al., 2005). The elliptical structure with diameters ranging between 700 and 950 m is composed of numerous depressions which are 0.5 to 15 m deeper than the surrounding seafloor (Marcon et al., 2014a). Remotely operated vehicle-borne micro-bathymetry and backscatter data of the entire structure, and high-resolution photo-mosaicking, side-scan sonar mapping of gas emissions, and maps of faunal distribution as well as of carbonate crust occurrence were combined to provide detailed information on fluid flow regimes in the subsurface (Marcon et al., 2014a). One prominent feature of the REGAB Pockmark is the presence of abundant authigenic carbonate (Ondréas et al., 2005; Pierre & Fouquet, 2007). Seismic profiles showed that the REGAB Pockmark is linked to a deep channel system that acts as a reservoir for seeping fluids by a 300-m deep chimney rooted in the channels, along which gas escapes (Ondréas et al., 2005). Gas seepage has been observed at several locations, and gas hydrates have been detected in the shallow subsurface at depths of 6 m or outcropping on the seafloor (Olu-Le Roy et al., 2007). The gas hydrates are composed mainly of biogenic

methane (up to 99%) and traces of other gases, such as carbon dioxide, ethane, and hydrogen sulfide (Charlou et al., 2004), which sustain an abundant and diverse population of megafauna and microbial communities, including aerobic and anaerobic methanotrophs (Bouloubassi et al., 2009; Marcon et al., 2014b).

Figure 4.1 Location of the study area within the REGAB Pockmark



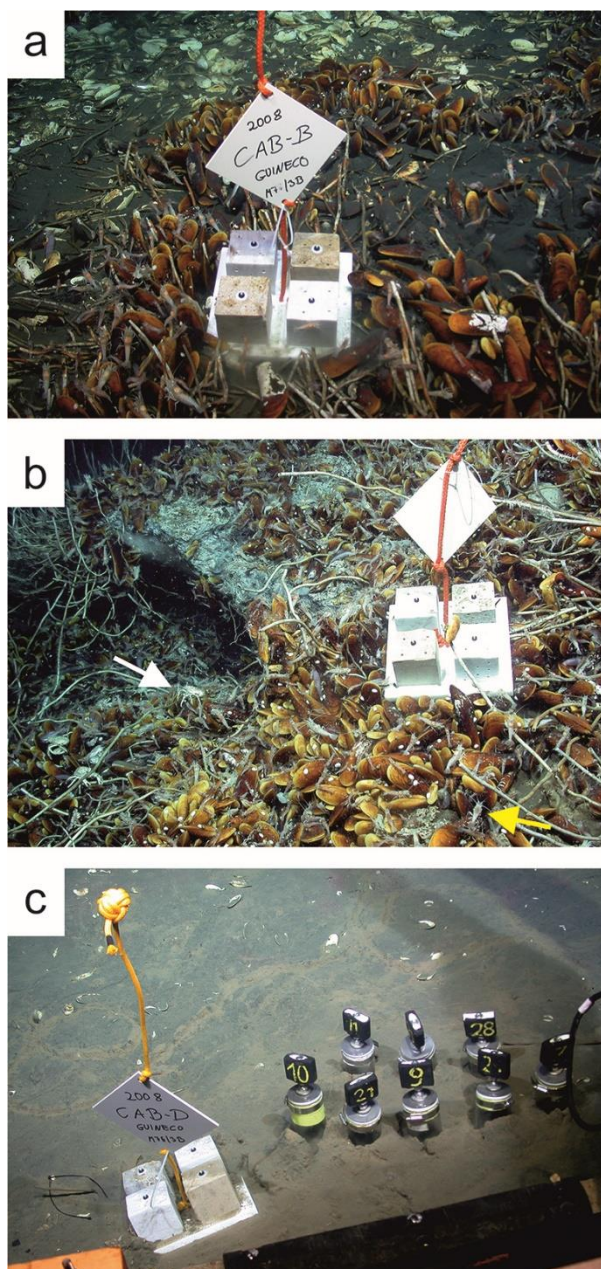
Source: modified from Marcon et al. (2014b).

4.4 Methods

Non-seep carbonate samples were deployed in three habitats within the REGAB seep field (Congo area) at ca. 3170 m water depth as part of the “corrosion and bioerosion” (CAB) carbonate experiments launched during cruise GUINECO M76/3b with the research vessel *Meteor* in July-August 2008 (Fig. 4.2; Zabel et al., 2012). Each of the experiments were comprised of four limestone cubes with 10 cm side length, including two cubes of marble and two cubes of fossiliferous limestone (Fig. 4.2). Experiment CAB-B was deployed in a mussel bed, experiment CAB-C was placed on gas hydrate at a site of active seepage and abundant chemosymbiotic benthos, and experiment CAB-D was deployed on the seafloor at a site where no evidence of seepage was recognized. Before deployment, the limestone cubes had been fixed on a square-cut plastic board (edge length 25 cm), which was regularly pierced by drill holes to allow for fluid flow through the equidistantly pierced limestone cubes. Each of the limestone cubes was pierced by four vertical drill holes and attached to the plastic board by a central metal screw. The samples were retrieved in January-February 2011 during the West Africa Cold Seeps (WACS) cruise aboard the R/V *Pourquoi Pas?* (Olu, 2011). For this study, only the marble cubes have been used. The marble cubes were divided

into subsamples for petrographic, 16S rRNA sequencing, and organic geochemical analyses.

Figure 4.2 Carbonate experiments with four limestone cubes each, deployed for 2.5 years within the REGAB Pockmark in the Lower Congo Basin at ca. 3170 m water depth. (a) Upon deployment of CAB-B in a mussel bed, gas escaped from the sediment. (b) CAB-C placed onto an active hydrate site with mussels and tubeworms; yellow arrow indicating a shrimp, white arrow pointing to a crab. (c) CAB-D located in a reference area with no apparent seepage activity.



For lipid biomarker analysis, biofilms attached to the carbonate surfaces were scraped off with a scalpel. The surface coatings were gently grounded and hydrolyzed with 6% KOH in methanol to cleave ester-bond lipids, and then extracted with a mixture of dichloromethane/methanol (3:1, v/v) by ultrasonication until the solvents became colorless. An aliquot of the resulting lipid extracts was separated by column chromatography (using aminopropyl-bonded silica gel column) into four fractions: (1) hydrocarbons (n-hexane), (2) ketones (n-hexane/dichloromethane, 3:1, v/v), (3)

alcohols (dichloromethane/acetone, 9:1, v/v), and (4) carboxylic acids ((2% formic acid in dichloromethane; cf. Cordova-Gonzalez et al., 2020). Alcohols were analyzed as trimethylsilyl-ether derivatives and fatty acids as fatty acid methyl esters derivatives (cf. Birgel & Peckmann, 2008). The double bond position of monounsaturated fatty acids was determined by analysis of their dimethyl disulfide adducts following Nichols et al. (1986). A second aliquot of the lipid extract was acetylated by reaction with a mixture of acetic anhydride/pyridine (1:1, v/v) for 1 h at 50 °C for analyses of bacteriohopanepolyols.

Lipid biomarkers were analyzed by means of gas chromatography–flame ionization detection (GC–FID) for quantification and gas chromatography–mass spectrometry (GC–MS) for identification using a Thermo Electron Trace DSQ II instrument at the MARUM, University of Bremen, equipped with a Rxi-5 MS fused silica capillary column (30 m, 0.25 mm inner diameter, 0.25 µm film thickness). The GC temperature program was: injection at 60 °C (1 min) to 150 °C at 10 °C min⁻¹, then from 150 °C to 320 °C at 4 °C min⁻¹, 37 min isothermal. The identification by GC–MS was based on GC retention times and comparison of mass spectra with published data. Internal standards (cholestane, 1-nonadecanol, 2-methyl-octadecanoic acid) with known concentrations were added prior to sample hydrolysis and extraction. Compound-specific carbon isotope analysis was performed using a Thermo Fisher Trace GC Ultra connected via a Thermo Fisher GC Isolink Interface to a Thermo Fisher Delta V Advantage isotope-ratio-monitoring mass spectrometer (IRM–MS), at the Department of Terrestrial Ecosystem Research, University of Vienna, Austria. Compound-specific carbon isotope values are given as δ values in per mil (‰) relative to Vienna Peedee Belemnite (V-PDB). The $\delta^{13}\text{C}$ values of alcohols (TMS-derivatives) and carboxylic acids (methyl esters) were corrected for the additional carbons introduced during derivatization.

The conditions for GC–IRM–MS analyses were identical to those used for GC analyses. Each measurement was calibrated using several pulses of carbon dioxide gas with known composition at the beginning and the end of the run. The precision of measurements was checked with a mixture of n-alkanes (C₁₄–C₃₈) with known isotopic composition. The analytical standard deviation was smaller than 0.4‰.

Screening for bacteriohopanepolyols was done with high-performance liquid chromatography with atmospheric pressure chemical ionization mass spectrometry

(HPLC–APCI–MS), as described in Birgel et al. (2011), at the MARUM, University of Bremen. Briefly, chromatographic separation was achieved using an Agilent 1200 series HPLC system with a flow of 0.2 ml/min and the following linear gradient: 100% A (3 min hold), then ramp to 100% B (at 25 min), isocratic (for 30 min), with A = MeOH:deionized water (90:10, v:v) and B = MeOH:deionized water:propan-2-ol (54:1:45). The oven was equipped with a reversed phase column (Alltech Prevail C₁₈, 150×2.1 mm, 3 µm) and a guard column of the same material (7.5×2.1 mm), and oven temperature was set to 30 °C. Prior to injection, the acetylated aliquots of the total extract were dissolved in 10 µl of MeOH/propan-2-ol (60:40 v/v). A Thermo Finnigan LCQ Deca XP Plus ion trap mass spectrometer with APCI source in positive mode was used for compound identification.

To determine the phylogenetic affiliation of microorganisms, present on surfaces of the marble cubes of experiment CAB-C, we performed sequencing of the 16S rRNA gene. For studying traces of microbial microbioerosion, surfaces of the marble cubes were treated with hydrogen peroxide and cleaned in an ultrasonic bath to remove any organic biofilm. Surfaces were then examined with a Tescan VEGA3 xmu scanning electron microscope (SEM) at 15 keV using a secondary electron detector. Subsamples were embedded in epoxy resin under vacuum conditions in a Struers CitoVac impregnation chamber, followed by dissolution of the carbonate with hydrochloric acid (for further detail, see Wisshak, 2012), yielding epoxy casts with the positive infills of microbioerosion traces that were then visualized with SEM after sputter-coating with gold.

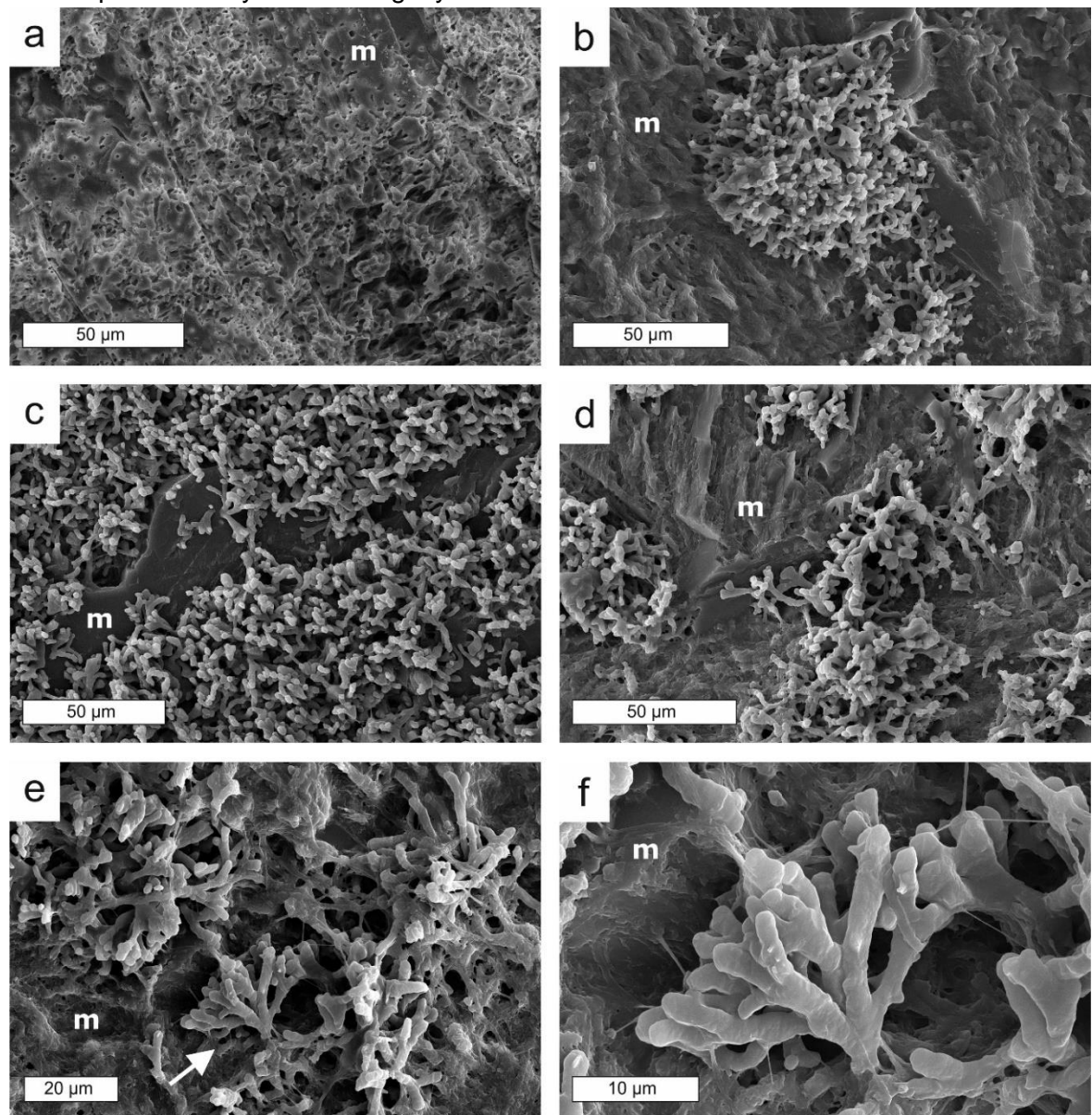
4.5 Results

4.5.1 Carbonate corrosion features

SEM surface examination of the marble cubes of experiment CAB-C showed the pristine coarsely crystalline texture of the carbonate rock and, in places, intense surface pitting indicative of microbioerosion (Fig. 4.3a). Accordingly, the epoxy casts revealed clusters of microborings of a yet unknown morphology (Fig. 4.3b-f). These range from individual, circumradial tunnel systems (Fig. 4.3b) to dense carpets of borings with little or no areas of pristine matrix between (Fig. 4.3c-d). Close-up SEM micrographs showed that individual tunnels are ca. 2 to 3 µm in diameter and radiate from a central point of entry in all directions while repeatedly bi- or trifurcating in acute angles. These tunnels slightly expand towards their rounded terminations that may

reach a diameter of up to 5 μm (Fig. 4.3e-f). This new type of microboring with some affinity to the ichnospecies *Fascichnus bellafurcus* (Radtke et al., 2010), formerly *Abeliella bellafurca* (see Wisshak et al., 2019), is by far the dominant in all the investigated samples, complemented only by very few, larger and strictly prostrate tunnels of the presumed fungal microboring *Orthogonum tubulare* (Radtke, 1991), a ubiquitous bioerosion trace in aphotic marine settings.

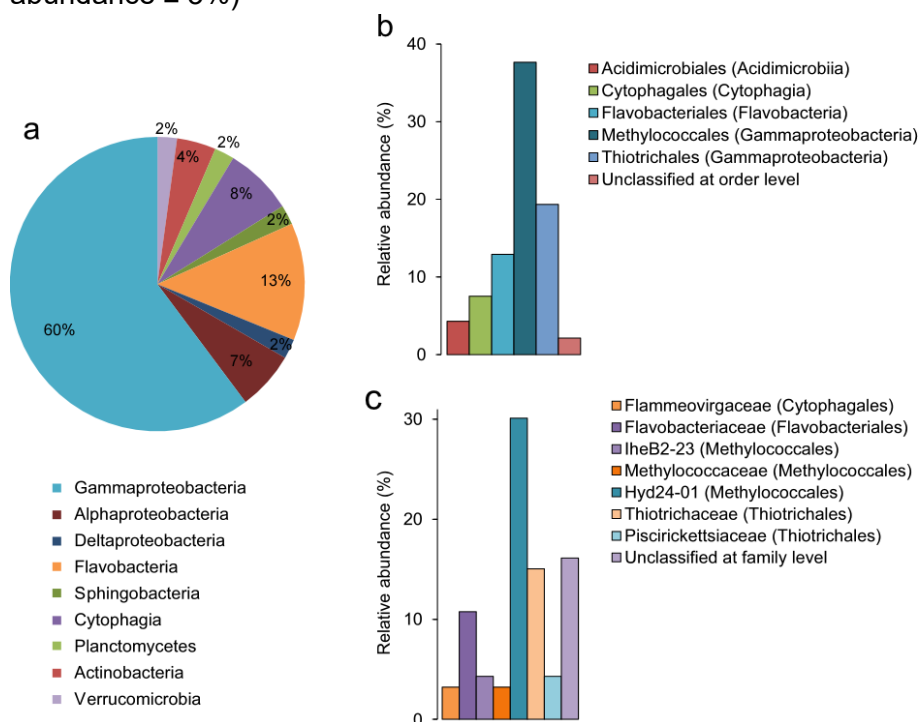
Figure 4.3 Scanning electron imaging of experimental marble substrates CAB-C (a) and epoxy casts thereof (b-f), showing distinctive signs of microbioerosion: (a) intense surface pitting in the coarsely crystalline carbonate matrix (m); (b) epoxy cast with circumradial microboring structure; (c-d) dense clusters of the same type of microborings; (e-f) close-ups of individual tunnels radiating and ramifying from a central point of entry towards slightly widened terminations



4.5.2 Composition of the microbial community

16S rRNA gene sequencing was carried out to decipher the microbial community in the biofilms attached to the corroded surface of the CAB-C carbonate cube from a hydrate-bearing active seep site (Fig. 4.4), for which SEM analyses revealed evidence of microbioerosion. Biofilms were adhering to all cube surfaces exposed to seawater, including the upper surface. A total of 93 bacterial clones was detected (See Table C.1, Appendix C for the full taxonomy). Phylogenetic information shows that Proteobacteria predominate, accounting for 69% of the total clones. Among them, Gammaproteobacteria are the predominant class (60% of total clones; Fig. 4.4a). The majority of the gammaproteobacterial community (Fig. 4.4b) belongs to relatives of aerobic methanotrophs (i.e., Type I methanotrophs) of the order Methylococcales (38% of total clones; Fig. 4.4c). Within this community, most methanotrophs are relatives of the uncultured clade Hyd24-01 (see Fig. 4.4c), followed by relatives of the uncultured clade IheB2-23, and ecotypes of the family Methylococcaceae ((now subdivided in Type Ia Methylomonadaceae and Type Ib Methylococcaceae; Parks et al., 2018), such as members of the genus *Methylomonas* (see Table C.1, Appendix C). Other members of the class Gammaproteobacteria, known to be sulfide-oxidizing bacteria were detected as well, accounting for 21% of the total clones. Detected sulfide-oxidizing bacteria include members of the order *Thiotrichales* (e.g., genera *Leucothrix* and *Thiothrix* of the family Thiotrichaceae) and *Chromatiales* (e.g., genus *Granulosicoccus* of the family Granulosicoccaceae).

Figure 4.4 Diversity and relative abundance (%) of dominant phylogenetic groups in the corroded surface of CAB-C. Each color represents the percentage of the total sample contributed by each taxon group at (a) phylum level, except for Proteobacteria and Bacteroidetes, which are shown by class; (b) order level (dominant phylotypes with relative abundance $\geq 3\%$), (c) family level (dominant phylotypes with relative abundance $\geq 3\%$)



4.5.3 Lipid biomarkers

The lipid biomarker compound inventories of the hydrocarbon, alcohol, and fatty acid fractions of biofilms from the CAB-B, CAB-C, and CAB-D cubes are presented in Table 4.1. Overall, highest contents of lipid biomarkers were detected for CAB-C (277.96 $\mu\text{g/g}$ wet weight), followed by the reference sample CAB-D (61.84 $\mu\text{g/g}$), while lowest contents were found for CAB-B (48.48 $\mu\text{g/g}$). In all samples, fatty acids are the most abundant compounds, representing 87% of all lipid biomarkers in the CAB-B cube, 82% in CAB-C, and 96% in CAB-D. The second largest group are alcohols, representing 12% in CAB-B, 17% in CAB-C, and 3% in CAB-D. Hydrocarbons were detected in trace amounts only in all samples, making up less than 3% of the total lipid biomarkers. Hopanoids and steroids dominate the alcohol and hydrocarbon fractions. Only phospholipid derived fatty acids, released after base hydrolysis, were detected in the carboxylic acid fraction of the three samples. Of particular interest are saturated and monounsaturated fatty acids with 16 and 18 carbon atoms. These compounds are the dominant phospholipid derived fatty acids of aerobic methanotrophs (Hanson &

Hanson, 1996), which are the most abundant fatty acids in the samples (>75% of fatty acid content). The full range of fatty acids is shown in Fig. 4.5. No bacteriohopanepolyols were found in any of the samples.

Table 4.1. Contents ($\mu\text{g/g}$) and $\delta^{13}\text{C}$ (‰ vs V-PDB) values of lipid biomarkers from biofilms attached to CAB-B, CAB-C, and CAB-D cubes

	CAB-B		CAB-C		CAB-D	
	Content ($\mu\text{g/g}$ ww)	$\delta^{13}\text{C}$ (‰ vs V- PDB)	Content ($\mu\text{g/g}$ ww)	$\delta^{13}\text{C}$ (‰ vs V- PDB)	Content ($\mu\text{g/g}$ ww)	$\delta^{13}\text{C}$ (‰ vs V- PDB)
<i>Alcohols</i>						
Cholesterol I	3.13	-58	6.23	-69	1.63	-34
Cholestanol II			0.89	n.m.		
Desmosterol III			12.59	-77		
4 α -Methylcholest-8(14)-en-3 β -ol IV			0.62	n.m.		
24-Methylcholesta-5,24(28)-dien-3 β -ol V	0.57	n.m.	4.14	-76		
4 α -Methylcholesta-8(14),24-dien-3 β -ol VI			10.89	-85		
Lanosterol VII			1.77	-76		
4,4-Dimethylcholesta-8(14),24-dien-3 β -ol VIII			0.30	n.m.		
Cycloartenol IX			2.51	-68		
4 α -Methylcholest-8(14)-en-3 β ,25-diol X			2.00	-77		
Diplopterol XI	1.91	-76	3.20	-84	0.34	-61
17 α (H),21 β (H)-32-hopanol XIIa			1.65			
17 β (H),21 α (H)-32-hopanol XIIb			0.99			
<i>Fatty acids</i>						
<i>n</i> -C _{14:0}	4.17	-51	10.58	-56	6.17	-29
<i>n</i> -C _{16:1ω8c}	8.00	-76	68.51	-69	4.59	-71
<i>n</i> -C _{16:1ω7c}	3.94	-69	39.38	-60	3.47	-60
<i>n</i> -C _{16:1ω6c}	1.30	n.m.	32.24	n.m.	2.65	n.m.
<i>n</i> -C _{16:1ω7t} & 16:1 ω 5c/t*	2.78	n.m.	30.51	n.m.	2167	n.m.
<i>n</i> -C _{16:0}	12.32	-41	34.22	-35	23.47	-32
<i>n</i> -C _{18:1ω9c}	4.20	-33	13.28	-52	8.82	-34
<i>n</i> -C _{18:1ω7c}	4.55	-55	18.69	-66	2.87	coelution
<i>n</i> -C _{18:0}	3.88	-35	9.95	-59	7.65	-30
Total <i>n</i> -C ₁₆ FA	25.56		174.35		34.18	
Total <i>n</i> -C ₁₈ FA	12.63		41.91		19.34	
<i>Hydrocarbons</i>						
17 α (H),21 β (H)-25,28,30-Trisnorhopane			0.57	n.m.		
17 β (H), 21 β (H)-25-Norhopane	0.13		1.49	-31		
Hop-17(21)-ene	0.24		0.37	n.m.	0.20	
Diploptene	0.14		0.92	-79		
Total lipid biomarkers	48.48		277.96		61.84	

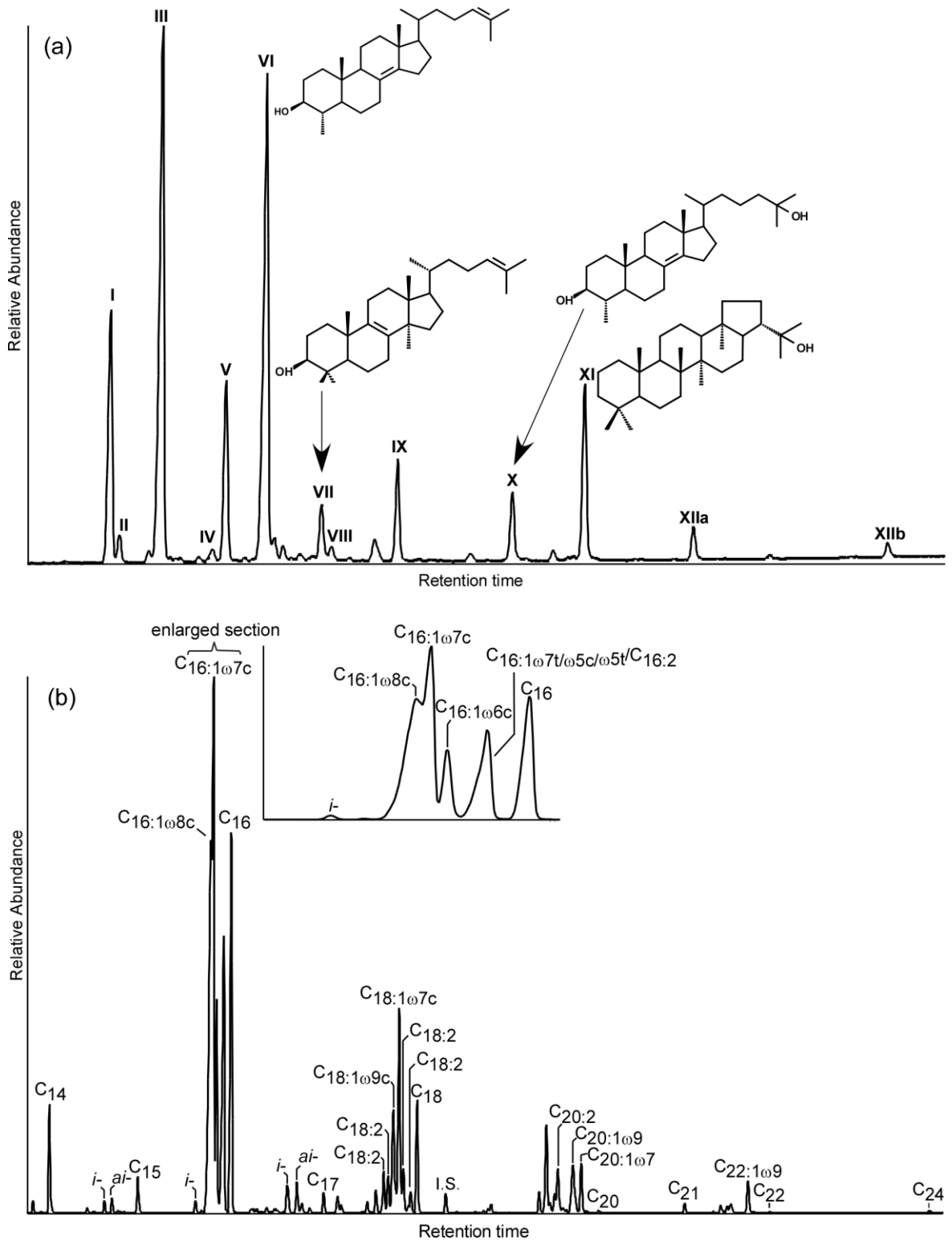
* Excluded from calculations due to coelution of *n*-C_{16:1 ω 7t}, and *n*-C_{16:1 ω 5c/t} with *n*-C_{16:2} on GC-FID. n.m. = not measured, ww = wet weight

CAB-B

In the hydrocarbon fraction of sample CAB-B, the most abundant lipid is hop-17(21)-ene (47%). 17 β (H),21 β (H)-30-norhopane and diploptene are also present in this fraction, representing approximately 25% each. The alcohol fraction is dominated by sterols, comprising cholesterol (56%) and 24-methylcholesta-5,24(28)-dien-3 β -ol (10%). The only hopanoid detected in the alcohol fraction is diplopterol (34%; Fig. 4.6). The fatty acid fraction of CAB-B is dominated by monounsaturated fatty acids (52% of the fraction). The distribution of saturated fatty acids in order of decreasing abundance is *n*-C_{16:0} (29%), *n*-C_{14:0} (10%), and *n*-C_{18:0} (9%). The most prominent

monounsaturated fatty acids are $n\text{-C}_{16:1\omega 8c}$ (19%), followed by $n\text{-C}_{18:1\omega 7c}$ (11%), $n\text{-C}_{18:1\omega 9c}$ (10%), $n\text{-C}_{16:1\omega 7c}$ (9%), and $n\text{-C}_{16:1\omega 6c}$ (3%; Fig. .4.6).

Figure 4.5 Partial gas chromatograms of alcohol (a) and fatty acid (b) fractions of CAB-C biofilm.



Notes: *i* = iso, *ai* = anteiso. Roman numerals in (a) explained Table 4.1

The $\delta^{13}\text{C}$ values of selected fatty acids (Table 4.1, Fig. 4.6) vary from -76‰ ($n\text{-C}_{16:1\omega 8}$) to -33‰ ($n\text{-C}_{18:1\omega 9}$). Monounsaturated fatty acids $n\text{-C}_{16}$ have the lowest $\delta^{13}\text{C}$ values (average -72‰). In the alcohol fraction, $\delta^{13}\text{C}$ values range between -76‰ (diplopterol) and -58‰ (cholesterol). The $\delta^{13}\text{C}$ values of hydrocarbons were not measured due to too low contents.

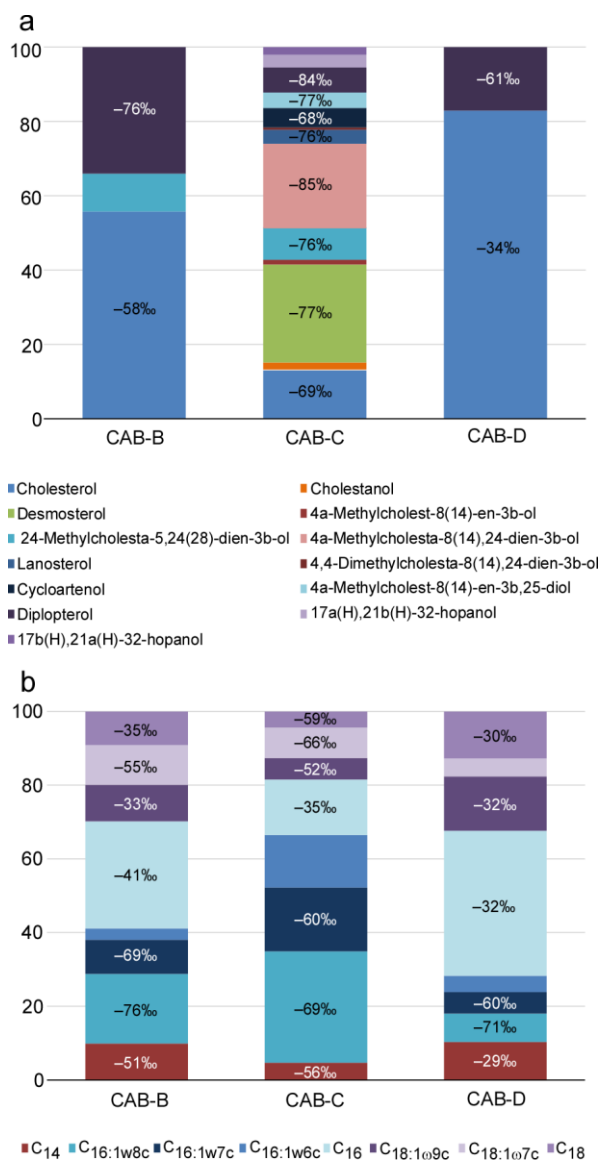
CAB-C

The most abundant hydrocarbon in the sample CAB-C is $17\beta(\text{H}), 21\beta(\text{H})\text{-}30\text{-norhopane}$ (44%, Fig. 4.6). Diploptene (27%), $17\alpha(\text{H}), 21\beta(\text{H})\text{-}25, 28, 30\text{-trishopane}$ (17%), and minor amounts of hop-17(21)-ene (11%) were detected as well (Table 4.1). In the alcohol fraction, sterols account for 88% of all compounds. Most abundant sterols are desmosterol (26%), various 4-methyl sterols (25%), cholesterol (13%), and 24-methylcholesta-5,24(28)-dien- $3\beta\text{-ol}$ (9%; Fig. 4.6). Besides the commonly reported 4-methyl sterols (4 α -methylcholest-8(14)-en- $3\beta\text{-ol}$, 4 α -methylcholesta-8(14),24-dien- $3\beta\text{-ol}$, 4,4-dimethylcholesta-8(14),24-dien- $3\beta\text{-ol}$)), minor amounts of an unusual 4-methyl steroid diol (4%) were detected, a compound that was first described by Elvert and Niemann (2008) from Haakon Mosby Mud Volcano sediments. Further sterols include cycloartenol, lanosterol, and cholestanol (Table 4.1, Fig. 4.5). Few hopanoids were detected in the alcohol fraction, including diplopterol (7%), and $17\alpha(\text{H}), 21\beta(\text{H})\text{-}$ and $17\beta(\text{H}), 21\alpha(\text{H})$ isomers of $\text{C}_{32}\text{-hopanol}$ (bishomohopanol; 5%). The fatty acid fraction of CAB-C is dominated by monounsaturated fatty acids, representing 76% of the target fatty acids. In sample CAB-C, the most abundant fatty acid is $n\text{-C}_{16:1\omega 8c}$ (30%) followed by $n\text{-C}_{16:1\omega 7c}$ (17%) and $n\text{-C}_{16:1\omega 6c}$ (14%; Fig. 4.6). Monounsaturated fatty acids with 18 carbon atoms, $n\text{-C}_{18:1\omega 7c}$ (8%), and $n\text{-C}_{18:1\omega 9c}$ (6%) are present in smaller amounts. Fatty acids $n\text{-C}_{16:0}$ (15%), $n\text{-C}_{14:0}$ (5%), and $n\text{-C}_{18:0}$ (4%) are present as well, although they are less prominent than the respective monounsaturated compounds (Table 4.1, Fig. 4.5).

Diploptene shows the lowest $\delta^{13}\text{C}$ value (-79‰) among the hydrocarbons, while the other measured compound, $17\beta(\text{H}), 21\beta(\text{H})\text{-}30\text{-norhopane}$, is considerably less ^{13}C -depleted with a $\delta^{13}\text{C}$ value of -31‰ . In the alcohol fraction, diplopterol exhibits the lowest $\delta^{13}\text{C}$ value (-84‰). Among sterols, the lowest $\delta^{13}\text{C}$ value was found for 4 α -methylcholesta-8(14),24-dien- $3\beta\text{-ol}$ (-85‰), whereas cholesterol and cycloartenol show the highest values (average -68‰). The $\delta^{13}\text{C}$ values for other sterols vary between -77‰ and -76‰ (Table 4.1, Fig. 4.6). Fatty acids were found to be considerably less depleted than alcohols (Table 4.1, Fig. 4.6). The most ^{13}C -depleted

fatty acids are monounsaturated fatty acids $n\text{-C}_{16}$ (average -65‰) and $n\text{-C}_{18:1\omega 7}$ (-66‰). The highest $\delta^{13}\text{C}$ value was found for $n\text{-C}_{16:0}$ (-33‰).

Figure 4.6 Relative abundance of lipids in the alcohol (a) and fatty acid (b) fractions of biofilms from CAB-B, CAB-C, and CAB-D cubes



Notes: Values within each stacked column represent $\delta^{13}\text{C}$ values of lipids. $\delta^{13}\text{C}$ value of $n\text{-C}_{16:1\omega 6c}$ not provided due to coelution with $\text{C}_{16:1\omega 7c}$ on GC-IRM-MS.

CAB-D

The only hydrocarbon detected in the reference sample CAB-D is hop-17(21)-ene. In the alcohol fraction, only cholesterol and diplopterol are present (83% and 17% of the fraction, respectively). The fatty acids are dominated by saturated fatty acids (62%). $n\text{-C}_{16:0}$ (39%) is the most abundant fatty acid, followed by $n\text{-C}_{18:0}$ (13%) and $n\text{-C}_{14:0}$ (10%). Monounsaturated fatty acids represent 38% of the fraction, including $n\text{-C}_{16:1\omega 8c}$ (8%), $n\text{-C}_{16:1\omega 7c}$ (6%), $n\text{-C}_{16:1\omega 6c}$ (4%), $n\text{-C}_{18:1\omega 9c}$ (15%), and $n\text{-C}_{18:1\omega 7c}$ (5%; Table 4.1, Fig. 4.6).

The $\delta^{13}\text{C}$ values of alcohols in reference sample CAB-D (Table 4.1, Fig. 4.6) fall between -61‰ (diplopterol) and -34‰ (cholesterol). The $\delta^{13}\text{C}$ values of fatty acids vary widely from -71‰ to -30‰ . No $\delta^{13}\text{C}$ values were obtained for compounds of the hydrocarbon fraction due to too low contents.

4.6 Discussion

Some biogeochemical processes strongly affect the carbonate system in sedimentary environments, causing either the formation of authigenic carbonate minerals or the dissolution of skeletal or authigenic carbonate in the sediment or at the sediment surface. Biogeochemical processes affect the carbonate system by the production or consumption of protons or by the production of carbonate species (Coleman, 1993). Apart from such effects driven by the metabolism itself, extracellular polymeric substances (EPS) are known to affect the carbonate system (Dupraz et al., 2009). Microbial sulfate reduction is an example to highlight that the effect of a biogeochemical process is not straightforward. It depends on factors including environmental conditions (e.g., presence and speciation of iron), the types of electron donors metabolized, and the EPS composition if sulfate reduction results in carbonate formation or dissolution (Meister, 2013; Gallagher et al., 2014; Baumann et al., 2016). The effects of other biogeochemical processes on the carbonate system are more straightforward. This includes the calcium pump (i.e., ATPase-mediated transcellular Ca^{2+} transport) of cyanobacteria (Garcia-Pichel, 2006; Garcia-Pichel et al., 2010), which is one of the mechanisms, apart from local acidification caused by respiration, that might also apply for other agents of microbial bioerosion in marine environments. With respect to marine methane seeps, aerobic methanotrophy and sulfide oxidation have been held responsible for carbonate dissolution (Matsumoto, 1990; Himmler et al., 2011). Yet, experiments to assess the effect of biogeochemical processes on the carbonate system in marine methane-rich environments are scarce.

4.6.1 Are aerobic methanotrophic bacteria corroding carbonate at seeps?

The SEM analyses revealed evidence of microbioerosion associated with the presence of biofilms adhering to the carbonate substrate of cube CAB-C, which was exposed to active methane seepage and outcropping hydrates for 2.5 years. In contrast, the CAB-B and CAB-D cubes revealed no signs of bioerosion or carbonate dissolution, although the experiment CAB-B was also exposed to active seepage. Such pattern provides circumstantial evidence for a methane-dependent bioerosion

process in case of the CAB-C cube, given the dominance of aerobic methanotrophs in the adhering biofilm suggested by 16S rRNA and biomarker data. This line of reasoning receives further support from the observation of a nearly monochthonospecific bioerosion trace assemblage with the dominant microbioerosion trace being new to science and having a very high abundance in the samples studied. These microbioerosion traces have been formed in a purely inorganic substrate (marble) being of limited attraction for organotrophic microendoliths such as marine fungi, which would have been expected in a much higher abundance and diversity in a biogenic substrate (e.g., skeletal carbonate) after more than two years of exposure in this aphotic environment (e.g., Golubic et al., 2005; Wisshak et al., 2011). Together, the ichnological observations suggest that the dominant agent of microbioerosion observed in the marble cubes exposed to active seepage is a bacterium with a methane- or hydrogen sulfide-based metabolism. Even at the most active seeps, hydrogen sulfide tends to be oxidized rapidly above the seafloor, and its concentration in the bottom water is typically lower than the concentration of methane (Sahling et al., 2002; Niemann et al., 2005; Boetius & Wenzhoefer, 2013). The position of the marble surfaces some centimeters above the seafloor and fluid exchange restriction caused by the perforated plastic boards, on which the cubes were resting, seem to be in favor of aerobic methanotrophy rather than sulfide oxidation.

Aerobic methanotrophy commonly occurs at methane seeps (Cordova-Gonzalez et al., 2020, and references therein). The composition of a community of aerobic methanotrophs can be assessed by phylogenetic analyses and lipid biomarkers (Hanson & Hanson, 1996). In this respect, the bioeroded surface of the marble cubes in the CAB-C experiment and the close to exclusive occurrence of a new type of microbioerosion trace suggest that site-specific microorganisms were involved in carbonate corrosion. Based on 16S rRNA analysis, aerobic methanotrophs of the order Methylococcales were among the most abundant bacteria identified. Among the Methylococcales, relatives of the Hyd24-01 clade, followed by the IheB2-23 clade, and representatives of the genus *Methylomonas* were most abundant. To date, no pure cultures of bacteria of the Hyd24-01 clade exist, however this clade has been reported from other methane-rich sites, including surface sediments of Haakon Mosby Mud Volcano (Lösekann et al., 2007). The uncultured clade IheB2-23 was first detected in the water column of the northern South China Sea (Mau et al., 2020). Apart from aerobic methanotrophs, the CAB-C biofilms contained abundant Thiotrichales. These and other sulfide-oxidizing bacteria are potential candidates other than aerobic

methanotrophs that may have caused the observed microbioerosion of marble. The biomarker inventory of the CAB-C biofilms helps to evaluate the phylogenetic affiliation of the microbioeroder. Unlike 16S rRNA analysis, lipid biomarker analysis provides a quantitative assessment of the relative abundance of microbial taxa (e.g., Biddle et al., 2006). Although, lipid biomarkers are affected by taphonomic processes (e.g., Xie et al., 2013), the circumstance that active biofilms have been sampled renders it unlikely that the obtained lipid inventory was compromised by degradation processes. Biomarkers are therefore suitable to determine the microorganisms that dominated the CAB-C biofilms and to identify the probable bioeroder.

The lipid biomarker inventory of the biofilm adhering to the CAB-C marble chiefly includes fatty acids, accompanied by sterols and hopanoids, most of them commonly reported from aerobic methanotrophic bacteria. Phospholipid fatty acids can be used to fingerprint methanotrophic bacteria, since fatty acids of Type I and X methanotrophs possess predominantly 16 carbon atoms with unsaturations at $\omega 5$, $\omega 7$, and $\omega 8$, while fatty acids with 18 carbons with unsaturations at $\omega 7$ and $\omega 8$ are predominant in Type II methanotrophs (Hanson & Hanson, 1996; Bowman, 2006). The fatty acid profile of the CAB-C biofilm is dominated by $n\text{-C}_{16:1\omega 8}$ ($\delta^{13}\text{C}$: -69‰), a lipid biomarker, which is only known to be produced by Type I methanotrophic bacteria (Bowman, 2006; Willers et al., 2015), but especially by members of the genus *Methylomonas* (Hanson & Hanson, 1996), which were detected by 16S rRNA sequencing. Another fatty acid related to Type I methanotrophs of the genus *Methylomonas* is $n\text{-C}_{16:1\omega 5t}$, which represents an excellent environmental marker for aerobic methanotrophy since, apart from some Type I methanotrophs, it is not common in bacteria (Bowman, 2006; Willers et al., 2015). The *cis* isomer $n\text{-C}_{16:1\omega 5c}$ is known to be produced by sulfate-reducing bacteria involved in AOM (Elvert et al., 2003); unfortunately, no ^{13}C values for $n\text{-C}_{16:1\omega 5}$ fatty acids were measured due to coelution with other compounds. However, since no evidence of AOM was found for the CAB-C biofilm, and is also not to be expected considering the environmental setting of the exposed marble cubes, sulfate reducers can be excluded, rendering aerobic methanotrophs the most likely source of $n\text{-C}_{16:1\omega 5c}$ as well.

Abundant $n\text{-C}_{16:1\omega 7}$ ($\delta^{13}\text{C}$: -60‰), a fatty acid found in high concentration in *Methylomonas* strains (Bowman, 2006), is a ubiquitous fatty acid sourced by many organisms including algae and bacteria, among the latter, sulfide-oxidizing bacteria (McCaffrey et al., 1989). Thiotrichales, sulfide-oxidizing bacteria, were among the Gammaproteobacteria in the 16S rRNA analyses of the CAB-C biofilm. However,

based on the presence of $\omega 8$ unsaturated fatty acids and the ^{13}C values of $n\text{-C}_{16:1\omega 7}$, aerobic methanotrophs are the most likely source organisms of this compound since lipids of sulfide-oxidizing bacteria are typically less ^{13}C -depleted than lipids of aerobic methanotrophs (Pond et al., 1998; Kellermann et al., 2012), providing additional evidence that methane-oxidizing bacteria and not sulfide-oxidizing bacteria dominate the CAB-C biofilms and are responsible for bioerosion.

The observed high contents of $n\text{-C}_{18:1\omega 7c}$ fatty acid ($\delta^{13}\text{C}$: -66‰) are surprising since this compound is considered a biomarker of Type II methanotrophs (Alphaproteobacteria), and the 16S rRNA analysis yielded only sequences of gammaproteobacterial methanotrophs. Similar inconsistencies were found by Kellermann et al. (2012) when studying mussel symbionts from *B. childressi* collected at a hydrocarbon seep in the Gulf of Mexico. The authors found a lipid composition consistent with Type II methanotrophs, yet only sequences of Type I methanotrophs were detected with the 16S rRNA analysis. Although Type I methanotrophs are the dominant methanotrophs in marine environments, there are reports of Type II methanotrophs from the Black Sea water column, accounting for up to 10% of the methanotrophic population (Durisch-Kaiser et al., 2005). However, despite the common use of fatty acid profiles to distinguish between Type I and II methanotrophs, most members of the family Methylothermaceae (Type I: *Methylohalobius crimeensis*, *Methylothermus subterraneus*, and *Methylomarinovum caldicuralii*), some of them isolated from marine environments, produce significant amounts of $n\text{-C}_{18:1\omega 7c}$ (Knief, 2015). Since similar fatty acid profiles have been described for Type I and II methanotrophs (e.g., Knief, 2015), additional evidence is needed for such comparison. The assignment of $n\text{-C}_{18:1\omega 7c}$ fatty acid to a source organism is further complicated by the circumstance that this compound is also produced by sulfide-oxidizing bacteria (McCaffrey et al., 1989). Its low $\delta^{13}\text{C}$ value rather agrees with aerobic methanotrophs as dominant source microorganisms (cf. Pond et al., 1998; Kellermann et al., 2012), although mixed input from both groups seems probable. Therefore, aerobic methanotrophy is most likely carried out by Type I methanotrophs based on the combined genetic and biomarker data, whereas sulfide-oxidizing bacteria are apparently subordinate members of the CAB-C biofilm community.

Additional evidence for the assignment of the biota of the CAB-C biofilms comes from sterols and hopanoids. Sterols are valuable biomarkers in marine systems and sediments, reflecting input from multiple sources (Bianchi & Canuel, 2011). Some

sterols, such as cholesterol, cholestanol, desmosterol, and 24-methylcholesta-5,24(28)-dien-3 β -ol, have been previously reported to occur in seep carbonates; yet the sources of these compounds are mostly unspecific (Guan et al., 2021). On the other hand, sterols with one or two methyl groups at the C-4 position (4 α -methylcholest-8(14)-en-3 β -ol, 4 α -methylcholesta-8(14),24-dien-3 β -ol, 4,4-dimethylcholesta-8(14),24-dien-3 β -ol) are of high specificity for aerobic methanotrophic bacteria. These compounds are produced by few bacteria only, including several strains of methanotrophs (*Methylosphaera hansonii*: Schouten et al., 2000; *Methylobacter luteus*, *Methylobacter whittenburyi*, *Methylococcus capsulatus*, *Methylosarcina lacus*: Wei et al., 2016; *Methylotheobacterium kenyense*, *Methylotheobacterium alcaliphilum*: Cordova-Gonzalez et al., 2020). ^{13}C -depleted 4-methyl sterols produced by aerobic methanotrophs have been detected in seep carbonates from the Gulf of Mexico (Birgel et al., 2011), sediments from Haakon Mosby Mud Volcano (Elvert & Niemann, 2008), and mussel gills (*Bathymodiolus childressi*, *Bathymodiolus brooksi*) hosting methane-oxidizing symbionts (Kellermann et al., 2012). The low $\delta^{13}\text{C}$ values of 4-methyl sterols (4 α -methylcholesta-8(14),24-dien-3 β -ol: -85‰ and 4 α -methylcholest-8(14)-en-3 β ,25-diol: -77‰) of the CAB-C biofilms agree with methanotrophic bacteria as source organisms.

Of special interest is the presence of the uncommon sterol 4 α -methylcholest-8(14)-en-3 β ,25-diol ($\delta^{13}\text{C}$: -77‰) in the CAB-C biofilm, a compound first reported from Haakon Mosby Mud Volcano (Elvert & Niemann, 2008) and assigned to aerobic methanotrophs. Remarkably, 16S rRNA analyses of Haakon Mosby sediments revealed the dominance of Methylococcales strains divided into two clusters, one of which closely related to the Hyd24-01 clade (Lösekann et al., 2007), the clade dominant in the CAB-C biofilm. Our study is only the second report of 4 α -methylcholest-8(14)-en-3 β ,25-diol. Our new finding suggests that this uncommon sterol is a lipid biomarker of the Hyd24-01 clade. Generally, 4-methyl sterols are thought to be biosynthesized via demethylation and desaturations of lanosterol (Bouvier et al., 1976; Summons et al., 2006); although lanosterol has not been identified to date in modern methane-seep carbonates, its diagenetic product lanostane is commonly found in ancient seep carbonates in cases where lipid biomarkers of aerobic methanotrophic bacteria are preserved (Birgel & Peckmann, 2008; Sandy et al., 2012; Natalicchio et al., 2015).

Hopanoids—ubiquitously present in the geological record—occur in many groups of bacteria (Bianchi & Canuel, 2011). Although the synthesis of hopanoids by anaerobic bacteria has been confirmed by culture studies (Härtner et al., 2005; Blumenberg et

al., 2006), aerobic methanotrophs still remain a probable source candidate of ^{13}C -depleted hopanoids at modern seeps, especially when co-occurring with other lipids of aerobic methanotrophs (e.g., sterols, Elvert & Niemann, 2008; Birgel et al., 2011). Accordingly, the presence of diplopterol ($\delta^{13}\text{C}$: -84‰) in the CAB-C biofilm, similarly ^{13}C -depleted as the associated 4-methyl sterols, is best explained by input from aerobic methanotrophs. Hopanoid synthesis from squalene either yields simple hopanoids such as diplopterol or hopanoid skeletons are modified by the addition of a polyfunctionalized side chains to produce bacteriohopanepolyols (Summons et al., 2006). Interestingly, no bacteriohopanepolyols—commonly found together with diplopterol in cultures of aerobic methanotrophs (*M. capsulatus*: Summons et al., 1994; *Methylomonas methanica*: Jahnke et al., 1999; *M. alcaliphilum* and *M. kenyense*: Cordova-Gonzalez et al., 2020) and at methane seeps (Birgel & Peckmann, 2008; Birgel et al., 2011; Himmler et al., 2015)—were found in the CAB-C biofilm. A similar inventory of cyclic terpenoids was described for sediments from Haakon Mosby Mud Volcano, containing abundant diplopterol and 4-methyl sterols (Elvert & Niemann, 2008), but no bacteriohopanepolyols (Marcus Elvert, personal communication). The biomarker pattern of Haakon Mosby sediments was at least partially reflecting input from methanotrophs closely related to the Hyd24-01 clade, the clade dominant in the CAB-C biofilm.

Biomarkers of aerobic methanotrophs are typically ^{13}C -depleted due to fractionation relative to the already ^{13}C -depleted methane source. Thus, compound-specific isotope composition represents a valuable tool for the interpretation of biomarkers of methanotrophs in recent and ancient environments (Jahnke et al., 1999; Cordova-Gonzalez et al., 2020). Considering a $^{13}\text{C}_{\text{methane}}$ value of ca. -69‰ , measured in shallow gas hydrates recovered from the REGAB Pockmark (Charlou et al., 2004), the fractionation ($\Delta\delta^{13}\text{C}$) between methane and aerobic methanotroph specific biomarkers averages -12‰ (from -16‰ to -7‰) for steroids and hopanoids. Previous studies on cultures of aerobic methanotrophs revealed a fractionation of terpenoids relative to methane ($\Delta\delta^{13}\text{C}_{\text{terpenoids-methane}}$) of -16‰ and -25‰ for Type I *M. alcaliphilum* and *M. kenyense*, respectively (Cordova-Gonzalez et al., 2020), and -1‰ for Type II *M. trichosporium* (Jahnke et al., 1999), in accordance with the $\Delta\delta^{13}\text{C}_{\text{terpenoids-methane}}$ found for the CAB-C biofilms herein. Yet, the $\Delta\delta^{13}\text{C}$ of fatty acids relative to methane is $+6\text{‰}$ on average (from 0‰ to $+13\text{‰}$). Such ^{13}C enrichment is best explained by cellular physiology and intermediate metabolites causing fatty acids to be ^{13}C enriched relative to hopanoids in methanotrophs (cf. Jahnke et al., 1999) or by additional input of $\omega 7$

fatty acids from sulfide-oxidizing bacteria. Moreover, ^{13}C values of methane are not necessarily homogenous throughout the REGAB Pockmark, and the ^{13}C values of methane consumed by methanotrophs in the study area might differ from those determined by Charlou et al. (2004).

Both aerobic methanotrophy and sulfide oxidation potentially lower the pH and have the potential to induce carbonate corrosion (Matsumoto, 1990; Leprich et al., 2021). However, considering the presence and abundance of ^{13}C -depleted fatty acids (*n*- $\text{C}_{16:1\omega 8\text{c}}$, *n*- $\text{C}_{18:1\omega 8\text{c}}$, *n*- $\text{C}_{16:1\omega 5\text{t}}$), 4-methyl sterols, and diplopterol, aerobic methanotrophic bacteria dominate the CAB-C biofilm. Together with the predominance of aerobic methanotrophs revealed by 16S rRNA analyses and the supposedly greater potential for methane oxidation rather than sulfide oxidation several centimeters above the seafloor on the surface of the exposed marble cubes (Sahling et al., 2002; Niemann et al., 2005; Boetius & Wenzhoefer, 2013), the observed bioerosion below the CAB-C biofilm was probably caused by methanotrophic bacteria.

4.6.2 Carbonate microbioerosion and aerobic methanotrophy

Our carbonate corrosion experiment in the REGAB seep field confirms that carbonate rocks are susceptible to corrosion when exposed to methane seepage in an oxic environment. The corrosion surfaces, in this case microbioerosion traces were found to be associated with biofilms dominated by aerobic methanotrophic bacteria. After 2.5 years of exposure to a seepage environment, the CAB-C marble blocks were found to exhibit densely pitted surfaces resulting from microbioerosion. The CAB-C trace fossil (Fig. 4.3) has not previously been reported elsewhere (Fig. 4.3). Pitting was apparently a chemically driven process, supposedly relying on a metabolism that produced acidity. It cannot be excluded that the trace maker used organic acids or chelating compounds in addition to metabolites or, possibly, took advantage of the chemical environment created in the biofilm (low pH caused by aerobic methanotrophy and subordinate sulfide oxidation), but was not a methanotroph or thiotroph itself. Based on our data, the phylogenetic affiliation cannot be assessed with certainty. However, the new data of the CAB experiment confirm that aerobic methanotrophy at seeps can be closely associated with substantial carbonate corrosion.

Abundant corrosion surfaces had already been identified in ancient seep carbonates; in some cases, together with lipid biomarkers of aerobic methanotrophs. For instance, Natalicchio et al. (2015) reported corrosion surfaces in Eocene seep carbonates from

northwestern Istria (Croatia) and suggested aerobic methane oxidation as the major cause of carbonate corrosion, supported by the presence of ^{13}C -depleted lanostanes. Another example of seep carbonates with corrosion features are the Cretaceous Tepee Buttes (Birgel et al., 2006a), where corrosion is accompanied by the presence of rearranged ^{13}C -depleted hopanoids, interpreted to derive from the alteration of bacteriohopanepolyols of aerobic methanotrophs. Examples of carbonate corrosion in modern seep environments stem from the Mediterranean Sea, such as the Amsterdam and Athina Mud Volcanoes (Himmler et al., 2011) and the Nadir Brine Lake (Aloisi et al., 2000). In some cases, lacking biomarker evidence, corrosion of seep carbonates was also attributed to aerobic methanotrophy (Aloisi et al., 2000; Himmler et al., 2011), sulfide oxidation (Campbell et al., 2002), or a combination thereof (Himmler et al., 2011).

Laboratory experiments conducted by Krause et al. (2014) demonstrated the potential of aerobic methanotrophy to affect carbonate stability, facilitating dissolution. The addition of cells of the methanotrophic bacterium *Methylosinus trichosporium* under saline conditions led to considerable calcite dissolution caused by the production of carbon dioxide (Equation 4.1). Cai et al. (2006) deployed bivalve shells in an experiment over eight years at two locations in the Gulf of Mexico—an active hydrocarbon seep and a site unaffected by seepage. Shells exposed to seepage were substantially affected by carbonate corrosion. Carbon mass balances led the authors to conclude that aerobic oxidation of methane was the dominant mechanism lowering the porewater pH and consequently causing carbonate dissolution. Our experiment in the REGAB seep field supports this interpretation, providing new microtextural, phylogenetic, and biomarker evidence for the crucial role of aerobic methanotrophy in carbonate corrosion at methane seeps.

Given the current concern about climate change and resultant ocean acidification, it becomes pertinent to pay more attention to the mechanisms involved in carbonate dissolution including microbially driven corrosion. The CAB experiment conducted in the REGAB seep field provides new insight on the potential of aerobic methanotrophy to induce carbonate corrosion. However, more research, and in particular more laboratory studies (e.g., Leprich et al., 2021) should be made to understand the mechanisms and the dynamics of carbonate corrosion and microbioerosion. With seawater on projected trend of declining pH, the demand on quantitative estimates of

the influence of aerobic methanotrophy and other biogeochemical processes on carbonate corrosion in marine environments is increasing.

4.7 Conclusions

A carbonate corrosion experiment conducted over the course of 2.5 years in the REGAB seep field confirms that carbonate rocks exposed to methane seepage are susceptible to corrosion when exposed to oxic conditions. After retrieval, purely inorganic marble cubes were found to be covered by biofilms dominated by aerobic methanotrophic bacteria. Underneath biofilms, marble surfaces were affected by corrosion, more precisely microbioerosion. The discovered microbioerosion trace with its circumradial tunnels, ca. 2 to 3 μm in diameter and radiating from a central point of entry while repeatedly bi- or trifurcating in acute angles, is new to science. The genetic data obtained from biofilms reflect the dominance of Type I aerobic methanotrophs of the order Methylococcales; among these, most methanotrophs are relatives of the uncultured clade Hyd24-01. Similar to the genetic data, the biofilm's lipid biomarker inventory including abundant ^{13}C -depleted fatty acids ($n\text{-C}_{16:1\omega 8c}$, $n\text{-C}_{18:1\omega 8c}$, $n\text{-C}_{16:1\omega 5t}$), 4-methyl sterols, and diplopterol suggests a close tie between methanotrophs and their acidity-generating metabolism and microbioerosion; however, our data do not allow for the assignment of the trace maker to a certain phylogenetic affiliation. This study is only the second report of the uncommon sterol 4 α -methylcholest-8(14)-en-3 β ,25-diol. As for the first report of this compound, it is associated with abundant methanotrophs of the Hyd24-01 clade. Such coincidence renders it likely that 4 α -methylcholest-8(14)-en-3 β ,25-diol is a biomarker for the Hyd24-01 clade. The microtextural, phylogenetic, and biomarker evidence compiled during the examination of the REGAB carbonate corrosion experiment supports the concept of aerobic methanotrophy as a potent trigger of carbonate corrosion at marine methane seeps. With levels of ocean acidification increasing, more experimental work is needed to assess the effects of biogeochemical processes like methane oxidation and sulfide oxidation on seawater alkalinity and the marine carbon cycle.

5. Chapter V

Outcomes and perspectives

5.1 Outcomes

The scientific questions raised were: 1) studying the tolerances and limitations of cultured aerobic methanotrophs to better decipher the biomarker record in ancient sedimentary rocks, especially of authigenic carbonates; 2) assessing the scope and limitations of ^{13}C -depleted tetrahymanol and gammacerane as a proxy for aerobic methanotrophy; 3) evaluate the carbon stable isotope patterns of molecular fossils of aerobic methanotrophs to better classify their carbon isotope signatures in modern and ancient environments, and 4) appraise the role of aerobic methanotrophy in the corrosion of authigenic carbonates at marine methane seeps. The first three questions were addressed by testing the hypotheses by culture-based experiments and analyzing the cyclic terpenoid inventory of two strains of aerobic methanotrophic bacteria, *M. alcaliphilum* and *M. kenyense*, under optimal growing conditions. A second experiment with *M. alcaliphilum* was conducted under varying salinities from normal marine towards high and low salinity and high nitrate concentrations, with the overarching aim to pose stress to the bacteria and monitor their reaction on deteriorating conditions.

The analyses of *M. alcaliphilum* and *M. kenyense* revealed that both strains, produce a suite of ^{13}C -depleted lipid biomarkers, including 4-methyl sterols, tetrahymanol, and hopanoids. Among the hopanoids were C_{30} hopanols (diplopterol, diploptene), and various BHPs (aminotetrol and aminotriol). Both groups of hopanoids were methylated at C-3, or desmethylated. This finding confirms that aerobic methanotrophs are

sources of tetrahymanol, although in *M. kenyense* tetrahymanol is much less abundant as in *M. alcaliphilum*. Besides the inventory of previously reported BHPs, *M. alcaliphilum* additionally synthesizes four novel N-containing BHPs identified as aminodiol, 3-methyl-aminodiol, and early eluting isomers of aminotriol and 3-methyl-aminotriol. The average carbon stable isotope fractionation relative to the methane source in *M. kenyense* and *M. alcaliphilum* were found to be -25‰ and -16‰ , respectively, considerably higher than isotope fractionation in Type II methanotrophs.

When grown at different salinities and nitrate concentrations, *M. alcaliphilum* strains show higher growth rates and shorter lag phases at low salinity (1% NaCl) and higher nitrate concentration (100 mM), while the experiment at higher salinity (8.7%) yielded the slowest growth rate. The abundance and composition of pentacyclic triterpenoids are also affected by salinity changes and varying nitrate concentration. Hopanoid contents are increased at low salinity (1% NaCl), particularly reflected in the production of BHPs, especially desmethylated aminotriol. On the other hand, higher salinity (3% NaCl) favors the synthesis of 3-methyl-aminotetrol and tetrahymanol. Generally, 3-methyl compounds are more abundant at higher salinity (3%), reflected by an increase of the 3-methylated over desmethylated ratios for all compounds. In experiments with varying nitrate concentrations, higher nitrate concentrations correlate with an increased production of BHPs (desmethylated aminotriol and 3-methyl-aminotriol).

The outcomes of this research allow a more confident interpretation of biomarkers of aerobic methanotrophy found in sediments and the rock record. After revisiting some marine seep deposits and reviewing published data, it is plausible to make a case for 4-methyl sterols as reliable biomarkers of Type I aerobic methanotrophs in young sediments and sedimentary rocks, although with apparently low preservation potential. This is especially true for ancient methane-seep deposits, where 4-methyl sterols can only be traced by their defunctionalized derivatives, the lanostanes. BHPs occur in recent and subrecent samples, but are absent in older rocks, where only their early degradation products (e.g., anhydroBHT) and later diagenetic products like hopanoic acids are found. 3-methyl hopanoids are reliable markers in some ancient seep deposits and allow to trace Type I methanotrophs into the rock record, because the extra methyl group can be preserved over very long time periods. When present along with other biomarkers of aerobic methanotrophs, ^{13}C -depleted tetrahymanol, and its degradation product gammacerane—biomarkers for stratification of the water column and hypersaline conditions—are also likely sourced by this group of bacteria. Although

biomarkers of aerobic methanotrophs are most often strongly depleted in ^{13}C , fractionation between methane and cyclic terpenoids of aerobic methanotrophs seems to vary greatly as a function of environmental conditions, and in some instances the extent of fractionation cannot be used to unequivocally discriminate Type I and Type II methanotrophs.

The fourth research question was addressed by performing a carbonate corrosion experiment in the REGAB Pockmark, off-Congo, exposing carbonate substrates to sites with and without apparent methane seepage. Petrography of the corrosion patterns documented for carbonates exposed to active methane seepage, combined with 16s rRNA and lipid biomarker analyses confirms that carbonate rocks exposed to methane seepage are indeed susceptible to corrosion, with corrosion surfaces hosting abundant aerobic methanotrophic bacteria. The scanning electron microscope (SEM) analyses of the sample exposed to active methane seepage revealed evidence of monoichnospecific bioerosion traces associated with the presence of biofilms adhering to the marble (purely abiogenic carbonate) substrate of the experiment. This is suggesting that the dominant agent of microbioerosion observed in the marble cube is a bacterium with a metabolism related to methane. The presence and abundance of a suit of ^{13}C -depleted fatty acids (*n*-C_{16:1ω8c}, *n*-C_{18:1ω8c}, *n*-C_{16:1ω5t}), 4-methyl sterols, and diplopterol, points towards aerobic methanotrophic bacteria as the dominant microorganism responsible for the microbioerosion patterns. Together with the predominance of aerobic methanotrophs revealed by 16S rRNA analyses, aerobic methanotrophy is apparently responsible, at least partially, for the microbioerosion in the carbonate cube exposed to methane seeping. The microtextural, phylogenetic, and biomarker evidence in this study supports the hypothesis of aerobic methanotrophy as an important trigger of carbonate corrosion in methane seeps, and marine environments.

5.2 Perspectives

In what direction will future research on aerobic methanotrophic bacteria be heading? A limitation of the study of aerobic methanotrophs in marine environments is the lack of the availability of marine strains in the collections of microorganisms and cell cultures. Molecular ecology studies have revealed that there are considerably more methanotrophs present in the environment than in culture collections. This is especially true for the marine environment, and for this reason it is difficult to create a whole database of biomarkers from aerobic methanotrophic bacteria. In order to close

this gap, it is essential to grow and isolate more strains and make them available to the scientific community, which is often a time-consuming task and needs some experience in culturing techniques. Further, more culture-based experiments are needed. It is still unknown, for example, how the ^{13}C isotopic composition of biomarkers from aerobic methanotrophs is affected by varying culture conditions, not only salinity and nitrate concentration, but also of other parameters such as oxygen and methane availability, and pH. On the other hand, this research made a case for aerobic methanotrophy as a trigger of microbiocorrosion at marine methane seeps; however, more work needs to be done to quantitatively estimate the influence of aerobic methanotrophy and other biogeochemical processes on carbonate corrosion in marine environments, especially considering the current concerns related to climate change and ocean acidification.

6. References

- Aloisi, G., Catherine, P., Rouchy, J.-M., Foucher, J.-P., & Woodside, J. (2000). Methane-related authigenic carbonates of Eastern Mediterranean Sea mud volcanoes and their possible relation to gas hydrate destabilisation. *Earth and Planetary Science Letters*, *184*, 321–338. [https://doi.org/10.1016/S0012-821X\(00\)00322-8](https://doi.org/10.1016/S0012-821X(00)00322-8)
- Archer, D., Buffett, B., & Brovkin, V. (2009). Ocean methane hydrates as a slow tipping point in the global carbon cycle. *Proceedings of the National Academy of Sciences*, *106*, 20596. <https://doi.org/10.1073/pnas.0800885105>
- Arning, E., Birgel, D., Schulz-Vogt, H., Holmkvist, L., Jørgensen, B., Larson, A., & Peckmann, J. (2008). Lipid biomarker patterns of phosphogenic sediments from upwelling regions. *Geomicrobiology Journal*, *25*, 69–82. <https://doi.org/10.1080/01490450801934854>
- Bale, N. J., Rijpstra, W. I. C., Sahonero-Canavesi, D. X., Oshkin, I. Y., Belova, S. E., Dedysh, S. N., & Sinninghe Damsté, J. S. (2019). Fatty acid and hopanoid adaptation to cold in the methanotroph *Methylovulum psychrotolerans*. *Frontiers in Microbiology*, *10*, 589. <https://doi.org/10.3389/fmicb.2019.00589>
- Banta, A. B., Wei, J. H., & Welander, P. V. (2015). A distinct pathway for tetrahymanol synthesis in bacteria. *Proceedings of the National Academy of Sciences of the United States of America*, *112*, 13478–13483. <https://doi.org/10.1073/pnas.1511482112>
- Baumann, L., Birgel, D., Wagneich, M., & Peckmann, J. (2016). Microbially-driven formation of Cenozoic siderite and calcite concretions from eastern Austria. *Austrian Journal of Earth Sciences*, *109*. <https://doi.org/10.17738/ajes.2016.0016>
- Baxter, N. J., Hirt, R. P., Bodrossy, L., Kovacs, K. L., Embley, M. T., Prosser, J. I., & Murrell, J. C. (2002). The ribulose-1,5-bisphosphate carboxylase/oxygenase gene cluster of *Methylococcus capsulatus* (Bath). *Archives of Microbiology*, *177*, 279–289. <https://doi.org/10.1007/s00203-001-0387-x>
- Bednarczyk, A., Hernandez, T. C., Schaeffer, P., Adam, P., Talbot, H. M., Farrimond, P., Riboulleau, A., Largeau, C., Derenne, S., Rohmer, M., & Albrecht, P. (2005). 32,35-Anhydrobacteriohopanetetrol: An unusual bacteriohopanepolyol widespread in recent and past environments. *Organic Geochemistry*, *36*, 673–677. <https://doi.org/10.1016/j.orggeochem.2004.10.014>
- Berndmeyer, C., Thiel, V., Schmale, O., & Blumenberg, M. (2013). Biomarkers for aerobic methanotrophy in the water column of the stratified Gotland Deep (Baltic Sea). *Organic Geochemistry*, *55*, 103–111. <https://doi.org/10.1016/j.orggeochem.2012.11.010>
- Bessette, S., Moalic, Y., Gautey, S., Lesongeur, F., Godfroy, A., & Toffin, L. (2017). Relative abundance and diversity of bacterial methanotrophs at the oxic–anoxic interface of the Congo deep-sea fan. *Frontiers in Microbiology*, *8*, 715. <https://doi.org/10.3389/fmicb.2017.00715>
- Bianchi, T. S., & Canuel, E. A. (2011). *Chemical Biomarkers in Aquatic Ecosystems*. Princeton University Press. <https://doi.org/10.1515/9781400839100>

- Biastoch, A., Treude, T., Rüpke, L. H., Riebesell, U., Roth, C., Burwicz, E. B., Park, W., Latif, M., Böning, C. W., Madec, G., & Wallmann, K. (2011). Rising Arctic Ocean temperatures cause gas hydrate destabilization and ocean acidification. *Geophysical Research Letters*, *38*. <https://doi.org/10.1029/2011GL047222>
- Biddle, J. F., Lipp, J. S., Lever, M. A., Lloyd, K. G., Sørensen, K. B., Anderson, R., Fredricks, H. F., Elvert, M., Kelly, T. J., Schrag, D. P., Sogin, M. L., Brenchley, J. E., Teske, A., House, C. H., & Hinrichs, K.-U. (2006). Heterotrophic Archaea dominate sedimentary subsurface ecosystems off Peru. *Proceedings of the National Academy of Sciences*, *103*, 3846–3851. <https://doi.org/10.1073/pnas.0600035103>
- Bird, C. W., Lynch, J. M., Pirt, S. J., & Reid, W. W. (1971). The identification of hop-22(29)-ene in prokaryotic organisms. *Tetrahedron Letters*, *12*, 3189–3190. [https://doi.org/10.1016/S0040-4039\(01\)97127-8](https://doi.org/10.1016/S0040-4039(01)97127-8)
- Birgel, D., Feng, D., Roberts, H. H., & Peckmann, J. (2011). Changing redox conditions at cold seeps as revealed by authigenic carbonates from Alaminos Canyon, northern Gulf of Mexico. *Chemical Geology*, *285*, 82–96. <https://doi.org/10.1016/j.chemgeo.2011.03.004>
- Birgel, D., Himmler, T., Freiwald, A., & Peckmann, J. (2008). A new constraint on the antiquity of anaerobic oxidation of methane: Late Pennsylvanian seep limestones from southern Namibia. *Geology*, *36*, 543–546. <https://doi.org/10.1130/G24690a.1>
- Birgel, D., & Peckmann, J. (2008). Aerobic methanotrophy at ancient marine methane seeps: A synthesis. *Organic Geochemistry*, *39*, 1659–1667. <https://doi.org/10.1016/j.orggeochem.2008.01.023>
- Birgel, D., Peckmann, J., Klautzsch, S., Thiel, V., & Reitner, J. (2006a). Anaerobic and aerobic oxidation of methane at Late Cretaceous seeps in the Western Interior Seaway, USA. *Geomicrobiology Journal*, *23*, 565–577. <https://doi.org/10.1080/01490450600897369>
- Birgel, D., Thiel, V., Hinrichs, K.-U., Elvert, M., Campbell, K. A., Reitner, J., Farmer, J. D., & Peckmann, J. (2006b). Lipid biomarker patterns of methane-seep microbialites from the Mesozoic convergent margin of California. *Organic Geochemistry*, *37*, 1289–1302. <https://doi.org/10.1016/j.orggeochem.2006.02.004>
- Blumenberg, M., Hoppert, M., Krüger, M., Dreier, A., & Thiel, V. (2012). Novel findings on hopanoid occurrences among sulfate reducing bacteria: Is there a direct link to nitrogen fixation? *Organic Geochemistry*, *49*, 1–5. <https://doi.org/10.1016/j.orggeochem.2012.05.003>
- Blumenberg, M., Krüger, M., Nauhaus, K., Talbot, H. M., Oppermann, B. I., Seifert, R., Pape, T., & Michaelis, W. (2006). Biosynthesis of hopanoids by sulfate-reducing bacteria (genus *Desulfovibrio*). *Environmental Microbiology*, *8*, 1220–1227. <https://doi.org/10.1111/j.1462-2920.2006.01014.x>
- Bodelier, P. L. E., & Laanbroek, H. J. (2004). Nitrogen as a regulatory factor of methane oxidation in soils and sediments. *FEMS Microbiology Ecology*, *47*, 265–277. [https://doi.org/10.1016/S0168-6496\(03\)00304-0](https://doi.org/10.1016/S0168-6496(03)00304-0)
- Bodelier, P. L. E., Roslev, P., Henckel, T., & Frenzel, P. (2000). Stimulation by ammonium-based fertilizers of methane oxidation in soil around rice roots. *Nature*, *403*, 421–424. <https://doi.org/10.1038/35000193>
- Boetius, A., Ravensschlag, K., Schubert, C. J., Rickert, D., Widdel, F., Gieseke, A., Amann, R., Jørgensen, B. B., Witte, U., & Pfannkuche, O. (2000). A marine microbial consortium apparently mediating anaerobic oxidation of methane. *Nature*, *407*, 623–626. <https://doi.org/10.1038/35036572>
- Boetius, A., & Wenzhoefer, F. (2013). Seafloor oxygen consumption fueled by methane from cold seeps. *Nature Geoscience*, *6*, 725–734. <https://doi.org/10.1038/ngeo1926>

- Bohrmann, G., Greinert, J., Suess, E., & Torres, M. (1998). Authigenic carbonates from the Cascadia subduction zone and their relation to gas hydrate stability. *Geology*, *26*, 647–650. [https://doi.org/10.1130/0091-7613\(1998\)026<0647:ACFTCS>2.3.CO;2](https://doi.org/10.1130/0091-7613(1998)026<0647:ACFTCS>2.3.CO;2)
- Bohrmann, G., & Torres, M. (2006). Gas hydrates in marine sediments. In *Marine Geochemistry* (pp. 481–512). https://doi.org/10.1007/3-540-32144-6_14
- Bouloubassi, I., Nabais, E., Pancost, R. D., Lorre, A., & Taphanel, M. H. (2009). First biomarker evidence for methane oxidation at cold seeps in the Southeast Atlantic (REGAB pockmark). *Deep-Sea Research Part II-Topical Studies in Oceanography*, *56*, 2239–2247. <https://doi.org/10.1016/j.dsr2.2009.04.006>
- Bouvier, P., Rohmer, M., Benveniste, P., & Ourisson, G. (1976). $\Delta^{8(14)}$ -Steroids in the bacterium *Methylococcus capsulatus*. *Biochemical Journal*, *159*, 267–271. <https://doi.org/DOI 10.1042/bj1590267>
- Bowman, J. (2006). The methanotrophs — The families *Methylococcaceae* and *Methylocystaceae*. In M. Dworkin, S. Falkow, E. Rosenberg, K.-H. Schleifer, & E. Stackebrandt (Eds.), *The Prokaryotes* (pp. 266–289). New York, NY, USA: Springer.
- Bowman, J. (2014). The family *Methylococcaceae*. In E. Rosenberg, E. F. DeLong, S. Lory, E. Stackebrandt, & F. Thompson (Eds.), *The Prokaryotes: Gammaproteobacteria* (pp. 411–440). Berlin-Heidelberg: Springer. Retrieved from https://doi.org/10.1007/978-3-642-38922-1_237
- Bowman, J., Sly, L. I., Nichols, P. D., & Hayward, A. C. (1993). Revised taxonomy of the methanotrophs: Description of *Methylobacter* gen. nov., emendation of *Methylococcus*, validation of *Methylosinus* and *Methylocystis* species, and a proposal that the family *Methylococcaceae* includes only the group I methanotrophs. *International Journal of Systematic and Evolutionary Microbiology*. Microbiology Society. <https://doi.org/10.1099/00207713-43-4-735>
- Buffett, B., & Archer, D. (2004). Global inventory of methane clathrate: Sensitivity to changes in the deep ocean. *Earth and Planetary Science Letters*, *227*, 185–199. <https://doi.org/10.1016/j.epsl.2004.09.005>
- Cai, W.-J., Chen, F., Powell, E. N., Walker, S. E., Parsons-Hubbard, K. M., Staff, G. M., Wang, Y., Ashton-Alcox, K. A., Callender, W. R., & Brett, C. E. (2006). Preferential dissolution of carbonate shells driven by petroleum seep activity in the Gulf of Mexico. *Earth and Planetary Science Letters*, *248*, 227–243. <https://doi.org/10.1016/j.epsl.2006.05.020>
- Campbell, K. A. (2006). Hydrocarbon seep and hydrothermal vent paleoenvironments and paleontology: Past developments and future research directions. *Palaeogeography, Palaeoclimatology, Palaeoecology*, *232*, 362–407. <https://doi.org/10.1016/j.palaeo.2005.06.018>
- Campbell, K. A., Farmer, J. D., & Des Marais, D. (2002). Ancient hydrocarbon seeps from the Mesozoic convergent margin of California: Carbonate geochemistry, fluids and palaeoenvironments. *Geofluids*, *2*, 63–94. <https://doi.org/10.1046/j.1468-8123.2002.00022.x>
- Ceramicola, S., Dupré, S., Somoza, L., & Woodside, J. (2018). Cold seep systems. In A. Micallef, S. Krastel, & A. Savini (Eds.), *Submarine Geomorphology* (pp. 367–387). Cham: Springer International Publishing. https://doi.org/10.1007/978-3-319-57852-1_19
- Charlou, J. L., Donval, J. P., Fouquet, Y., Ondreas, H., Knoery, J., Cochonat, P., Levaché, D., Poirier, Y., Jean-Baptiste, P., Fourré, E., & Chazallon, B. (2004). Physical and chemical characterization of gas hydrates and associated methane plumes in the Congo–Angola Basin. *Chemical Geology*, *205*, 405–425. <https://doi.org/10.1016/j.chemgeo.2003.12.033>
- Chistoserdova, L. (2018). Methanotrophy: An evolving field. In M. G. Kalyuzhnaya & X.-H. Xing (Eds.), *Methane Biocatalysis: Paving the Way to Sustainability* (pp.

- 1–15). Cham: Springer International Publishing. https://doi.org/10.1007/978-3-319-74866-5_1
- Chistoserdova, L., Kalyuzhnaya, M. G., & Lidstrom, M. E. (2009). The expanding world of methylotrophic metabolism. *Annual Review of Microbiology*, *63*, 477–499. <https://doi.org/10.1146/annurev.micro.091208.073600>
- Ciais, P., Sabine, C., Bala, G., Bopp, L., Brovkin, V., Canadell, J., Chhabra, A., DeFries, R., Galloway, J., Heimann, M., Jones, C., Le Quere, C., Myneni, R. B., Piao, S. L., & Thornton, P. (2013). Carbon and other biogeochemical cycles. In T. F. Stocker, D. Qin, G.-K. Plattner, M. Tignor, S. K. Allen, J. Boschung, A. Nauels, Y. Xia, V. Bex, & P. M. Midgley (Eds.), *Climate change 2013: The physical science basis, in contribution of Working Group I (WGI) to the Fifth Assessment Report (AR5) of the Intergovernmental Panel on Climate Change (IPCC)* (pp. 465–570). Cambridge, United Kingdom and New York, NY, USA: Cambridge University Press.
- Coleman, M. L. (1993). Microbial processes: Controls on the shape and composition of carbonate concretions. *Marine Sediments, Burial, Pore Water Chemistry, Microbiology and Diagenesis*, *113*, 127–140. [https://doi.org/10.1016/0025-3227\(93\)90154-N](https://doi.org/10.1016/0025-3227(93)90154-N)
- Collister, J. W., Summons, R. E., Lichtfouse, E., & Hayes, J. M. (1992). An isotopic biogeochemical study of the Green River oil shale. *Organic Geochemistry*, *19*, 265–276. [https://doi.org/10.1016/0146-6380\(92\)90042-V](https://doi.org/10.1016/0146-6380(92)90042-V)
- Connan, J., & Dessort, D. (1987). Novel family of hexacyclic hopanoid alkanes (C₃₂–C₃₅) occurring in sediments and oils from anoxic paleoenvironments. *Organic Geochemistry*, *11*, 103–113. [https://doi.org/10.1016/0146-6380\(87\)90032-5](https://doi.org/10.1016/0146-6380(87)90032-5)
- Coolen, M. J., Talbot, H. M., Abbas, B. A., Ward, C., Schouten, S., Volkman, J. K., & Sinninghe Damsté, J. S. (2008). Sources for sedimentary bacteriohopanepolyols as revealed by 16S rDNA stratigraphy. *Environmental Microbiology*, *10*, 1783–803. <https://doi.org/10.1111/j.1462-2920.2008.01601.x>
- Cordova-Gonzalez, A., Birgel, D., Kappler, A., & Peckmann, J. (2020). Carbon stable isotope patterns of cyclic terpenoids: A comparison of cultured alkaliphilic aerobic methanotrophic bacteria and methane-seep environments. *Organic Geochemistry*, *139*, 103940. <https://doi.org/10.1016/j.orggeochem.2019.103940>
- Crémière, A., Pierre, C., Blanc-Valleron, M.-M., Zitter, T., Çağatay, M. N., & Henry, P. (2012). Methane-derived authigenic carbonates along the North Anatolian fault system in the Sea of Marmara (Turkey). *Deep Sea Research Part I: Oceanographic Research Papers*, *66*, 114–130. <https://doi.org/10.1016/j.dsr.2012.03.014>
- Dedysh, S. N., & Knief, C. (2018). Diversity and phylogeny of described aerobic methanotrophs. In M. G. Kalyuzhnaya & X.-H. Xing (Eds.), *Methane biocatalysis: Paving the way to sustainability* (pp. 17–42). Cham: Springer International Publishing. https://doi.org/10.1007/978-3-319-74866-5_2
- Deppenmeier, U. (2002). The unique biochemistry of methanogenesis. *Progress in Nucleic Acid Research and Molecular Biology, Vol 71*, *71*, 223–283. [https://doi.org/10.1016/S0079-6603\(02\)71045-3](https://doi.org/10.1016/S0079-6603(02)71045-3)
- Deutzmann, J. S., Hoppert, M., & Schink, B. (2014). Characterization and phylogeny of a novel methanotroph, *Methyloglobulus morosus* gen. nov., spec. nov. *Systematic and Applied Microbiology*, *37*, 165–169. <https://doi.org/10.1016/j.syapm.2014.02.001>
- Doughty, D. M., Hunter, R. C., Summons, R. E., & Newman, D. K. (2009). 2-Methylhopanoids are maximally produced in akinetes of *Nostoc punctiforme*: geobiological implications. *Geobiology*, *7*, 524–532. <https://doi.org/10.1111/j.1472-4669.2009.00217.x>

- Dunfield, P., & Knowles, R. (1995). Kinetics of inhibition of methane oxidation by nitrate, nitrite, and ammonium in a humisol. *Applied and Environmental Microbiology*, *61*, 3129–3135.
- Duperron, S., Sibuet, M., MacGregor, B. J., Kuypers, M. M. M., Fisher, C. R., & Dubilier, N. (2007). Diversity, relative abundance and metabolic potential of bacterial endosymbionts in three *Bathymodiolus* mussel species from cold seeps in the Gulf of Mexico. *Environmental Microbiology*, *9*, 1423–1438. <https://doi.org/10.1111/j.1462-2920.2007.01259.x>
- Dupraz, C., Reid, R. P., Braissant, O., Decho, A. W., Norman, R. S., & Visscher, P. T. (2009). Processes of carbonate precipitation in modern microbial mats. *Microbial Mats in Earth's Fossil Record of Life: Geobiology*, *96*, 141–162. <https://doi.org/10.1016/j.earscirev.2008.10.005>
- Durisch-Kaiser, E., Klauser, L., Wehrli, B., & Schubert, C. (2005). Evidence of intense archaeal and bacterial methanotrophic activity in the Black Sea water column. *Applied and Environmental Microbiology*, *71*, 8099–8106. <https://doi.org/10.1128/AEM.71.12.8099-8106.2005>
- Eickhoff, M., Birgel, D., Talbot, H. M., Peckmann, J., & Kappler, A. (2013a). Bacteriohopanoid inventory of *Geobacter sulfurreducens* and *Geobacter metallireducens*. *Organic Geochemistry*, *58*, 107–114. <https://doi.org/10.1016/j.orggeochem.2013.02.013>
- Eickhoff, M., Birgel, D., Talbot, H. M., Peckmann, J., & Kappler, A. (2013b). Oxidation of Fe(II) leads to increased C-2 methylation of pentacyclic triterpenoids in the anoxygenic phototrophic bacterium *Rhodospseudomonas palustris* strain TIE-1. *Geobiology*, *11*, 268–278. <https://doi.org/10.1111/gbi.12033>
- Eickhoff, M., Birgel, D., Talbot, H. M., Peckmann, J., & Kappler, A. (2014). Diagenetic degradation products of bacteriohopanepolyols produced by *Rhodospseudomonas palustris* strain TIE-1. *Organic Geochemistry*, *68*, 31–38. <https://doi.org/10.1016/j.orggeochem.2014.01.002>
- Elvert, M., Boetius, A., Knittel, K., & Jørgensen, B. B. (2003). Characterization of specific membrane fatty acids as chemotaxonomic markers for sulfate-reducing bacteria involved in anaerobic oxidation of methane. *Geomicrobiology Journal*, *20*, 403–419. <https://doi.org/10.1080/01490450303894>
- Elvert, M., & Niemann, H. (2008). Occurrence of unusual steroids and hopanoids derived from aerobic methanotrophs at an active marine mud volcano. *Organic Geochemistry*, *39*, 167–177. <https://doi.org/10.1016/j.orggeochem.2007.11.006>
- Elvert, M., Suess, E., & Whiticar, M. (1999). Anaerobic methane oxidation associated with marine gas hydrates: Superlight C-isotopes from saturated and unsaturated C₂₀ and C₂₅ irregular isoprenoids. *Naturwissenschaften*, *86*, 295–300. <https://doi.org/10.1007/s001140050619>
- Emil Ruff, S. (2020). Microbial communities and metabolisms at hydrocarbon seeps. In A. Teske & V. Carvalho (Eds.), *Marine hydrocarbon seeps: Microbiology and biogeochemistry of a global marine habitat* (pp. 1–19). Cham: Springer International Publishing. https://doi.org/10.1007/978-3-030-34827-4_1
- Farrimond, P., Griffiths, T., & Evdokiadis, E. (2002). Hopanoic acids in Mesozoic sedimentary rocks: Their origin and relationship with hopanes. *Organic Geochemistry*, *33*, 965–977. [https://doi.org/Pii S0146-6380\(02\)00059-1](https://doi.org/Pii S0146-6380(02)00059-1) Doi 10.1016/S0146-6380(02)00059-1
- Gallagher, K. L., Dupraz, C., & Visscher, P. T. (2014). Two opposing effects of sulfate reduction on carbonate precipitation in normal marine, hypersaline, and alkaline environments: COMMENT. *Geology*, *42*, e313–e314. <https://doi.org/10.1130/G34639C.1>
- Garcia-Pichel, F. (2006). Plausible mechanisms for the boring on carbonates by microbial phototrophs. *Sedimentary Geology*, *185*, 205–213. <https://doi.org/10.1016/j.sedgeo.2005.12.013>

- Garcia-Pichel, F., Ramírez-Reinat, E., & Gao, Q. (2010). Microbial excavation of solid carbonates powered by P-type ATPase-mediated transcellular Ca^{2+} transport. *Proceedings of the National Academy of Sciences of the United States of America*, *107*, 21749–54. <https://doi.org/10.1073/pnas.1011884108>
- Golubic, S., Radtke, G., & Campion-Alsumard, T. L. (2005). Endolithic fungi in marine ecosystems. *Trends in Microbiology*, *13*, 229–235. <https://doi.org/10.1016/j.tim.2005.03.007>
- Greinert, J., Bohrmann, G., & Suess, E. (2013). Gas hydrate-associated carbonates and methane-venting at Hydrate Ridge: Classification, distribution, and origin of authigenic lithologies. *Natural Gas Hydrates: Occurrence, Distribution, and Detection, Geophysical Monograph Series*, *124*. <https://doi.org/10.1029/GM124p0099>
- Guan, H., Birgel, D., Feng, D., Peckmann, J., Liu, L., Liu, L., & Tao, J. (2021). Lipids and their $\delta^{13}\text{C}$ values reveal carbon assimilation and cycling in the methane-seep tubeworm *Paraescarpia echinospica* from the South China Sea. *Deep Sea Research Part I: Oceanographic Research Papers*, *174*, 103556. <https://doi.org/10.1016/j.dsr.2021.103556>
- Hanson, R. S., & Hanson, T. E. (1996). Methanotrophic bacteria. *Microbiological Reviews*, *60*, 439–471.
- Härtner, T., Straub, K. L., & Kannenberg, E. L. (2005). Occurrence of hopanoid lipids in anaerobic *Geobacter* species. *FEMS Microbiology Letters*, *243*, 59–64.
- Hayes, J. M. (1993). Factors controlling ^{13}C contents of sedimentary organic compounds: Principles and evidence. *Marine Geology*, *113*, 111–125. [https://doi.org/10.1016/0025-3227\(93\)90153-M](https://doi.org/10.1016/0025-3227(93)90153-M)
- Hayes, J. M., Freeman, K. H., Popp, B. N., & Hoham, C. H. (1990). Compound-specific isotopic analyses: A novel tool for reconstruction of ancient biogeochemical processes. *Organic Geochemistry*, *16*, 1115–1128. [https://doi.org/10.1016/0146-6380\(90\)90147-R](https://doi.org/10.1016/0146-6380(90)90147-R)
- Himmler, T., Birgel, D., Bayon, G., Pape, T., Ge, L., Bohrmann, G., & Peckmann, J. (2015). Formation of seep carbonates along the Makran convergent margin, northern Arabian Sea and a molecular and isotopic approach to constrain the carbon isotopic composition of parent methane. *Chemical Geology*, *415*, 102–117. <https://doi.org/10.1016/j.chemgeo.2015.09.016>
- Himmler, T., Brinkmann, F., Bohrmann, G., & Peckmann, J. (2011). Corrosion patterns of seep-carbonates from the eastern Mediterranean Sea. *Terra Nova*, *23*, 206–212. <https://doi.org/10.1111/j.1365-3121.2011.01000.x>
- Hinrichs, K.-U., & Boetius, A. (2002). The anaerobic oxidation of methane: new insights in microbial ecology and biogeochemistry. In G. Wefer, D. Billett, D. Hebbeln, B. B. Jørgensen, M. Schlüter, & T. C. E. van Weering (Eds.), *Ocean Margin Systems* (pp. 457–477). Berlin Heidelberg: Springer.
- Hinrichs, K.-U., Hayes, J. M., Sylva, S. P., Brewer, P. G., & DeLong, E. F. (1999). Methane-consuming archaeobacteria in marine sediments. *Nature*, *398*, 802–805.
- Hirayama, H., Abe, M., Miyazaki, M., Nunoura, T., Furushima, Y., Yamamoto, H., & Takai, K. (2014). *Methylomarinovum caldicuralii* gen. nov., sp. nov., a moderately thermophilic methanotroph isolated from a shallow submarine hydrothermal system, and proposal of the family *Methylothermaceae* fam. nov. *International Journal of Systematic and Evolutionary Microbiology*, *64*, 989–999.
- Hirayama, H., Fuse, H., Abe, M., Miyazaki, M., Nakamura, T., Nunoura, T., Furushima, Y., Yamamoto, H., & Takai, K. (2013). *Methylomarinum vadi* gen. nov., sp. nov., a methanotroph isolated from two distinct marine environments. *International Journal of Systematic and Evolutionary Microbiology*. Microbiology Society. <https://doi.org/10.1099/ijs.0.040568-0>

- Hoefman, S., van der Ha, D., Boon, N., Vandamme, P., De Vos, P., & Heylen, K. (2014). Niche differentiation in nitrogen metabolism among methanotrophs within an operational taxonomic unit. *BMC Microbiology*, *14*, 83. <https://doi.org/10.1186/1471-2180-14-83>
- Howarth, R. W., Santoro, R., & Ingraffea, A. (2011). Methane and the greenhouse-gas footprint of natural gas from shale formations. *Climatic Change*, *106*, 679. <https://doi.org/10.1007/s10584-011-0061-5>
- Hussler, G., Connan, J., & Albrecht, P. (1984). Novel families of tetra- and hexacyclic aromatic hopanoids predominant in carbonate rocks and crude oils. *Organic Geochemistry*, *6*, 39–49. [https://doi.org/10.1016/0146-6380\(84\)90025-1](https://doi.org/10.1016/0146-6380(84)90025-1)
- Innes, H. E., Bishop, A. N., Head, I. M., & Farrimond, P. (1997). Preservation and diagenesis of hopanoids in recent lacustrine sediments of Priest Pot, England. *Organic Geochemistry*, *26*, 565–576. [https://doi.org/10.1016/S0146-6380\(97\)00017-X](https://doi.org/10.1016/S0146-6380(97)00017-X)
- Jahnke, L. L., & Nichols, P. D. (1986). Methyl sterol and cyclopropane fatty acid composition of *Methylococcus capsulatus* grown at low oxygen tensions. *Journal of Bacteriology*, *167*, 238–242. <https://doi.org/10.1128/jb.167.1.238-242.1986>
- Jahnke, L. L., Summons, R. E., Dowling, L. M., & Zahiralis, K. D. (1995). Identification of methanotrophic lipid biomarkers in cold-seep mussel gills: Chemical and isotopic analysis. *Appl Environ Microbiol*, *61*, 576–82.
- Jahnke, L. L., Summons, R. E., Hope, J. M., & des Marais, D. J. (1999). Carbon isotopic fractionation in lipids from methanotrophic bacteria II: The effects of physiology and environmental parameters on the biosynthesis and isotopic signatures of biomarkers. *Geochimica et Cosmochimica Acta*, *63*, 79–93. [https://doi.org/10.1016/S0016-7037\(98\)00270-1](https://doi.org/10.1016/S0016-7037(98)00270-1)
- Jorgensen, A. D., Picel, K. C., & Stamoudis, V. C. (1990). Prediction of gas chromatography flame ionization detector response factors from molecular structures. *Analytical Chemistry*, *62*, 683–689. <https://doi.org/10.1021/ac00206a007>
- Joseph, A. (2017). Seafloor hot chimneys and cold seeps: Mysterious life around them. In A. Joseph (Ed.), *Investigating seafloors and oceans* (pp. 307–375). Elsevier. <https://doi.org/10.1016/B978-0-12-809357-3.00006-0>
- Kalyuzhnaya, M. G., Gomez, O. A., & Murrell, J. C. (2019). The methane-oxidizing bacteria (methanotrophs). In T. J. McGenity (Ed.), *Taxonomy, genomics and ecophysiology of hydrocarbon-degrading microbes* (pp. 1–34). Cham: Springer International Publishing. https://doi.org/10.1007/978-3-319-60053-6_10-1
- Kalyuzhnaya, M. G., Khmelenina, V., Eshinimaev, B., Sorokin, D., Fuse, H., Lidstrom, M., & Trotsenko, Y. (2008). Classification of halo(alkali)philic and halo(alkali)tolerant methanotrophs provisionally assigned to the genera *Methylomicrobium* and *Methylobacter* and emended description of the genus *Methylomicrobium*. *International Journal of Systematic and Evolutionary Microbiology*, *58*, 591–596. <https://doi.org/10.1099/ijs.0.65317-0>
- Kannenbergh, E. L., & Poralla, K. (1999). Hopanoid biosynthesis and function in bacteria. *Naturwissenschaften*, *86*, 168–176. <https://doi.org/10.1007/s001140050592>
- Karstens, J., Hafliadason, H., Becker, L. W. M., Berndt, C., Rüpke, L., Planke, S., Liebetrau, V., Schmidt, M., & Mienert, J. (2018). Glacigenic sedimentation pulses triggered post-glacial gas hydrate dissociation. *Nature Communications*, *9*, 635. <https://doi.org/10.1038/s41467-018-03043-z>
- Kellermann, M. Y., Schubotz, F., Elvert, M., Lipp, J. S., Birgel, D., Prieto-Mollar, X., Dubilier, N., & Hinrichs, K.-U. (2012). Symbiont-host relationships in chemosynthetic mussels: A comprehensive lipid biomarker study. *Organic Geochemistry*, *43*, 112–124. <https://doi.org/10.1016/j.orggeochem.2011.10.005>

- Kennett, J. P., Cannariato, K., Hendy, I., & Behl, R. (2003). *Methane Hydrates in Quaternary Climate Change: The Clathrate Gun Hypothesis* (1st ed.). Washington DC: American Geophysical Union. <https://doi.org/10.1029/054SP>
- Khider, M., Brautaset, T., & Irla, M. (2021). Methane monooxygenases: Central enzymes in methanotrophy with promising biotechnological applications. *World Journal of Microbiology and Biotechnology*, *37*. <https://doi.org/10.1007/s11274-021-03038-x>
- Khmelenina, V. N., Colin Murrell, J., Smith, T. J., & Trotsenko, Y. A. (2018). Physiology and biochemistry of the aerobic methanotrophs. In F. Rojo (Ed.), *Aerobic Utilization of Hydrocarbons, Oils and Lipids* (pp. 1–25). Cham: Springer International Publishing. https://doi.org/10.1007/978-3-319-39782-5_4-1
- Killops, S., & Killops, V. (2005). *Introduction to Organic Geochemistry* (2nd ed.). Oxford: Blackwell Publishing.
- Knief, C. (2015). Diversity and habitat preferences of cultivated and uncultivated aerobic methanotrophic bacteria evaluated based on *pmoA* as molecular marker. *Frontiers in Microbiology*, *6*, 1346. <https://doi.org/10.3389/fmicb.2015.01346>
- Knoblauch, C., Zimmermann, U., Blumenberg, M., Michaelis, W., & Pfeiffer, E.-M. (2008). Methane turnover and temperature response of methane-oxidizing bacteria in permafrost-affected soils of northeast Siberia. *Soil Biology and Biochemistry*, *40*, 3004–3013. <https://doi.org/10.1016/j.soilbio.2008.08.020>
- Krause, S., Aloisi, G., Engel, A., Liebetrau, V., & Treude, T. (2014). Enhanced calcite dissolution in the presence of the aerobic methanotroph *Methylosinus trichosporium*. *Geomicrobiology Journal*, *31*, 325–337. <https://doi.org/10.1080/01490451.2013.834007>
- Krause, S., Niemann, H., & Treude, T. (2017). 1. Methane seeps in a changing climate. In J. Kallmeyer (Ed.), *Life at Vents and Seeps* (pp. 1–32). <https://doi.org/10.1515/9783110493672-001>
- Kulkarni, G., Wu, C.-H., & Newman, D. K. (2013). The general stress response factor EcfG regulates expression of the C-2 hopanoid methylase HpnP in *Rhodopseudomonas palustris* TIE-1. *Journal of Bacteriology*, *195*, 2490–2498. <https://doi.org/10.1128/JB.00186-13>
- Lanoil, B. D., Sassen, R., La Duc, M. T., Sweet, S. T., & Neilson, K. H. (2001). Bacteria and archaea physically associated with Gulf of Mexico gas hydrates. *Appl Environ Microbiol*, *67*, 5143–5153. <https://doi.org/10.1128/Aem.67.11.5143-5153.2001>
- Leprich, D. J., Flood, B. E., Schroedl, P. R., Ricci, E., Marlow, J. J., Girguis, P. R., & Bailey, J. V. (2021). Sulfur bacteria promote dissolution of authigenic carbonates at marine methane seeps. *The ISME Journal*. <https://doi.org/10.1038/s41396-021-00903-3>
- Lösekan, T., Knittel, K., Nadalig, T., Fuchs, B., Niemann, H., Boetius, A., & Amann, R. (2007). Diversity and abundance of aerobic and anaerobic methane oxidizers at the Haakon Mosby Mud Volcano, Barents Sea. *Applied and Environmental Microbiology*, *73*, 3348–3362. <https://doi.org/10.1128/Aem.00016-07>
- Lupascu, M., Wadham, J. L., Hornibrook, E. R. C., & Pancost, R. D. (2014). Methanogen biomarkers in the discontinuous permafrost zone of Stordalen, Sweden. *Permafrost and Periglacial Processes*, *25*, 221–232. <https://doi.org/10.1002/ppp.1823>
- Ma, G., Zhan, L., Lu, H., & Hou, G. (2021). Structures in shallow marine sediments associated with gas and fluid migration. *Journal of Marine Science and Engineering*, *9*. <https://doi.org/10.3390/jmse9040396>
- Mangiarotti, A., Genovese, D. M., Naumann, C. A., Monti, M. R., & Wilke, N. (2019). Hopanoids, like sterols, modulate dynamics, compaction, phase segregation

- and permeability of membranes. *Biochimica et Biophysica Acta (BBA) - Biomembranes*, 1861, 183060. <https://doi.org/10.1016/j.bbamem.2019.183060>
- Marcon, Y., Ondréas, H., Sahling, H., Bohrmann, G., & Olu, K. (2014a). Fluid flow regimes and growth of a giant pockmark. *Geology*, 42, 63–66. <https://doi.org/10.1130/G34801.1>
- Marcon, Y., Sahling, H., Allais, A.-G., Bohrmann, G., & Olu, K. (2014b). Distribution and temporal variation of mega-fauna at the Regab pockmark (Northern Congo Fan), based on a comparison of videomosaics and geographic information systems analyses. *Marine Ecology*, 35, 77–95. <https://doi.org/10.1111/maec.12056>
- Matsumoto, R. (1990). Vuggy carbonate crust formed by hydrocarbon seepage on the continental shelf of Baffin Island, northeast Canada. *Geochemical Journal*, 24, 143–158.
- Mau, S., Tu, T.-H., Becker, M., dos Santos Ferreira, C., Chen, J.-N., Lin, L.-H., Wang, P.-L., Lin, S., & Bohrmann, G. (2020). Methane seeps and independent methane plumes in the South China Sea offshore Taiwan. *Frontiers in Marine Science*, 7, 543. <https://doi.org/10.3389/fmars.2020.00543>
- McCaffrey, M. A., Farrington, J. W., & Repeta, D. J. (1989). Geochemical implications of the lipid composition of *Thioploca* spp. from the Peru upwelling region—15°S. *Organic Geochemistry*, 14, 61–68. [https://doi.org/10.1016/0146-6380\(89\)90019-3](https://doi.org/10.1016/0146-6380(89)90019-3)
- McDonald, I. R., Kenna, E. M., & Murrell, J. C. (1995). Detection of methanotrophic bacteria in environmental samples with the PCR. *Applied and Environmental Microbiology*, 61, 116–121. <https://doi.org/10.1128/aem.61.1.116-121.1995>
- Meister, P. (2013). Two opposing effects of sulfate reduction on carbonate precipitation in normal marine, hypersaline, and alkaline environments. *Geology*, 41, 499–502. <https://doi.org/10.1130/G34185.1>
- Nalin, R., Putra, S. R., Domenach, A.-M., Rohmer, M., Gourbiere, F., & Berry, A. M. (2000). High hopanoid/total lipids ratio in *Frankia* mycelia is not related to the nitrogen status. *Microbiology*. Microbiology Society. <https://doi.org/10.1099/00221287-146-11-3013>
- Natalicchio, M., Peckmann, J., Birgel, D., & Kiel, S. (2015). Seep deposits from northern Istria, Croatia: a first glimpse into the Eocene seep fauna of the Tethys region. *Geological Magazine*, 152, 444–459. <https://doi.org/10.1017/S0016756814000466>
- Naviaux, J. D., Subhas, A. V., Rollins, N. E., Dong, S., Berelson, W. M., & Adkins, J. F. (2019). Temperature dependence of calcite dissolution kinetics in seawater. *Geochimica et Cosmochimica Acta*, 246, 363–384. <https://doi.org/10.1016/j.gca.2018.11.037>
- Nazaries, L., Pan, Y., Bodrossy, L., Baggs, E. M., Millard, P., Murrell, J. C., & Singh, B. K. (2013). Evidence of microbial regulation of biogeochemical cycles from a study on methane flux and land use change. *Applied and Environmental Microbiology*, 79, 4031–4040. <https://doi.org/10.1128/AEM.00095-13>
- Neunlist, S., & Rohmer, M. (1985). Novel hopanoids from the methylotrophic bacteria *Methylococcus capsulatus* and *Methylomonas methanica*: (22S)-35-aminobacteriohopane-30,31,32,33,34-pentol and (22S)-35-amino-3β-methylbacteriohopane-30,31,32,33,34-pentol. *Biochemical Journal*, 231, 635–639.
- Nichols, P. D., Guckert, J. B., & White, D. C. (1986). Determination of monosaturated fatty acid double-bond position and geometry for microbial monocultures and complex consortia by capillary GC-MS of their dimethyl disulphide adducts. *Journal of Microbiological Methods*, 5, 49–55. [https://doi.org/10.1016/0167-7012\(86\)90023-0](https://doi.org/10.1016/0167-7012(86)90023-0)

- Niemann, H., Elvert, M., Hovland, M., Orcutt, B., Judd, A., Suck, I., Gutt, J., Joye, S., Damm, E., Finster, K., & Boetius, A. (2005). Methane emission and consumption at a North Sea gas seep (Tommeliten area). *Biogeosciences*, 2, 335–351. <https://doi.org/10.5194/bg-2-335-2005>
- Niemann, H., Lösekann, T., de Beer, D., Elvert, M., Nadalig, T., Knittel, K., Amann, R., Sauter, E. J., Schluter, M., Klages, M., Foucher, J. P., & Boetius, A. A. (2006). Novel microbial communities of the Haakon Mosby mud volcano and their role as a methane sink. *Nature*, 443, 854–8. <https://doi.org/10.1038/nature05227>
- Noll, M., Frenzel, P., & Conrad, R. (2008). Selective stimulation of type I methanotrophs in a rice paddy soil by urea fertilization revealed by RNA-based stable isotope probing. *FEMS Microbiology Ecology*, 65, 125–132. <https://doi.org/10.1111/j.1574-6941.2008.00497.x>
- Nyerges, G., Han, S.-K., & Stein, L. Y. (2010). Effects of ammonium and nitrite on growth and competitive fitness of cultivated methanotrophic bacteria. *Applied and Environmental Microbiology*, 76, 5648. <https://doi.org/10.1128/AEM.00747-10>
- Nyerges, G., & Stein, L. Y. (2009). Ammonia cometabolism and product inhibition vary considerably among species of methanotrophic bacteria. *FEMS Microbiology Letters*, 297, 131–136. <https://doi.org/10.1111/j.1574-6968.2009.01674.x>
- Olu, K. (2011). *WACS cruise, RV Pourquoi pas? R/V. Brest: Ifremer*. Retrieved from <http://dx.doi.org/10.17600/11030010>
- Olu-Le Roy, K., Caprais, J.-C., Fifis, A., Fabri, M.-C., Galéron, J., Budzinsky, H., Le Ménach, K., Khripounoff, A., Ondréas, H., & Sibuet, M. (2007). Cold-seep assemblages on a giant pockmark off West Africa: Spatial patterns and environmental control. *Marine Ecology*, 28, 115–130. <https://doi.org/10.1111/j.1439-0485.2006.00145.x>
- Ondréas, H., Olu, K., Fouquet, Y., Charlou, J. L., Gay, A., Dennielou, B., Donval, J. P., Fifis, A., Nadalig, T., Cochonat, P., Cauquil, E., Bourillet, J. F., Moigne, M. L., & Sibuet, M. (2005). ROV study of a giant pockmark on the Gabon continental margin. *Geo-Marine Letters*, 25, 281–292. <https://doi.org/10.1007/s00367-005-0213-6>
- Orata, F. D., Meier-Kolthoff, J. P., Sauvageau, D., & Stein, L. Y. (2018). Phylogenomic analysis of the gammaproteobacterial methanotrophs (order *Methylococcales*) Calls for the reclassification of members at the genus and species levels. *Frontiers in Microbiology*, 9, 3162. <https://doi.org/10.3389/fmicb.2018.03162>
- Orphan, V. J., House, C. H., Hinrichs, K.-U., McKeegan, K. D., & DeLong, E. F. (2002). Multiple archaeal groups mediate methane oxidation in anoxic cold seep sediments. *Proceedings of the National Academy of Sciences of the United States of America*, 99, 7663–7668. <https://doi.org/10.1073/pnas.072210299>
- Osborne, K. A., Gray, N. D., Sherry, A., Leary, P., Mejeha, O., Bischoff, J., Rush, D., Sidgwick, F. R., Birgel, D., Kalyuzhnaya, M. G., & Talbot, H. M. (2017). Methanotroph-derived bacteriohopanepolyol signatures as a function of temperature related growth, survival, cell death and preservation in the geological record. *Environmental Microbiology Reports*, 9, 492–500. <https://doi.org/10.1111/1758-2229.12570>
- Ourisson, G., & Albrecht, P. (1992). Hopanoids. 1. Geohopanoids: The most abundant natural products on Earth? *Accounts of Chemical Research*, 25, 398–402. <https://doi.org/10.1021/ar00021a003>
- Parks, D. H., Chuvochina, M., Waite, D. W., Rinke, C., Skarshewski, A., Chaumeil, P.-A., & Hugenholtz, P. (2018). A standardized bacterial taxonomy based on genome phylogeny substantially revises the tree of life. *Nature Biotechnology*, 36, 996–1004. <https://doi.org/10.1038/nbt.4229>

- Pearson, A. (2014). Lipidomics for geochemistry. In *Treatise on Geochemistry: Second Edition* (Vol. 12, pp. 291–336). <https://doi.org/10.1016/B978-0-08-095975-7.01022-6>
- Pearson, E. J., Farrimond, P., & Juggins, S. (2007). Lipid geochemistry of lake sediments from semi-arid Spain: Relationships with source inputs and environmental factors. *Organic Geochemistry*, 38, 1169–1195. <https://doi.org/10.1016/j.orggeochem.2007.02.007>
- Peckmann, J., Reimer, A., Luth, U., Luth, C., Hansen, B. T., Heinicke, C., Hoefs, J., & Reitner, J. (2001). Methane-derived carbonates and authigenic pyrite from the northwestern Black Sea. *Marine Geology*, 177, 129–150. [https://doi.org/10.1016/S0025-3227\(01\)00128-1](https://doi.org/10.1016/S0025-3227(01)00128-1)
- Peckmann, J., & Thiel, V. (2004). Carbon cycling at ancient methane-seeps. *Chemical Geology*, 205, 443–467. <https://doi.org/10.1016/j.chemgeo.2003.12.025>
- Peckmann, J., Thiel, V., Michaelis, W., Clari, P., Gaillard, C., Martire, L., & Reitner, J. (1999). Cold seep deposits of Beauvoisin (Oxfordian; southeastern France) and Marmorito (Miocene; northern Italy): Microbially induced authigenic carbonates. *International Journal of Earth Sciences*, 88, 60–75. [https://doi.org/DOI 10.1007/s005310050246](https://doi.org/DOI%2010.1007/s005310050246)
- Peckmann, J., Thiel, V., Reitner, J., Taviani, M., Aharon, P., & Michaelis, W. (2004). A microbial mat of a large sulfur bacterium preserved in a Miocene methane-seep limestone. *Geomicrobiology Journal*, 21, 247–255. <https://doi.org/10.1080/01490450490438757>
- Peters, K. E., Walters, C. C., & Moldowan, J. M. (2004a). *The Biomarker Guide: Volume 1: Biomarkers and Isotopes in the Environment and Human History* (2nd ed., Vol. 1). Cambridge: Cambridge University Press. <https://doi.org/10.1017/CBO9780511524868>
- Peters, K. E., Walters, C. C., & Moldowan, J. M. (2004b). *The Biomarker Guide: Volume 2: Biomarkers and Isotopes in Petroleum Systems and Earth History* (2nd ed., Vol. 2). Cambridge: Cambridge University Press. <https://doi.org/10.1017/CBO9781107326040>
- Pierre, C., & Fouquet, Y. (2007). Authigenic carbonates from methane seeps of the Congo deep-sea fan. *Geo-Marine Letters*, 27, 249–257. <https://doi.org/10.1007/s00367-007-0081-3>
- Pond, D. W., Bell, M. V., Dixon, D. R., Fallick, A. E., Segonzac, M., & Sargent, J. R. (1998). Stable-carbon-isotope composition of fatty acids in hydrothermal vent mussels containing methanotrophic and thiotrophic bacterial endosymbionts. *Applied and Environmental Microbiology*, 64, 370–375. <https://doi.org/10.1128/AEM.64.1.370-375.1998>
- Poralla, K., Härtner, T., & Kannenberg, E. (1984). Effect of temperature and pH on the hopanoid content of *Bacillus acidocaldarius*. *FEMS Microbiology Letters*, 23, 253–256. <https://doi.org/10.1111/j.1574-6968.1984.tb01073.x>
- Radtke, G. (1991). *Die mikroendolithischen Spurenfossilien im Alt-Tertiär West-Europas und ihre palökologische Bedeutung*. Stuttgart, Germany: Schweizerbart Science Publishers. Retrieved from http://www.schweizerbart.de/publications/detail/isbn/9783510611294/CFS_Courier_Forschungsinstitut_Senckenbe
- Radtke, G., Glaub, I., Vogel, K., & Golubic, S. (2010). A new dichotomous microboring: *Abeliella bellafurca* sp. nov., distribution, variability and biological origin. *Ichnos*, 17, 25–33. <https://doi.org/10.1080/10420940903358628>
- Rahalkar, M., Bussmann, I., & Schink, B. (2007). *Methylosoma difficile* gen. nov., sp. nov., a novel methanotroph enriched by gradient cultivation from littoral sediment of Lake Constance. *International Journal of Systematic and Evolutionary Microbiology*. Microbiology Society. <https://doi.org/10.1099/ijs.0.64574-0>

- Rashby, S. E., Sessions, A. L., Summons, R. E., & Newman, D. K. (2007). Biosynthesis of 2-methylbacteriohopanepolyols by an anoxygenic phototroph. *Proc Natl Acad Sci U S A*, *104*, 15099–15104. <https://doi.org/10.1073/pnas.0704912104>
- Reeburgh, W. S. (2007). Oceanic methane biogeochemistry. *Chem Rev*, *107*, 486–513. <https://doi.org/10.1021/cr050362v>
- Rohmer, M., Bouvier, P., & Ourisson, G. (1979). Molecular evolution of biomembranes: Structural equivalents and phylogenetic precursors of sterols. *Proceedings of the National Academy of Sciences*, *76*, 847. <https://doi.org/10.1073/pnas.76.2.847>
- Rohmer, M., Bouviernave, P., & Ourisson, G. (1984). Distribution of hopanoid triterpenes in prokaryotes. *Journal of General Microbiology*, *130*, 1137–1150.
- Rubin-Blum, M., Antony, C. P., Sayavedra, L., Martínez-Pérez, C., Birgel, D., Peckmann, J., Wu, Y.-C., Cardenas, P., MacDonald, I., Marcon, Y., Sahling, H., Hentschel, U., & Dubilier, N. (2019). Fueled by methane: Deep-sea sponges from asphalt seeps gain their nutrition from methane-oxidizing symbionts. *The ISME Journal*, *13*, 1209–1225. <https://doi.org/10.1038/s41396-019-0346-7>
- Rush, D., Osborne, K. A., Birgel, D., Kappler, A., Hirayama, H., Peckmann, J., Poulton, S. W., Nickel, J. C., Mangelsdorf, K., Kalyuzhnaya, M. G., Sidgwick, F. R., & Talbot, H. M. (2016). The bacteriohopanepolyol inventory of novel aerobic methane oxidising bacteria reveals new biomarker signatures of aerobic methanotrophy in marine systems. *PLoS One*, *11*, e0165635. <https://doi.org/10.1371/journal.pone.0165635>
- Rush, D., Sinninghe Damsté, J. S., Poulton, S. W., Thamdrup, B., Garside, A. L., González, J. [Acuña, Schouten, S., Jetten, M. S. M., & Talbot, H. M. (2014). Anaerobic ammonium-oxidising bacteria: A biological source of the bacteriohopanetetrol stereoisomer in marine sediments. *Geochimica et Cosmochimica Acta*, *140*, 50–64. <https://doi.org/10.1016/j.gca.2014.05.014>
- Sahling, H., Rickert, D., Lee, R. W., Linke, P., & Suess, E. (2002). Macrofaunal community structure and sulfide flux at gas hydrate deposits from the Cascadia convergent margin, NE Pacific. *Marine Ecology Progress Series*, *231*, 121–138. <https://doi.org/10.3354/meps231121>
- Saito, H., & Suzuki, N. (2007). Distributions and sources of hopanes, hopanoic acids and hopanols in Miocene to recent sediments from ODP Leg 190, Nankai Trough. *Organic Geochemistry*, *38*, 1715–1728.
- Sandy, M. R., Lazar, I., Peckmann, J., Birgel, D., Stoica, M., & Roban, R. D. (2012). Methane-seep brachiopod fauna within turbidites of the Sinaia Formation, Eastern Carpathian Mountains, Romania. *Palaeogeography Palaeoclimatology Palaeoecology*, *323*, 42–59. <https://doi.org/10.1016/j.palaeo.2012.01.026>
- Sato, S., Kudo, F., Rohmer, M., & Eguchi, T. (2020). Characterization of radical SAM adenosylhopane synthase, HpnH, which catalyzes the 5'-deoxyadenosyl radical addition to diploptene in the biosynthesis of C₃₅ bacteriohopanepolyols. *Angewandte Chemie International Edition*, *59*, 237–241. <https://doi.org/10.1002/anie.201911584>
- Schouten, S., Bowman, J. P., Rijpstra, W. I., & Sinninghe Damsté, J. S. (2000). Sterols in a psychrophilic methanotroph, *Methylosphaera hansonii*. *FEMS Microbiology Letters*, *186*, 193–195.
- Schwartz-Narbonne, R., Schaeffer, P., Hopmans, E. C., Schenese, M., Charlton, E. A., Jones, D. M., Sinninghe Damsté, J. S., Haque, M. [Farhan U., Jetten, M. S. M., Lengger, S. K., Murrell, J. C., Normand, P., Nuijten, G. H. L., Talbot, H. M., & Rush, D. (2020). A unique bacteriohopanetetrol stereoisomer of marine anammox. *Organic Geochemistry*, *143*, 103994. <https://doi.org/10.1016/j.orggeochem.2020.103994>

- Semrau, J. D., DiSpirito, A. A., & Yoon, S. (2010). Methanotrophs and copper. *FEMS Microbiology Reviews*, *34*, 496–531. <https://doi.org/10.1111/j.1574-6976.2010.00212.x>
- Sessions, A. L., Zhang, L., Welander, P. V., Doughty, D., Summons, R. E., & Newman, D. K. (2013). Identification and quantification of polyfunctionalized hopanoids by high temperature gas chromatography–mass spectrometry. *Organic Geochemistry*, *56*, 120–130. <https://doi.org/10.1016/j.orggeochem.2012.12.009>
- Sherry, A., Osborne, K. A., Sidgwick, F. R., Gray, N. D., & Talbot, H. M. (2016). A temperate river estuary is a sink for methanotrophs adapted to extremes of pH, temperature and salinity. *Environmental Microbiology Reports*, *8*, 122–131. <https://doi.org/10.1111/1758-2229.12359>
- Sinninghe Damsté, J. S., Kenig, F., Koopmans, M. P., Köster, J., Schouten, S., Hayes, J. M., & Leeuw, J. W. [de. (1995a). Evidence for gammacerane as an indicator of water column stratification. *Geochimica et Cosmochimica Acta*, *59*, 1895–1900. [https://doi.org/10.1016/0016-7037\(95\)00073-9](https://doi.org/10.1016/0016-7037(95)00073-9)
- Sinninghe Damsté, J. S., Van Duin, A. C. T., Hollander, D., Kohnen, M. E. L., & De Leeuw, J. W. (1995b). Early diagenesis of bacteriohopanepolyol derivatives: Formation of fossil homohopanoids. *Geochimica Et Cosmochimica Acta*, *59*, 5141–5147. [https://doi.org/10.1016/0016-7037\(95\)00338-x](https://doi.org/10.1016/0016-7037(95)00338-x)
- Sloan, E. D. (2003). Fundamental principles and applications of natural gas hydrates. *Nature*, *426*, 353–359. <https://doi.org/10.1038/nature02135>
- Smith, T. J., Trotsenko, Y. A., & Murrell, J. C. (2010). Physiology and biochemistry of the aerobic methane oxidizing bacteria. In K. N. Timmis (Ed.), *Handbook of Hydrocarbon and Lipid Microbiology* (pp. 767–779). Berlin, Heidelberg: Springer Berlin Heidelberg. https://doi.org/10.1007/978-3-540-77587-4_58
- Spencer-Jones, C. L., Wagner, T., Dinga, B. J., Schefuss, E., Mann, P. J., Poulsen, J. R., Spencer, R. G. M., Wabakanghanzi, J. N., & Talbot, H. M. (2015). Bacteriohopanepolyols in tropical soils and sediments from the Congo River catchment area. *Organic Geochemistry*, *89–90*, 1–13. <https://doi.org/10.1016/j.orggeochem.2015.09.003>
- Subhas, A. V., Adkins, J. F., Rollins, N. E., Naviaux, J., Erez, J., & Berelson, W. M. (2017). Catalysis and chemical mechanisms of calcite dissolution in seawater. *Proceedings of the National Academy of Sciences*, *114*, 8175. <https://doi.org/10.1073/pnas.1703604114>
- Suess, E. (2010). Marine cold seeps. In K. N. Timmis (Ed.), *Handbook of Hydrocarbon and Lipid Microbiology* (pp. 187–203). Berlin Heidelberg: Springer.
- Suess, E. (2014). Marine cold seeps and their manifestations: geological control, biogeochemical criteria and environmental conditions. *International Journal of Earth Sciences*, *103*, 1889–1916. <https://doi.org/10.1007/s00531-014-1010-0>
- Suess, E., Torres, M. E., Bohrmann, G., Collier, R. W., Greinert, J., Linke, P., Rehder, G., Trehu, A., Wallmann, K., Winckler, G., & Zuleger, E. (1999). Gas hydrate destabilization: Enhanced dewatering, benthic material turnover and large methane plumes at the Cascadia convergent margin. *Earth and Planetary Science Letters*, *170*, 1–15. [https://doi.org/10.1016/S0012-821X\(99\)00092-8](https://doi.org/10.1016/S0012-821X(99)00092-8)
- Summons, R. E., Bradley, A. S., Jahnke, L. L., & Waldbauer, J. R. (2006). Steroids, triterpenoids and molecular oxygen. *Philosophical Transactions of the Royal Society of London. Series B, Biological Sciences*, *361*, 951–968. <https://doi.org/10.1098/rstb.2006.1837>
- Summons, R. E., Jahnke, L. L., & Roksandic, Z. (1994). Carbon isotopic fractionation in lipids from methanotrophic bacteria: Relevance for interpretation of the geochemical record of biomarkers. *Geochimica Et Cosmochimica Acta*, *58*, 2853–2863. [https://doi.org/10.1016/0016-7037\(94\)90119-8](https://doi.org/10.1016/0016-7037(94)90119-8)

- Summons, R. E., Welander, P. V., & Gold, D. A. (2021). Lipid biomarkers: molecular tools for illuminating the history of microbial life. *Nature Reviews Microbiology*. <https://doi.org/10.1038/s41579-021-00636-2>
- Talbot, H. M., & Farrimond, P. (2007). Bacterial populations recorded in diverse sedimentary biohopanoid distributions. *Organic Geochemistry*, *38*, 1212–1225. <https://doi.org/10.1016/j.orggeochem.2007.04.006>
- Talbot, H. M., Handley, L., Spencer-Jones, C. L., Dinga, B. J., Schefuss, E., Mann, P. J., Poulsen, J. R., Spencer, R. G. M., Wabakanghanzi, J. N., & Wagner, T. (2014). Variability in aerobic methane oxidation over the past 1.2 Myrs recorded in microbial biomarker signatures from Congo fan sediments. *Geochimica Et Cosmochimica Acta*, *133*, 387–401. <https://doi.org/10.1016/j.gca.2014.02.035>
- Talbot, H. M., Rohmer, M., & Farrimond, P. (2007a). Rapid structural elucidation of composite bacterial hopanoids by atmospheric pressure chemical ionisation liquid chromatography/ion trap mass spectrometry. *Rapid Communications in Mass Spectrometry*, *21*, 880–892. <https://doi.org/10.1002/rcm.2911>
- Talbot, H. M., Rohmer, M., & Farrimond, P. (2007b). Structural characterisation of unsaturated bacterial hopanoids by atmospheric pressure chemical ionisation liquid chromatography/ion trap mass spectrometry. *Rapid Communications in Mass Spectrometry*, *21*, 1613–1622. <https://doi.org/10.1002/rcm.2997>
- Talbot, H. M., Sidgwick, F. R., Bischoff, J., Osborne, K. A., Rush, D., Sherry, A., & Spencer-Jones, C. L. (2016). Analysis of non-derivatised bacteriohopanepolyols by ultrahigh-performance liquid chromatography/tandem mass spectrometry. *Rapid Communications in Mass Spectrometry*, *30*, 2087–2098. <https://doi.org/10.1002/rcm.7696>
- Talbot, H. M., Watson, D. F., Murrell, J. C., Carter, J. F., & Farrimond, P. (2001). Analysis of intact bacteriohopanepolyols from methanotrophic bacteria by reversed-phase high-performance liquid chromatography-atmospheric pressure chemical ionisation mass spectrometry. *Journal of Chromatography A*, *921*, 175–185. [https://doi.org/10.1016/S0021-9673\(01\)00871-8](https://doi.org/10.1016/S0021-9673(01)00871-8)
- Talbot, H. M., Watson, D. F., Pearson, E. J., & Farrimond, P. (2003). Diverse biohopanoid compositions of non-marine sediments. *Organic Geochemistry*, *34*, 1353–1371. [https://doi.org/10.1016/S0146-6380\(03\)00159-1](https://doi.org/10.1016/S0146-6380(03)00159-1)
- Tavormina, P. L., Hatzenpichler, R., McGlynn, S., Chadwick, G., Dawson, K. S., Connon, S. A., & Orphan, V. J. (2015). *Methyloprofundus sedimenti* gen. nov., sp. nov., an obligate methanotroph from ocean sediment belonging to the 'deep sea-1' clade of marine methanotrophs. *International Journal of Systematic and Evolutionary Microbiology*. Microbiology Society. <https://doi.org/10.1099/ijs.0.062927-0>
- Tavormina, P. L., Ussler, W., & Orphan, V. J. (2008). Planktonic and sediment-associated aerobic methanotrophs in two seep systems along the North American margin. *Appl Environ Microbiol*, *74*, 3985–3995. <https://doi.org/10.1128/Aem.00069-08>
- Taylor, R. F. (1984). Bacterial triterpenoids. *Microbiological Reviews*, *48*, 181–198.
- Taylor, S. C., Dalton, H., & Dow, C. S. (1981). Ribulose-1,5-bisphosphate carboxylase/oxygenase and carbon assimilation in *Methylococcus capsulatus* (Bath). *Journal of General Microbiology*, *122*, 89–94.
- Tays, C., Guarnieri, M. T., Sauvageau, D., & Stein, L. Y. (2018). Combined effects of carbon and nitrogen source to optimize growth of proteobacterial methanotrophs. *Frontiers in Microbiology*, *9*, 2239–2239. <https://doi.org/10.3389/fmicb.2018.02239>
- Thiel, V., Peckmann, J., Seifert, R., Wehrung, P., Reitner, J., & Michaelis, W. (1999). Highly isotopically depleted isoprenoids: molecular markers for ancient methane venting. *Geochimica Et Cosmochimica Acta*, *63*, 3959–3966. [https://doi.org/10.1016/S0016-7037\(99\)00177-5](https://doi.org/10.1016/S0016-7037(99)00177-5)

- Trotsenko, Y. A., & Murrell, J. C. (2008). Metabolic aspects of aerobic obligate methanotrophy*. In *Advances in Applied Microbiology* (Vol. 63, pp. 183–229). Academic Press. [https://doi.org/10.1016/S0065-2164\(07\)00005-6](https://doi.org/10.1016/S0065-2164(07)00005-6)
- Wagner, T., Kallweit, W., Talbot, H. M., Mollenhauer, G., Boom, A., & Zabel, M. (2014). Microbial biomarkers support organic carbon transport from methane-rich Amazon wetlands to the shelf and deep sea fan during recent and glacial climate conditions. *Organic Geochemistry*, *67*, 85–98. <https://doi.org/10.1016/j.orggeochem.2013.12.003>
- Wei, J. H., Yin, X. C., & Welander, P. V. (2016). Sterol synthesis in diverse bacteria. *Frontiers in Microbiology*, *7*, 990. <https://doi.org/ARTN 990 10.3389/fmicb.2016.00990>
- Welander, P. V., Coleman, M. L., Sessions, A. L., Summons, R. E., & Newman, D. K. (2010). Identification of a methylase required for 2-methylhopanoid production and implications for the interpretation of sedimentary hopanes. *Proceedings of the National Academy of Sciences*, *107*, 8537. <https://doi.org/10.1073/pnas.0912949107>
- Welander, P. V., Hunter, R. C., Zhang, L. C., Sessions, A. L., Summons, R. E., & Newman, D. K. (2009). Hopanoids play a role in membrane integrity and pH homeostasis in *Rhodopseudomonas palustris* TIE-1. *Journal of Bacteriology*, *191*, 6145–6156. <https://doi.org/10.1128/Jb.00460-09>
- Welander, P. V., & Summons, R. E. (2012). Discovery, taxonomic distribution, and phenotypic characterization of a gene required for 3-methylhopanoid production. *Proceedings of the National Academy of Sciences of the United States of America*, *109*, 12905–10. <https://doi.org/10.1073/pnas.1208255109>
- Werne, J. P., Baas, M., & Sinninghe Damsté, J. S. (2002). Molecular isotopic tracing of carbon flow and trophic relationships in a methane-supported benthic microbial community. *Limnology and Oceanography*, *47*, 1694–1701. <https://doi.org/DOI 10.4319/lo.2002.47.6.1694>
- Willers, C., Jansen van Rensburg, P. J., & Claassens, S. (2015). Phospholipid fatty acid profiling of microbial communities—a review of interpretations and recent applications. *Journal of Applied Microbiology*, *119*, 1207–1218. <https://doi.org/10.1111/jam.12902>
- Wisshak, M. (2012). Chapter 8 - Microbioerosion. In D. Knaust & R. G. Bromley (Eds.), *Trace Fossils as Indicators of Sedimentary Environments. Developments in Sedimentology* (Vol. 64, pp. 213–243). Elsevier. <https://doi.org/10.1016/B978-0-444-53813-0.00008-3>
- Wisshak, M., Knaust, D., & Bertling, M. (2019). Bioerosion ichnotaxa: Review and annotated list. *Facies*, *65*, 24. <https://doi.org/10.1007/s10347-019-0561-8>
- Wisshak, M., Tribollet, A., Jakobsen, J., & Freiwald, A. (2011). Temperate bioerosion: Ichnodiversity and biodiversity from intertidal to bathyal depths (Azores). *Geobiology*, *9*, 492–520. <https://doi.org/10.1111/j.1472-4669.2011.00299.x>
- Xie, S., Lipp, J. S., Wegener, G., Ferdelman, T. G., & Hinrichs, K.-U. (2013). Turnover of microbial lipids in the deep biosphere and growth of benthic archaeal populations. *Proceedings of the National Academy of Sciences of the United States of America*, *110*, 6010–6014. <https://doi.org/10.1073/pnas.1218569110>
- Zabel, M., Boetius, A., Emeis, K.-C., Ferdelman, T. G., & Spieß, V. (2012). PROSA Process Studies in the Eastern South Atlantic – Cruise No. M76 – April 12 – August 24, 2008 – Cape Town (South Africa) – Walvis Bay (Namibia) Meteor R/V. Bremen: DFG-Senatskommission für Ozeanographie; https://doi.org/10.2312/cr_m76
- Zundel, M., & Rohmer, M. (1985). Prokaryotic triterpenoids. 1. 3-beta-methylhopanoids from *Acetobacter* species and *Methylococcus capsulatus*. *European Journal of Biochemistry*, *150*, 23–27. <https://doi.org/10.1111/j.1432-1033.1985.tb08980.x>

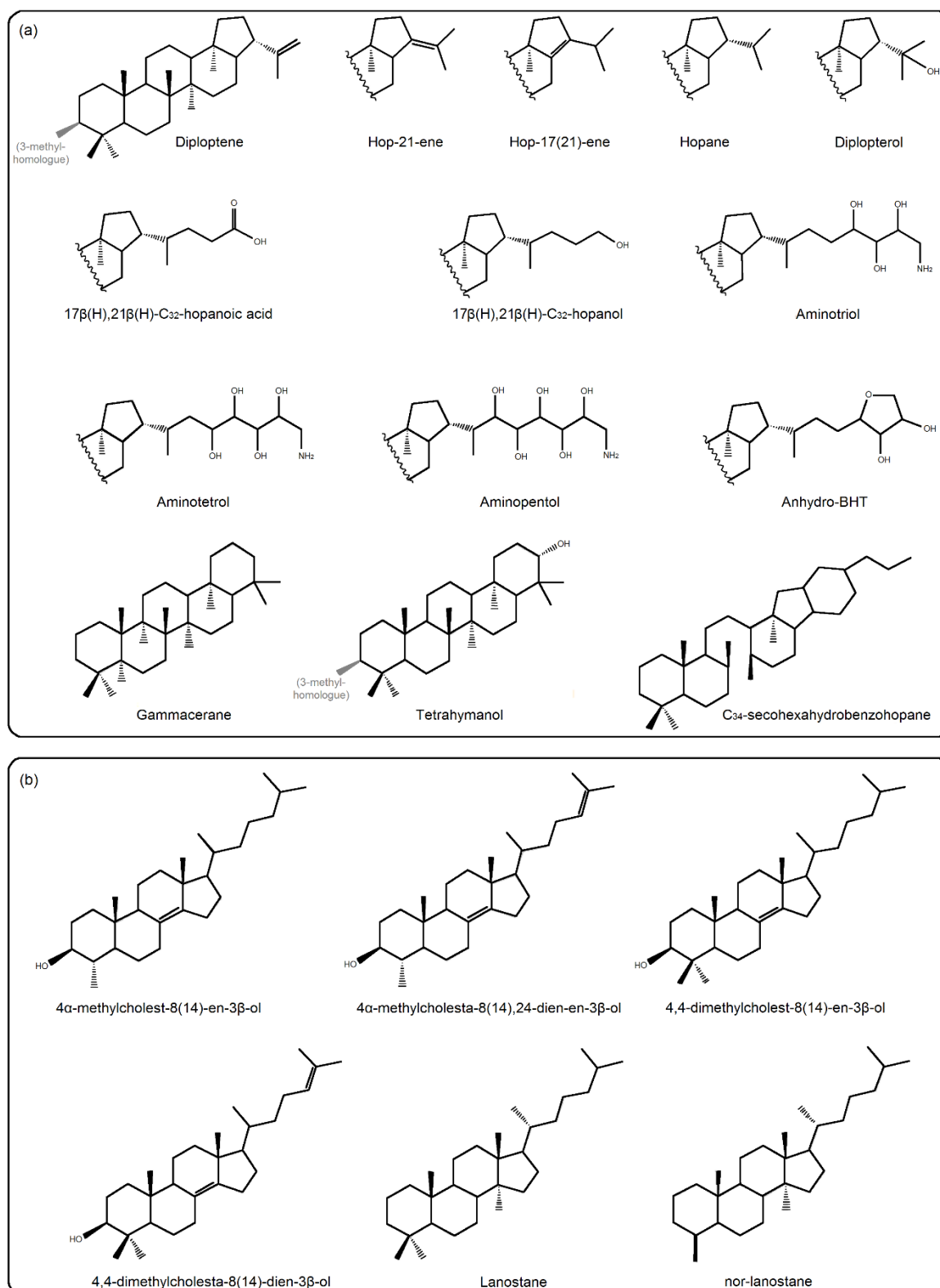
Appendix A

Table A.1 Carbon isotope values (‰ V-PDB) of biomarkers of Type I methanotrophs in individual batch cultures. n.d. = not detected; tr = traces.

Compounds	<i>M. alcaliphilum</i>			<i>M. kenyaense</i>		
	$\delta^{13}\text{C}$ (‰V-PDB)			$\delta^{13}\text{C}$ (‰ V-PDB)		
	Exp 1	Exp 2	Exp 3	Exp 1	Exp 2	Exp 3
Squalene	n.d.	n.d.	n.d.	traces	traces	-73
Diploptene	tr	tr	tr	-68	-70	-76
Hop-21-ene	tr	n.d.	n.d.	tr	tr	tr
3-me-diploptene	n.d.	n.d.	n.d.	n.d.	n.d.	tr
3-me-hop-21-ene	n.d.	n.d.	n.d.	n.d.	n.d.	tr
4 α -methylcholest-8(14)-en-3 α -ol	n.d.	n.d.	n.d.	tr	tr	tr
4 α -methylcholesta-8(14),24-dien-3 α -ol	n.d.	n.d.	n.d.	tr	tr	tr
4,4-dimethylcholest-8(14)-en-3 β -ol	tr	tr	tr	-75	-72	-76
4,4-dimethylcholesta-8(14),24-dien-3 β -ol	tr	tr	tr	tr	tr	tr
Diplopterol	tr	tr	tr	-72	-71	-78
Tetrahymanol	-63	-66	-66	tr	tr	tr
3-me-diplopterol	tr	tr	tr	tr	tr	-77
3-me-tetrahymanol	-60	-62	-63	tr	tr	tr
C ₃₁ 17 β (H),21 β (H)-hopanol*	tr	-61	-64	tr	tr	-67
Unsat. C ₃₂ 17 β (H),21 β (H)-hopanol*						
C ₃₂ 17 β (H),21 β (H)-hopanol*	-61	-64	-65	-65	-67	-67
3-me-C ₃₂ 17 β (H),21 β (H)-hopanol*	-57	-62	-62	n.d.	-66	-64

Products of periodic acid cleavage procedure; C₃₁ 17 β (H),21 β (H)-hopanol (homohopanol) is derived from aminotetrol, and C₃₂ 17 β (H),21 β (H)-hopanol (bishomohopanol) and 3-methyl C₃₂ 17 β (H),21 β (H)-hopanol (bishomohopanol) are derived from aminotriol and 3-methyl aminotriol, respectively.

Figure A.1 Lipid structures A



Appendix B

Table B.1 Contents of pentacyclic terpenoids in cultures of *M. alcaliphilum* provided with varying amounts of nitrate

	10 mM KNO ₃					100 mM KNO ₃				
	Content (µg/g dw)					Content (µg/g dw)				
	alc-1	alc-2	alc-3	Average	SD	alc-4	alc-5	alc-6	Average	SD
diploptene XIII	19	27	16	21	6	10	19	24	18	7
hop-21-ene XIV	10	14	7	10	3	5	10	11	9	3
3-me-diploptene XV	4	7	4	5	2	3	4	16	8	7
3-me-hop-21-ene XVI	2	4	4	3	1	2	2	11	2	0
diplopterol XVII	19	63	39	40	22	47	16	47	47	0
3-me-diplopterol XVIII	7	17	11	12	5	17	6	46	23	21
tetrahymanol XIX	60	56	34	50	14	53	121	235	136	92
3-me-tetrahymanol XX	6	5	2	4	2	5	11	41	19	19
aminodiol I	0	0	0	0	0	1	3		2	1
aminotriol a IIIa	0	0	9	3	5	15	24	41	27	14
aminotriol b IIIb	138	172	206	172	34	321	443	636	467	159
3-me-aminotriol a IVa	6	14	3	8	6	3	5		4	2
3-me-aminotriol b IVb	44	61	83	63	20	106	154	160	140	30
aminotetrol V	37	48	34	40	8	43	58	170	90	69
3-me-aminotetrol VI	106	143	93	114	26	125	182	496	267	200
Sum pentacyclic triterpenoids	457	632	544	544	88	754	1042	1922	1239	608

Bold values represent outliers according to Dixon test ($\alpha < 0.05$)

Table B.2 Contents of pentacyclic terpenoids in cultures of *M. alcaliphilum* grown at different salinities

	1% NaCl					3% NaCl				
	Content (µg/g dw)					Content (µg/g dw)				
	alc-7	alc-8	alc-9	Average	SD	alc-1	alc-2	alc-3	Average	SD
diploptene XIII	20	41	23	28	12	19	27	16	21	6
hop-21-ene XIV	13	23	13	16	6	10	14	7	10	3
3-me-diploptene XV	3	9	4	6	3	4	7	4	5	2
3-me-hop-21-ene XVI	2	5	2	2	0	2	4	4	3	1
diplopterol XVII	118	51	49	72	39	19	63	39	40	22
3-me-diplopterol XVIII	16	14	14	15	1	7	17	11	12	5
tetrahymanol XIX	53	58	55	55	2	60	56	34	50	14
3-me-tetrahymanol XX	2	3	1	2	1	6	5	2	4	2
aminodiol I	14	7	16	12	4	0	0	0	0	0
aminotriol a IIIa	10	8	9	9	1	0	0	9	3	5
aminotriol b IIIb	441	652	168	420	243	138	172	206	172	34
3-me-aminotriol a IVa	96	41	77	71	28	6	14	3	8	6
3-me-aminotriol b IVb	106	192	52	117	70	44	61	83	63	20
aminotetrol V	110	132	38	93	49	37	48	34	40	8
3-me-aminotetrol VI	119	182	78	127	52	106	143	93	114	26
Sum pentacyclic triterpenoids	1123	1414	599	1045	413	457	632	544	544	88

Bold values represent outliers according to Dixon test ($\alpha < 0.05$)

Table B.3 Calculated p values from t -tests

	Nitrogen availability	Salinity
	10 mM vs. 100 mM	1% vs. 3%
diploptene XIII	0.651	0.374
hop-21-ene XIV	0.562	0.196
3-me-diploptene XV	0.543	0.738
3-me-hop-21-ene XVI	0.497	0.414
diplopterol XVII	0.219	0.283
3-me-diplopterol XVIII	0.409	0.409
tetrahymanol XIX	0.185	0.603
3-me-tetrahymanol XX	0.267	0.071
aminotriol a IIIa	0.048	0.168
aminotriol b IIIb	0.035	0.251
3-me-aminotriol a IVa	0.257	0.018
3-me-aminotriol b IVb	0.020	0.269
aminotetrol V	0.336	0.201
3-me-aminotetrol VI	0.318	0.729
Sum pentacyclic triterpenoids	0.236	0.224

Bold values represent those variables showing statistically significant differences ($\alpha < 0.05$)

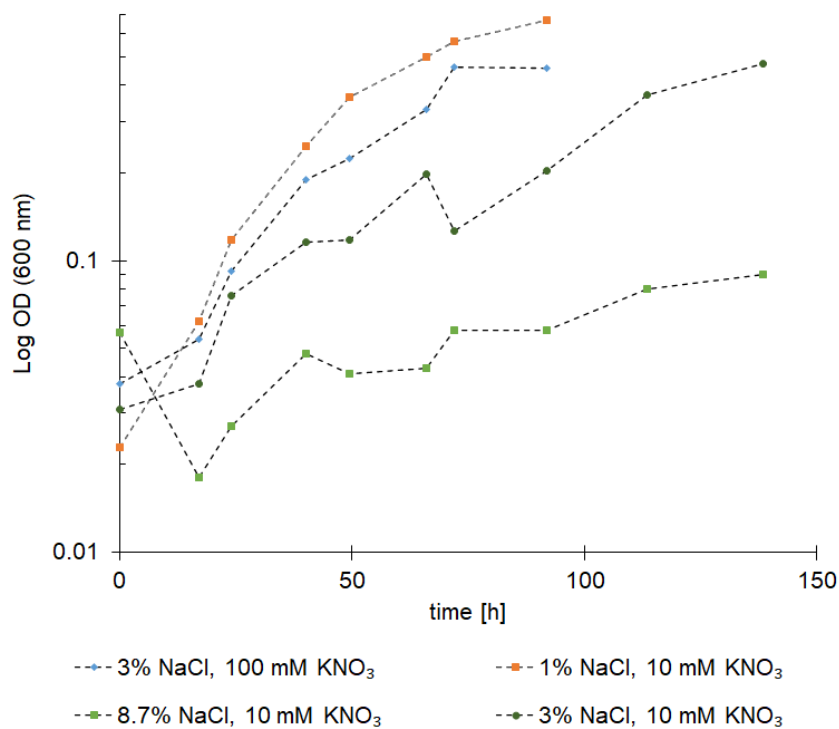
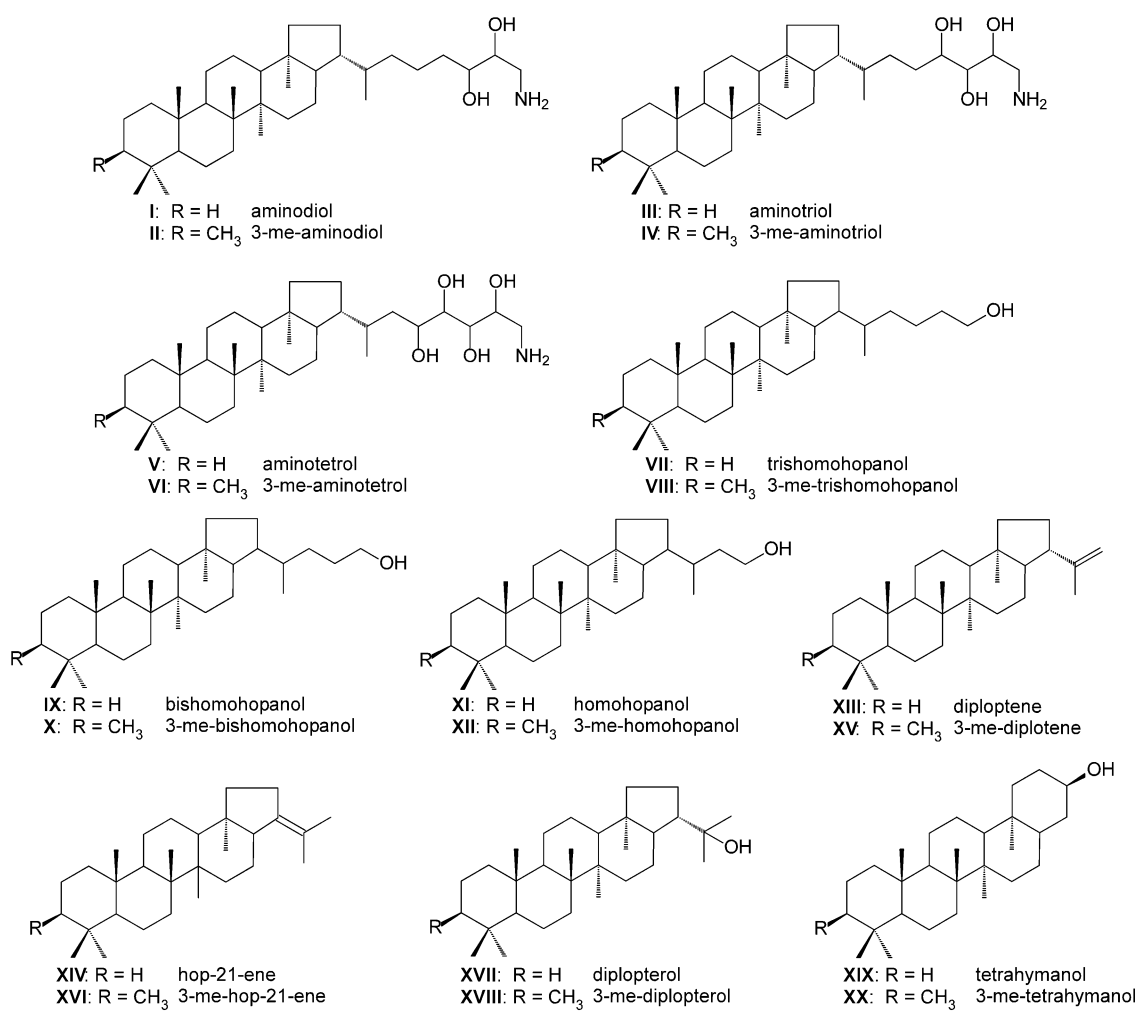
Figure B.1 Growth curves (OD_{600}) of *M. alcaliphilum* provided with varying amounts of nitrate and grown at different salinities.

Figure B.2 Lipid structures B



Appendix C

Table C.1 Taxonomy of microbial community in the corroded surface of sample CAB-C

Assignments at domain level		
Parent taxa	Taxa	Abundance
Cellular organisms	Bacteria	93
	Total	93
	Unclassified	0

Assignments at phylum level		
Parent taxa	Taxa	Abundance
Bacteria	Verrucomicrobia	2
Bacteria	Actinobacteria	4
Bacteria	Bacteroidetes	21
Bacteria	Planctomycetes	2
Bacteria	Proteobacteria	64
	Total	93
	Unclassified	0

Assignments at class level		
Parent taxa	Taxa	Abundance
Verrucomicrobia	Cytophagia	2
Actinobacteria	Acidimicrobiia	4
Bacteroidetes	Cytophagia	7
Bacteroidetes	Sphingobacteria	2
Bacteroidetes	Flavobacteria	12
Planctomycetes	Planctomycetacia	2
Proteobacteria	Deltaproteobacteria	2
Proteobacteria	Alphaproteobacteria	6
Proteobacteria	Gammaproteobacteria	56
	Total	93
	Unclassified	0

Assignments at order level		
Parent taxa	Taxa	Abundance
Spartobacteria	Chthoniobacterales	1
Acidimicrobiia	Acidimicrobiales	4
Cytophagia	Cytophagales	7
Sphingobacteria	Sphingobacteriales	2
Flavobacteria	Flavobacteriales	12
Planctomycetacia	Planctomycetales	2
Deltaproteobacteria	Myxococcales	2
Alphaproteobacteria	Caulobacterales	2
Alphaproteobacteria	Rhizobiales	2
Alphaproteobacteria	Rhodobacterales	2
Gammaproteobacteria	Methylococcales	35
Gammaproteobacteria	Chromatiales	2
Gammaproteobacteria	Thiotrichales	18
	Total	91
	Unclassified	2

Assignments at family level		
Parent taxa	Taxa	Abundance
Cytophagales	Flammeovirgaceae	3
Sphingobacteriales	Saprospiraceae	2
Flavobacteriales	Flavobacteriaceae	10
Planctomycetales	Planctomycetaceae	2
Myxococcales	Haliangiaceae	2
Nannocystineae		
Caulobacterales	Hyphomonadaceae	2
Rhizobiales	Rhodobiaceae	2
Rhodobacterales	Rhodobacteraceae	1
Methylococcales	IheB2-23	4
Methylococcales	Methylococcaceae	3
Methylococcales	Hyd24-01	28
Chromatiales	Granulosicoccaceae	1
Thiotrichales	Thiotrichaceae	14
Thiotrichales	Piscirickettsiaceae	4
	Total	78
	Unclassified	15

Assignments at genus level		
Parent taxa	Taxa	Abundance
Flavobacteriaceae	Lutibacter	2
Flavobacteriaceae	Aquimarina	2
Haliangiaceae	Haliangium	2
Hyphomonadaceae	Robiginitomaculum	2
Rhodobiaceae	Rhodobium	1
Rhodobacteraceae	Roseobacter clade	1
	NAC11-7 lineage	
Methylococcaceae	Methylomonas	2
Granulosicoccaceae	Granulosicoccus	1
Thiotrichaceae	Leucothrix	12
Thiotrichaceae	Thiothrix	2
	Total	27
	Unclassified	66

Assignments at species level		
Parent taxa	Taxa	Abundance
	Total	0
	Unclassified	93

Appendix D:

Author's contributions to publications

Cordova-Gonzalez, A., Birgel, D., Kappler, A., & Peckmann, J., 2020. Carbon stable isotope patterns of cyclic terpenoids: A comparison of cultured alkaliphilic aerobic methanotrophic bacteria and methane-seep environments. *Organic Geochemistry*, 139, 103940. DOI: 10.1016/j.orggeochem.2019.103940.

Author's contribution: data interpretation, results and discussion.

Cordova-Gonzalez, A., Birgel, D., Kappler, A., & Peckmann, J., 2021. Variation of salinity and nitrogen concentration affects the pentacyclic triterpenoid inventory of the haloalkaliphilic aerobic methanotrophic bacterium *Methylovumicrobium alcaliphilum*. *Extremophiles* 25(3):285-299. DOI: 10.1007/s00792-021-01228-x.

Author's contribution: idea, methods, data acquisition and interpretation, results and discussion.

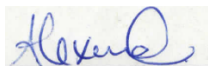
Cordova-Gonzalez A., Birgel D., Wisshak M., Urich T., Brinkmann F., Marcon Y., Bohrmann G. & Peckmann J. A carbonate corrosion experiment at a marine methane seep: The role of aerobic methanotrophic bacteria. (In preparation, to be submitted to *Geobiology*).

Author's contribution: data interpretation, results and discussion.

Eidesstattliche Versicherung

Hiermit versichere ich an Eides statt, dass ich die vorliegende Dissertation mit dem Titel: "Unchaining the biomarker potential of aerobic methanotrophic bacteria" selbstständig verfasst und keine anderen als die angegebenen Hilfsmittel – insbesondere keine im Quellenverzeichnis nicht benannten Internet-Quellen – benutzt habe. Alle Stellen, die wörtlich oder sinngemäß aus Veröffentlichungen entnommen wurden, sind als solche kenntlich gemacht. Ich versichere weiterhin, dass ich die Dissertation oder Teile davon vorher weder im In- noch im Ausland in einem anderen Prüfungsverfahren eingereicht habe und die eingereichte schriftliche Fassung der auf dem elektronischen Speichermedium entspricht.

Hamburg, 04.02.2022



Alexmar del Carmen Córdova González